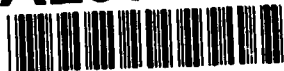AFOSR-TR-91-0250

University Research Initiative

Nonlinear Dynamics and Control of Flexible Structures

Cornell University
October 1986 - June 1990

Sponsored by the

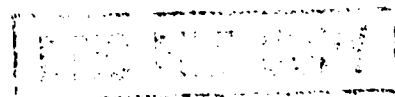Air Force Office of Scientific Research
Aerospace Division

FINAL REPORT

March 1991

APR 7 1991

Accession For

☑ ☐ ☐

A-1

91 4 16 063

REPORT DOCUMENTATION PAGE

Form Approved
OMB No. 0704-0188

1a. REPORT SECURITY CLASSIFICATION	1b. RESTRICTIVE MARKINGS
2a. SECURITY CLASSIFICATION AUTHORITY	3. DISTRIBUTION / AVAILABILITY OF REPORT
2b. DECLASSIFICATION / DOWNGRADING SCHEDULE	Approved for public release,' distribution unlimited

4. PERFORMING ORGANIZATION REPORT NUMBER(S)	5. MONITORING ORGANIZATION REPORT NUMBER(S)

6a. NAME OF PERFORMING ORGANIZATION	6b. OFFICE SYMBOL (If applicable)	7a. NAME OF MONITORING ORGANIZATION
Cornell University		AFOSR

6c. ADDRESS (City, State, and ZIP Code)	7b. ADDRESS (City, State, and ZIP Code)
105 Upson Hall Ithaca, NY 148537501	AFOSR/NA Bolling AFB DC 20332-6448

8a. NAME OF FUNDING / SPONSORING ORGANIZATION AFOSR/NA Bolling AFB DC 20332-6448.	8b. OFFICE SYMBOL (If applicable) NA	9. PROCUREMENT INSTRUMENT IDENTIFICATION NUMBER AFOSR-90-0211

8c. ADDRESS (City, State, and ZIP Code)	10. SOURCE OF FUNDING NUMBERS			
Bldg. 410, Rm. A227 Bolling Air Force Base, DC 20332-0448	PROGRAM ELEMENT NO. 61102F	PROJECT NO. 3484	TASK NO. A1	WORK UNIT ACCESSION NO.

11. TITLE (Include Security Classification)

NONLINEAR DYNAMICS AND CONTROL OF FLEXIBLE STRUCTURES (U)

12. PERSONAL AUTHOR(S)
Francis C. Moon, Editor

13a. TYPE OF REPORT Final	13b. TIME COVERED FROM 10/86 TO 6/90	14. DATE OF REPORT (Year, Month, Day) 1 March 1991	15. PAGE COUNT

16. SUPPLEMENTARY NOTATION

17.	COSATI CODES		18. SUBJECT TERMS (Continue on reverse if necessary and identify by block number)
FIELD	GROUP	SUB-GROUP	

19. ABSTRACT (Continue on reverse if necessary and identify by block number)

The goals of the Air Force sponsored University Research Initiative at Cornell were to examine the nonlinear dynamics and control of flexible structures, some of which might be used for space applications. This project was a collaborative one involving structural, electrical and mechanical engineers and resulted in nine doctoral dissertations and two masters theses wholly or partially supported by this grant. Because of the space application focus of the research, a major part of the research was on truss/frame type structures and five different truss structures from three to ten meters in size were constructed, two with active controls. However, nonlinear dynamics of continuous beam type structures were also investigated.

(continued)

20. DISTRIBUTION / AVAILABILITY OF ABSTRACT ☒ UNCLASSIFIED/UNLIMITED ☒ SAME AS RPT. ☐ DTIC USERS	21. ABSTRACT SECURITY CLASSIFICATION unclassified
22a. NAME OF RESPONSIBLE INDIVIDUAL Francis C. Moon SPENCER T WU	22b. TELEPHONE (Include Area Code) (607) 255-7146	22c. OFFICE SYMBOL AFOSR/NA

DD Form 1473, JUN 86   Previous editions are obsolete.

19.   On the dynamics side, one of the principal themes was to explore what types of nonlinearities would result in chaotic and unpredictable vibrations. Loose joints in truss structures, friction, buckling and geometric nonlinearities were all found to lead to chaotic motions under certain periodic forcing conditions. Several modern tools of nonlinear mathematics were used in the experimental investigation including Poincaré maps, fractal dimensions, bifurcation analysis and probability distribution functions. Given the pervasiveness of the chaotic phenomena, it was concluded that current methods of numerical structural analysis would not uncover these unpredictable regions.

On the control side optimal placement of actuators and sensors for space truss active vibration suppression was investigated. A common theme in these investigations was the concept of self-equilibrating non-local control systems for space structures. In one case a cable control actuator was developed for a ten-meter long truss. With a single actuator, the control force was distributed along the truss and was able to suppress the five lowest modes of vibration. In another experimental-theoretical study, vibrations of a six-meter truss was achieved with 10-15% critical damping using new magnetic, linear motor actuators with a high force/weight ratio.

On the theoretical side new methods were developed for structural control using techniques for simulated annealing for actuator placement, differential dynamic pro-gramming for optimal control, a method of analysis for nonlinear random vibrations of pin-jointed trusses, group theoretic methods for vibration analysis and new models to analyze chaotic dynamics in nonlinear structures with large deformations and friction forces.

Finally, a major numerical effort resulted in new codes to predict large motions of structures under active control using parallel processing algorithms. A listing of specific accomplishments is given below. Selected projects are described in more detail. Copies of reports and papers can be obtained upon request.

Nonlinear Dynamics and Control of Flexible Structures

Selected Thesis Abstracts

Nonlinear Dynamics and Control of Flexible Structures

University Research Initiative
Cornell University

Sponsored by the

Air Force Office of Scientific Research
Aerospace Division

Summary

The goals of the Air Force sponsored University Research Initiative at Cornell were to examine the nonlinear dynamics and control of flexible structures, some of which might be used for space applications. This project was a collaborative one involving structural, electrical and mechanical engineers and resulted in nine doctoral dissertations and two masters theses wholly or partially supported by this grant. Because of the space application focus of the research, a major part of the research was on truss/frame type structures and five different truss structures from three to ten meters in size were constructed, two with active controls. However, nonlinear dynamics of continuous beam type structures were also investigated.

On the dynamics side, one of the principal themes was to explore what types of nonlinearities would result in chaotic and unpredictable vibrations. Loose joints in truss structures, friction, buckling and geometric nonlinearities were all found to lead to chaotic motions under certain periodic forcing conditions. Several modern tools of nonlinear mathematics were used in the experimental investigation including Poincaré maps, fractal dimensions, bifurcation analysis and probability distribution functions. Given the pervasiveness of the chaotic phenomena, it was concluded that current methods of numerical structural analysis would not uncover these unpredictable regions.

On the control side optimal placement of actuators and sensors for space truss active vibration suppression was investigated. A common theme in these investigations was the concept of self-equilibrating non-local control systems for space structures. In one case a cable control actuator was developed for a ten-meter long truss. With a single actuator, the control force was distributed along the truss and was able to suppress the five lowest modes of vibration. In another experimental-theoretical study, vibrations of a six-meter truss was achieved with 10-15% critical damping using new magnetic, linear motor actuators with a high force/weight ratio.

On the theoretical side new methods were developed for structural control using techniques for simulated annealing for actuator placement, differential dynamic pro-gramming for optimal control, a method of analysis for nonlinear random vibrations of pin-jointed trusses, group theoretic methods for vibration analysis and new models to analyze chaotic dynamics in nonlinear structures with large deformations and friction forces.

Finally, a major numerical effort resulted in new codes to predict large motions of structures under active control using parallel processing algorithms. A listing of specific accomplishments is given below. Selected projects are described in more detail. Copies of reports and papers can be obtained upon request.

Nonlinear Dynamic and Control of Flexible Structures

Francis C. Moon, Mechanical and Aerospace Engineering
   Principal Investigator

Nonlinear Dynamics
Chaotic Vibrations
Controlled Structures

James S. Thorp, Electrical Engineering
   Co-Principal Investigator

Nonlinear Feedback Control
Optimal Sensor and Actuator Location

Peter Gergely, Civil Engineering
   Co-Principal Investigator

Experimental Structural Dynamics
Controlled Structures

John F. Abel, Civil Engineering

Nonlinear Structural Analysis

Christine A. Shoemaker, Civil Engineering

Optimal Control of Nonlinear Systems

Other Faculty Participants:

H.-D. Chiang, Electrical Engineering

Optimal Control

D.F. Delchamps, Electrical Engineering

Nonlinear Control Theory

M.D. Grigoriu, Civil Engineering

Nonlinear Random Vibration

T.J. Healey, Theoretical and Applied Mechanics

Nonlinear Structural Analysis

S. Mukherjee, Theoretical and Applied Mechanics

Elasto-Plastic Structural Dynamics

Graduate Students:

G.-X. Li	Theoretical and Applied Mechanics
J. Cusumano	Theoretical and Applied Mechanics
P.-Y. Chen	Theoretical and Applied Mechanics
B. Feeny	Theoretical and Applied Mechanics
J. Treacy	Theoretical and Applied Mechanics
R. Pratap	Theoretical and Applied Mechanics
O.M. O'Reilly	Theoretical and Applied Mechanics
S.M. Howard	Theoretical and Applied Mechanics
M. Davies	Mechanical and Aerospace Engineering
B. Aubert	Civil and Environmental Engineering
L. Larson	Civil and Environmental Engineering
J.F. Hajjar	Civil and Environmental Engineering
L.-Z. Liao	Operations Research and Industrial Engineering
J.Lu	Electrical Engineering
J.-C. Wang	Electrical Engineering

Postdocs:

G.-X. Li	Theoretical and Applied Mechanics
S. Islam	Civil and Environmental Engineering

URI Accomplishments

•Nonlinear Dynamics and Chaos in Flexible Structures

The effect of several different types of nonlinearities on the dynamics of flexible structures has been investigated including,

large elastic deformation
loose joints in Truss-frame structures
friction in structures and machines
buckling in truss structures

The general conclusion from these studies is that strong nonlinearities in structures can lead to complicated dynamical motions at the least and complex, even chaotic and unpredictable motions at worse.

•Chaotic vibrations of thin cantilevered beams under bending and torsional motions (Cusumano & Moon).
The major result of this work was the discovery of unstable out of plane motions under in-plane bending excitation. Both experimental and analytical results show that these out of plane bending-torsion motions become chaotic and unpredictable near all the natural frequencies and sums and differences of natural frequencies. Experimental tools such as fractal dimension algorithms were developed in this work which has been subsequently used in other experiments.

•Chaotic vibrations of truss structures with loose joints(G.-X. Li & Moon).
In this experimental and numerical study a 4-meter truss was constructed with pin joints. The principal result is that small play in the joints can lead to chaotic dynamics of the truss even for small excitation. However, a prestress in the truss using a tension cable was shown to delay the onset of chaotic vibration.

•Chaotic dynamics due to friction (Feeny &Moon).
Joints in truss structures often have dry friction nonlinearities. Also, dry friction plays a role in turbine blade vibrations. In this study the qualitative dynamics of a dry friction oscillator were explored using experiments, numerical simulation and analysis. This first of its kind study gives a complete picture of the strange attractors the results from the chaotic behavior. New techniques using symbol dynamics were developed in the thesis as well as a new method of measure friction properties of structural joints.

•Chaotic dynamics of a space truss with a buckled strutt (Davies & Moon).
In this experimental and analytical study, the dynamics of a 4-meter space truss with one bending-weak longeron strutt was studied under periodic excitation. The results showed period doubling behavior leading to chaotic fractal looking Poincaré maps when the weak strutt began to buckle. These results are the first of its kind for nonlinear structural dynamics.

•Active Vibration Damping using Magnetic Actuators for Truss Structures (Chen & Moon)
    In this experimental and analytical study, a six-meter truss was built with new linear motor magnetic actuators with high force/weight ratio. The forces were transmitted across several bays of the truss using a new link mechanism to achieve nonlocal force control. Damping ratios of 10-15% were obtained using co-located feedback for vibration level up to 1 cm amplitude.

•Group Theory Methods for Vibration Analysis of Space Structures (Healey & Treacy).

•Buckling Dynamics in Space Structures (Mukherjee & Pratap).

•Design and construction of a 10-meter, flexible truss for current and future testing of 2D and 3D controlled and uncontrolled dynamic behavior.

    •Preliminary tests, 2D prototype, open-loop control derived from DDP (Prof. Gergely)

    •Design of full system (Professors Gergely, Abel, Thorp, and Shoemaker)

    •Calculation of optimal locations and gains for tendon-control system (Prof. Thorp)

    •Computer simulation for design of structure and control system, and for analysis of robustness of control (Prof. Abel)

    •Initial testing with closed-loop tendon control system (Prof. Gergely)

•Development and application of computer simulations for nonlinear dynamics of controlled and uncontrolled space structures (Prof. Abel)

    •3D nonlinear simulations with interactive computer graphics

    •Parallel processing (coarse-grained) algorithms and implementation for nonlinear structural dynamics

    •Modeling of open-loop, constant-feedback gain, and collocated velocity feedback controls.

    •Comparison with experiments for verification

    •Effects of nonlinearities on nominally linear dynamic simulations

    •Studies of sensitivity of controls to structural imperfections

•Control Theory and Methods

    •Optimal location of controllers by simulated annealing (Professors Chiang and Thorp)

    •Optimal location of tendon control system by dynamic programming (Professor Thorp)

    •Extension of differential dynamic programming (DDP) to optimal control of nonlinear structural control behavior (Professor Shoemaker)

    •Improvements in the convergence and efficiency of DDP for large-scale nonlinear dynamic systems (Prof. Shoemaker)

4

•Effects of nonlinearities on performance and stability of controls derived from linear theories (Professors Thorp and Chiang)

•Partial eigenstructure assignment for modal control of very large space structures (Professors Thorp and Chiang)

•Nonlinear random vibration of pin-jointed trusses with imperfections (Prof. Grigoriu)

URI Dissertations

Aubert, B., "Numerical Simulation of the Transient Nonlinear Dynamics of Actively Controlled Space Structures," Ph.D. Thesis, Civil and Environmental Engineering, Cornell University, (expected) May 1991.

Chen, P.-Y., "Vibration Suppression of Flexible Structures Using Colocated Velocity Feedback and Nonlocal Actuator Control," Ph.D. Thesis, Depatment of Theoretical and Applied Mechancs, Cornell University, May 1990.

Cusumano, J,P., "Low-Dimensional Behavior in Chaotic Nonplanar Motions of a Forced Linearly Elastic Rod: Experiment and Theory," Ph.D. Thesis, Department of Theoretical and Applied Mechanics, Cornell University, August 1989.

Feeny, B., "Chaos and Friction," Ph.D. Thesis, Department of Theoretical and Applied Mechanics, Cornell University, August 1990.

Hajjar, J.E., "Parallel Processing for Transient Nonlinear Structural Dynamics and Three-Dimensional Framed Structures," Ph.D. Thesis, Department of Structural Engineering, Cornell University, January 1988.

Howard, S.M., "Transient Stress Waves in Trusses and Frames," Ph.D. Thesis, Department of Theoretical and Applied Mechanics, Cornell University, January 1990.

Larson, L.B., "Experimental Program for Active Control of Flexible Space Structures," M.S. Thesis, School of Civil and Environmental Engineering, Cornell University, August 1990.

Liao, Li-Zhi, "Numerically Efficient Algorithms for Unconstrained and Constrained Differential Dynamic Programming in Discrete-Time, Nonlinear Systems," Ph.D. Thesis, School of Operations Research and Industrial Engineering, Cornell University, August 1990.

O'Reilly, O.M., "A Pseudo Exponent for the Characterization of Periodic and Chaotic Data Sets from Forced Systems," M.S. Thesis, Department of Theoretical and Applied Mechanics, Cornell University, August 1988.

O'Reilly, O.M., "The Chaotic Vibration of a String," Ph.D. Thesis, Department of Theoretical and Applied Mechanics, Cornell University, August 1990.

Treacy, J.A., "Symmetry and Bifurcation in Frame Structures with Bending Degrees of Freedom," Ph.D. Thesis, Department of Theoretical and Applied Mechanics, Cornell University, in preparation.

URI Reports

Islam, Saiful and Mircea Grigoriu, "Nonlinear Random Vibration of Pin-Jointed Trusses with Imperfections," School of Civil and Environmental Engineering, Cornell University Report, October 1989.

Liao, L.-Z. and C.A. Shoemaker, "The Proof of Quadratic Convergence of Differential Dynamic Programming," Technical Report, No. 917, School of Operations Research and Industrial Engineering, Cornell University, 1990.

Moon, F.C., B. Feeny, "The Measurement of Friction and Chaotic Oscillations: Paper on Paper and Titanium on Titanium," Cornell University Report.

URI Papers

Aubert, B., J. Abel, J. Lu, and J. Thorp, "Effects of Structural Imperfections on Constant-Feedback-Gain Control of a Spatial Structure," Computing Systems in Engineering 1 (1990) 601-606.

Aubert, B. and J. Abel, "Computer Simulation of Control of Nonlinear Structural Dynamics," to appear in the Proceedings of the 3rd Air Force/NASA Symposium on Recent Advances in Multidisciplinary Analysis and Optimization, held September 1990.

Chen, P.-Y., F.C. Moon, "Experimental Vibration Suppression in a Space Truss Using Self-equilibrated Colocated Feedback Control," submitted to AIAA Journal.

Chen, P.-Y., F.C. Moon, "Experiments on Co-located Feedback Vibration Suppression in a Space Frame Using New Magnetic Actuators," Proceedings of the Joint U.S./Japan Conference on Adaptive Structures in Maui, Hawaii, 13-15 November 1990.

Chiang, H.-D., J.S. Thorp, JC. Wang and J. Lu, "Optimal Linear Controller Placements for Large Scale Systems," 1989 American Control Conference, June 1989, pp. 1615-1620.

Chiang, H.-D., J.S. Thorp, J.C. Wang and J. Lu, "Optimal Controller Placements for Large Scale Linear Systems," submitted to IEEE Trans. on Automatic Control for publication.

Cusumano, J.P., F.C. Moon, "Low Dimensional Behavior in Chaotic Nonplanar Motions of a Forced Elastic Rod: Experiment and Theory," IUTAM Symposium on Nonlinear Dynamics in Engineering Systems, Springer-Verlag: Berlin, 1990.

Delchamps, D.F., "Expanding Maps and the Statistical Stabilization of Linear Control Systems With quantized Measurements," Proceedings of the 1989 Conference on Information Sciences and Systems, Baltimore, MD, March 1989, pp. 112-118.

Delchamps, D.F., "Some Chaotic Consequences of Quantization in Digital Filters and Digital Control Systems," Proceedings of the IEEE International Symposium on Circuits and Systems, Portland, OR, May 1989, pp. 602-605.

Delchamps, D.F., "Extracting State Information From a Quantized Output Record," to appear in Systems and Control Letters, 1990.

Delchamps, D.F., "Controlling the Flow of Information in Feedback Systems With Measurement Quantization," to appear in Proceedings of the 28th IEEE Conference on Decision and Control, Tampa, FL, December 1989.

Delchamps, D.F., "Asymptotic Statistical Properties of Linear Systems Operating Under Quantized Feedback," to appear in Proceedings of the Twenty-Seventh Annual Allerton Conference on Communications, Control, and Computing, Urbana, IL, September 1989.

Delchamps, D.F., "Stabilizing a Linear System With Quantized State Feedback," submitted to IEEE Transactions on Automatic Control.

Feeny, B.F., F.C. Moon, "Autocorrelation on Symbol Dynamics for a Chaotic Dry-Friction Oscillator," Phys. Lett. A 141 (1989) 397-400.

Golnaraghi, M.F., F.C. Moon and Richard Rand, "Resonance in a High Speed Flexible-Arm Robot," International J. Dynamics and Stability of Systems 4 (1989) 169-188.

Grigoriu, M., "A New Closure Technique for Solution of Nonlinear Random Vibration Problems," in preparation.

Hajjar, J.F. and J.F. Abel, "On the Accuracy of Some Domain-by-domain Algorithms for Parallel Processing of Transient Structural Dynamics," International Journal for Numerical Methods in Engineering, 28 (1989) 1855-1874.

Hajjar, J.F., and J.F. Abel, "Parallel Processing for Transient Nonlinear Structural Dynamics of Three-Dimensional Framed Structures using Domain Decomposition," Computers and Structures 30 (1988) 1237-1254.

Hajjar, J.F., and J.F. Abel, "Parallel Processing of Central Difference Transient Analysis for Three-Dimensional Nonlinear Frames Structures," Communications in Applied Numerical Methods, 5 (1989) 39-46.

Healey, T.J., J.N. Papadopoulos, "Steady Axial Motions of Strings," J. Appl. Mech., 57 (1990) 785-787.

Healey, T.J., "Stability and Bifurcation of Rotating Nonlinear Elastic Loops," to be published in Quarterly of Appl. Math., XLVIII (1990) 679-698.

Healey, T.J., J.A. Treacy, "Exact Block Diagonalization of Large Eigenvalue Problems for Structures with Symmetry," 31 (1991) 265-285.

Islam, S. and M. Grigoriu, "Nonlinear Random Vibration of Pin-Jointed Trusses with Imperfections," in preparation.

Lee, C.-K., F.C. Moon, "Laminated Piezopolymer Plates for Torsion and Bending Sensors and Actuators," J. Acoust. Soc. Am. 85 (1989) 2432.

Li, G.X., F.C. Moon, "Criteria for Chaos of a Three-Well Potential Oscillator with Homoclinic and Heteroclinic Orbits," J. Sound and Vibration 136 (1990) 17-34.

Liao, L.-Z. and C.A. Shoemaker, "Convergence in Unconstrained Discrete-time Differential Dynamic Programming," IEEE Trans. Automat. Contr. (in press).

Liao, L.-Z. and C.A. Shoemaker, "Partitioning and QR Factorization to Avoid Numerical Ill-conditioning of Penalty Functions for Constrained Nonlinear Programming and Control," Proceedings of the 29th IEEE Conference on Decision and Control, Honolulu, HI Dec. 5-7, 1990.

Liao, L.-Z. and C.A. Shoemaker, "QR Penalty Function Method to Avoid Numerical Ill-conditioning in Constrained Nonlinear Programming and Control," submitted to SIAM Journal on Optimization.

Lu, J., H.-D. Chiang and J.S. Thorp, "Partial Eigenstructure Assignment and its Application to Model Control of Large Space Structures," submitted to IEEE Trans. on Automatic Control for publication.

Lu, J., J. Thorp, B. Aubert, and L. Larson, "Optimal Tendon Placement of Tendon Control Systems for Large Flexible Space Structures," Journal of Guidance, Control and Dynamics, submitted for publication.

Lu, J., J.S. Thorp, H.D. Chiang, "Design of Linear Multifunctional Observers with Unfixed Feedback Gain," Proceedings of the 1989 Conference on Information Sciences and Systems, Baltimore, MD, March 1989.

Moon, F.C., "Spacial and Temporal Chaos in Elastic Continua," IUTAM Symposium on Nonlinear Dynamics in Engineering Systems, Springer-Verlag: Berlin, 1990.

Moon, F.C., "Chaotic Dynamics in Solid Mechanics," Dynamical Systems Approaches to Nonlinear Problems in Systems and Circuits, ed. Fathi M.A. Salam and Mark L. Levi, SIAM, 1988.

Moon, F.C., T. Broschart, "Chaotic Sources of Noise in Machine Acoustics," accepted in Ingenieur Archiv.

Moon, F.C., Guangxuan Li, "Experimental Study of Chaotic Vibrations in a Pin-Jointed Space Truss Structure," AIAA Journal 28 (1990) 915-921.

Poddar, B., F.C. Moon, S. Mukherjee, "Chaotic Motion of an Elastic-Plastic Beam," J. Appl. Mech. 55 (1988) 185-189.

Pratap, R., S. Mukherjee, "Vibration of an Arch Under Axial Loading," submitted to J. Sound & Vibra.

Shoemaker, C.A., L.-Z. Liao, B. Aubert and J.F. Abel, "Optimal Control of Nonlinear Structures Described by Finite Element Models," to be submitted to Computers and Structures.

Shoemaker, C.A., L.-Z. Liao, H. Caffey and L.-C. Chang, "Optimal Control of Large Scale Nonlinear Engineering Systems," IBM Supercomputing Competition, 1990 (in press).

Shoemaker, C.A. and L.-Z. Liao, "Large Scale Nonlinear Optimal Control for Finite Element Models of Flexible Structures," Proceedings of the Third Annual Air Force/NASA Symposium on Multidisciplinary Analysis and Optimization, San Francisco, CA., Sept. 24-26, 1990.

Shoemaker, C.A., L.-Z. Liao, B.H. Aubert and J.F. Abel, "Optimal Nonlinear Control with Geometrically Nonlinear Finite Element Analysis for Flexible Structures: Some Preliminary Results," Computational Mechanics '88, S.N. Atluri and G. Yagawa (eds.), Springer-Verlag, 1988, pp. 64.i.1-4.

Shoemaker, C.A., L.-Z. Liao, J.F. Abel and B. Aubert, "Large Scale Nonlinear Numerical Optimal Control for Finite Element Models of Flexible Structures," in preparation.

URI Conference Presentations/Lectures/Seminars

J.F. Abel, "The Cornell 10-meter Truss: Simulation, Control Placement, and Initial Testing," 8th AFOSR Forum on Space Structures, Melbourne, FL, June 1990.

J.F. Abel, "Computer Simulation of Control of Nonlinear Structural Dynamics," 3rd AF/NASA Symposium on Recent Advances in Multidisciplinary Analysis and Optimization, San Francisco, CA, September 1990.

J.F. Abel, "Effects of Structural Imperfections on Constant-Feedback Gain Control of a Spatial Structure," Symposium on Computational Technology for Flight Vehicles, Arlington, VA, November 1990.

D.F. Delchamps, "Information and Uncertainty in Feedback Systems With Measurement Quantization," presented at the SIAM Conference on Control in the 90's, San Francisco, CA, May 1989.

D.F. Delchamps, "Stabilization and Pole Assignment for Linear Systems Using Quantized Measurements," presented at the 1989 Conference on the Mathematical Theory of Networks and Systems (MTNS-89), Amsterdam, The Netherlands, June 1989.

D.F. Delchamps, The Pseudorandom Asymptotic Behavior of Digitally Controlled Analog Systems," presented at the 28th IEEE Conference on Decision and Control, Tampa, FL, December 1989.

B. Feeny, "Nonlinear Dynamics and Chaos in Space Structures," 8th AFOSR Forum on Space Structures, Melbourne, FL, June 1990.

M. Grigoriu, "Probabilistic Analysis of Response of Duffing Oscillators to Narrow Band Stationary Gaussian Excitations," Proceedings, I Pan American Congress of Applied Mechanics (PACAM), Rio de Janeiro, Brazil, January 1989, pp. 652-655.

M. Grigoriu, "Reliability of Degrading Dynamic Systems," Proceedings, Euromech 250: Nonlinear Systems Under Random Conditions, Como, Italy, June 1989.

C.A. Shoemaker, "Partitioning and QR Factorization to Avoid Numerical Ill-Conditioning of Penalty Functions for Constrained Nonlinear Programming and Control," 29th IEEE Conference on Decision and Control, Honolulu, HI, December 1990.

C.A. Shoemaker, "Optimal Nonlinear Control with Geometrically Nonlinear Finite Element Analysis: Some Preliminary Results," International Conference on Computational Mechanics, Atlanta, GA, March 1988.

C.A. Shoemaker, "Large Scale Nonlinear Numerical Optimal Control for Finite Element Models of Flexible Structures," 3rd AF/NASA Symposium on Recent Advances in Multidisciplinary Analysis and Optimization, San Franciso, CA, September 1990.

URI Invited Lectures and Seminars

Francis C. Moon

1990

20 March	Symposium on Applications of Nonlinear Studies	Ann Arbor, MI	"Nonlinear Dynamics"
9 July	CISM Conference	Udiné, Italy	"Chaotic Dynamics"
5 August	Soviet-American Conference/ Workshop on Chaos	Tarusa, USSR	"Chaos"
8 October	Workshop on Enginering Applications of Chaos Theory	Argonne, IL	"Chaotic Dynamics"
13 November	Joint US/Japan Conference	Maui, HI	"Adaptive Structures"

1989

8 May	7th VPI&SU Symposium on Dynamics and Control of Large Space Structures	Blacksburg, VA	"Nonlinear Dynamics"
22 May	United Technologies Research Cntr	East Hartford, CT	"Chaotic Dynamics"
10 July	3rd Joint ASCE/ASME Mechanics Conference	La Jolla, CA	"Chaotic Dynamics"
21 August	Symposium on Nonlinear Dynamics in Engineering Systems	Stuttgart, FRG	"Nonlinear Dynamics"
1 November	Duke University	Durham, NC	"Chaos"
17 November	The Catholic University of America	Washington, DC	"Chaos"
25 November	250th Anniversary of the Royal Academy of Sciences	Stockholm, Sweden	"Chaos"

1988

14 February	AAAS Meeting	Boston, MA	"Chaotic Dynamics"
1988 Midwest	Mechanics Conference Tour		
22 March	Notre Dame University	Notre Dame, IN	"Chaotic Dynamics"
23 March	Illinois Institute of Technology	Chicago, IL	"Chaotic Dynamics"
24 March	University of Illinois	Urbana, IL	"Chaotic Dynamics"
25 March	Purdue University	West Lafayette, IN	"Chaotic Dynamics"
11 April	University of Michigan	Ann Arbor, MI	"Chaotic Dynamics"
12 April	Michigan State University	East Lansing, MI	"Chaotic Dynamics"
14 April	University of Wisconsin	Madison, WI	"Chaotic Dynamics"
15 April	University of Minnesota	Minneapolis, MN	"Chaotic Dynamics"
28 April	National Research Council	Washington, DC	"Chaotic Dynamics"

21 August	IUTAM - International Congress	Grenoble France	"Chaotic Dynamics"
19 October	Technische Universität	Wien	"Chaotic Dynamics"
1 November	Technische Hochschule Darmstadt	Darmstadt	"Chaotic Dynamics"
6 December	Technische Universität Karlsruhe	Karlsruhe	"Chaotic Dynamics"
8 December	Technische Universität München	München	"Chaotic Dynamics"
21 December	Swiss Federal Institue of Technology ETH-Zurich	Zurich	"Chaotic Dynamics" and "Superconducting Bearings"

1987

February	Air Force Wright Aeronautical Lab	Dayton, Ohio
May	University of Akron	Akron, OH
	University of Maryland	College Park, MD
	Johns Hopkins Physics Laboratory	Baltimore, MD
June	University of Montreal	Montreal, Canada
August	AFOSR, Bolling Air Force Base	Washington, D.C.

James S. Thorp

1988

June	Constructive Algorithm to Estimate Stability Region of Nonlinear Dynamical Systems	Espoo, Finland
November	Optimal control locations	Cambridge U. England

1989

March	Estimations of Stability Domains and Optimal Actuator Locations	VPI&SU, Blacksburg, VA

Project Title:
Low Dimensional Behavior in Chaotic Nonplanar Motions of a Forced Elastic Rod: Experiment and Theory

Faculty Leader:
Professor Francis C. Moon
Department of Mechanical & Aerospace Engineering

Graduate Research Assistant:
J.P. Cusumano
Theoretical and Applied Mechanics

Now at:
Department of Engineering Science & Mechanics
The Pennsylvania State University
University Park, PA 16802

Project Summary:

The results of an experimental and theoretical investigation of the dynamics of a thin elastic rod are presented. Regular, planar motions of the rod are observed to become unstable in wedge-shaped regions of the forcing frequency- forcing amplitude parameter plane. Inside of these wedges, motions are nonplanar and generally chaotic. Fractal dimension calculations from experimental data indicate that the dynamics of the rod may be modelled by between two and six degrees of freedom. A family of asymmetric bending-torsion nonlinear modes are discovered experimentally, and their frequency-amplitude characteristic is obtained. A two degree-of-freedom system is derived by starting with a geometrically exact linearly elastic rod theory and projecting onto the first bending and torsional modes. Numerical simulations indicate that this two-mode model exhibits much of the behavior observed experimentally.

Introduction

In this paper, the results of an experimental and theoretical study of the dynamics of a thin, cantilevered elastic rod are presented. A more detailed discussion, along with a complete bibliography, can be found in Cusumano [1], as well as in a forthcoming paper by the authors.

The study of elastic rods is an old one. In fact, we will often refer to the elastic rod under consideration as "the elastica" in reference to the name given the static problem by Euler. While the study of the dynamics of the elastica has a long history, the majority of

work done has dealt with small, linear vibrations. Space does not permit a complete review of the literature here, but a bibliography of works involving the nonlinear vibrations of beams can be found in the survey paper by Sathyamoorthy [2]. Of particular relevance to this study is the work of Crespo da Silva and Glynn [3,4], who used perturbation methods to show that planar motions of a fixed-free beam can lose stability. However, they neglected torsional inertia and assumed nearly equal bending rigidities, which is not the case here.

Experimental Observations

The elastica was clamped at the support end and oriented so that its undeformed neutral axis was vertical (see Fig. 1). The specimen studied was made of carbon steel. with overall dimensions of $28.8cm \times 1.27cm \times .21mm$. The support of the rod was harmonically displaced by means of an electro-mechanical shaker. The axis of displacement was aligned with the lateral axis of symmetry of the rod so that one would expect motions to remain in the x-y plane. Indeed, stable motions are observed in which the response of the rod is planar and regular (i.e. either periodic or quasiperiodic). However experiments showed that the planar motions become unstable in certain regions of the forcing frequency, forcing amplitude plane. The stability diagram of Fig. 2 shows a series of wedge-shaped regimes, each with its apex at a resonance of the system. In the diagram. the f_i, with $i = 2, 3, 4, 5$, are the second through the 5th in-plane bending natural frequencies. and f_τ is the first torsional natural frequency. Resonances occur at all in-plane natural frequencies. Combination resonances are present at frequencies equal to $f_2 + f_3$ and $f_\tau - f_1$. Another resonance at $f^* \cong 92$Hz is not readily identifiable as a combination resonance.

Inside of the regions of planar instability, motions were. in general. chaotic (the response was characterized by a broad-band. continuous power spectrum). Chaotic. nonplanar motions of the thin elastica exhibit dynamic two-well behavior: during excursions out of the x-y plane. the rod stays trapped away from the x-z plane. It should not be inferred that chaotic responses exist at all points inside of the nonplanar regions: in one instance. an asymmetric. period-two response was discovered.

A previously unobserved family of asymmetric bending-torsion nonlinear modes (periodic

motions in the conservative system which do not pass through the equilibrium configuration of the rod) were found. These solutions pass back and forth through the x-y plane while the rod stays bent away from the x-z plane. The weak damping in the system allowed the frequency-amplitude characteristic for the nonlinear modes to be obtained by estimating the instantaneous frequency of a transient torsional strain signal and plotting the result against the estimated instantaneous torsional strain amplitude (see Fig. 3). The result shows that the frequency of vibration of the nonlinear modes is a decreasing function of their amplitudes. Spectral analysis results taken just after the loss of planar stability near all resonances are qualitatively similar in shape, and an "energy cascading" phenomenon is apparent: most of the power in chaotic tip displacement signals (obtained using an optical edge tracking system) lies well below the driving frequencies, lying instead in low frequency first bending and nonlinear bending-torsion modes.

Fractal Dimension Calculations

The fractal dimensions of attracting sets in different resonant wedges were estimated directly from experimentally-obtained time series using a numerical code based on the correlation dimension method of Grassberger and Proccacia [5]. A key element of the algorithm is the reconstruction of the actual phase-space trajectories from scalar data by means of the delay-embedding procedure. An introduction to fractal dimensions. and to other ideas from dynamical systems theory, along with an extensive bibliography, can be found in [6]. The fractal dimension for a given attractor is estimated by plotting the correlation dimension d_c versus the embedding dimension m used in the delay-embedding procedure (m can be thought of as a guess at the phase space dimension needed to model the observed dynamics). For a deterministic signal. d_c will level out at some critical value of m. For random noise. d_c will continue to grow: in the limit of an infinite number of data points $d_c(m) = m$ for random noise. The resulting dimension estimates for the thin elastica. with one exception, were below 5, which implies from dimension theory that it should be possible to model the dynamics of the rod with between two and six degrees of freedom (see Fig. 4).

Derivation and Analysis of a Two-mode Model

By starting with the classical three-dimensional rod theory due to Love [7] a geometrically

14

exact theory for the experimental system can be developed. Physical scaling arguments show that an additional curvature constraint is needed: the curvature component corresponding to bending in the stiff cross-sectional direction is zero. If in addition it is assumed that the torsion of the rod varies slowly along its length, it can be shown that a Lagrangian density in a generalized bending variable U and a generalized torsional variable ϕ is given to second order in U by:

$$\ell = \frac{1}{2}\dot{d}^2 + \dot{d}\dot{U}\cos\phi - \dot{d}U\sin\phi\dot{\phi} + \frac{1}{2}\dot{U}^2 + \frac{1}{2}(\mu + U^2)\dot{\phi}^2 - \frac{1}{1+\nu}(\phi')^2 + \frac{1}{2}(U'')^2 \quad (1)$$

where $d \equiv D\cos\Omega t$, $(\dot{\ }) = \frac{\partial}{\partial t}$, and $()' = \frac{\partial}{\partial x}$. Then, application of Hamilton's principle leads to the set of partial differential equations:

$$\ddot{U} + U'''' - U\dot{\phi}^2 = D\Omega^2\cos(\Omega t)\cos\phi \quad (2)$$

and

$$(\mu + U^2)\ddot{\phi} - \frac{2}{1+\nu}\phi'' + 2U\dot{U}\dot{\phi} = D\Omega^2 U\cos(\Omega t)\sin\phi, \quad (3)$$

with boundary conditions $U(0,t) = U'(0,t) = U''(\bar{l},t) = U'''(\bar{l},t) = 0$ and $\phi(0,t) = \phi'(\bar{l},t) = 0$ (in the preceding, $\bar{l}$ is the dimensionless rod length). We remark that the unforced, linearized versions of equations (2) and (3) correspond to the Bernoulli-Euler beam equation, and the equation for torsional waves on a rod, respectively. Nonlinear coupling in the system comes from coriolis and centripetal acceleration terms, as well as a nonlinear inertia term in equation (3). Observe also that the condition $\dot{\phi} = 0$, which corresponds to planar motions, defines an invariant manifold for the nonlinear system.

By means of the assumed-modes method, the above partial differential equations can be used to obtain a two-mode model system using the first bending and the first torsional mode of the system. The resulting model system can be put into the following form after the addition of linear modal damping terms:

$$\ddot{q}_1 + \Delta_1\dot{q}_1 + q_1 - \gamma q_1\dot{q}_2^2 = \alpha D\Omega^2\cos\Omega t + \beta q_2\dot{q}_2 D\Omega\sin\Omega t \quad (4)$$

and

$$(\mu + \gamma q_1^2)\ddot{q}_2 + \mu\Delta_2\dot{q}_2 + \mu\omega^2 q_2 + 2\gamma q_1\dot{q}_1\dot{q}_2 = -\beta q_2\frac{d}{dt}(q_1 D\Omega\sin\Omega t), \quad (5)$$

where q_1 and q_2 are, respectively, the bending and torsional modal amplitudes.

The dynamics of the two-mode model represented by equations (4) and (5) were studied numerically. A family of nonlinear modes analogous to those observed experimentally were found, and the computed frequency-amplitude characteristic of the family is qualitatively similar to that found for the rod (Fig. 5). A wedge of planar instability was found for the model inside of which the motions were chaotic and nonplanar (Fig. 6).

Conclusion

The behavior of a two-mode model captures much of the observed dynamics of the thin elastica studied experimentally. Thus, it appears that the precise mechanism of the planar instability observed in the thin elastica can be elucidated by studying a much simpler system. Future work will focus on the nature of modal coupling in the model system of partial differential equations (2) and (3), with the goal of understanding the energy cascading phenomenon observed in the experiments.

References

1. Cusumano, J.P.: Low-Dimensional Behavior in Chaotic Nonplanar Motions of a Forced Linearly Elastic Rod: Experiment and Theory. Ph. D. Thesis, Department of Theoretical and Applied Mechanics, Cornell University: 1989.

2. Sathyamoorthy, M: Nonlinear Analysis of Beams. Part I: Survey of Recent Advances. Shock and Vibration Digest, 14 (1982) 19-35.

3. Crespo da Silva, M.R.M. and Glynn, C.C.: Nonlinear Flexural Torsional Dynamics of Inextensional Beams. I: Equations of Motion. Journal of Structural Mechanics. 6 (1978) 437-448.

4. Crespo da Silva, M.R.M. and Glynn, C.C.: Nonlinear Flexural Torsional Dynamics of Inextensional Beams. II: Forced Motion. Journal of Structural Mechanics. 6 (1978) 449-461.

5. Grassberger, P. and Proccacia, I.: Characterization of Strange Attractors. Physical Review Letters, 50 (1983) 346-349.

6. Moon. F.C.: Chaotic Vibrations: An Introduction for Applied Scientists and Engineers. New York: Wiley 1987.

7. Love. A.E.H.: A Treatise on the Mathematical Theory of Elasticity, 4th edition. New York: Dover 1944.
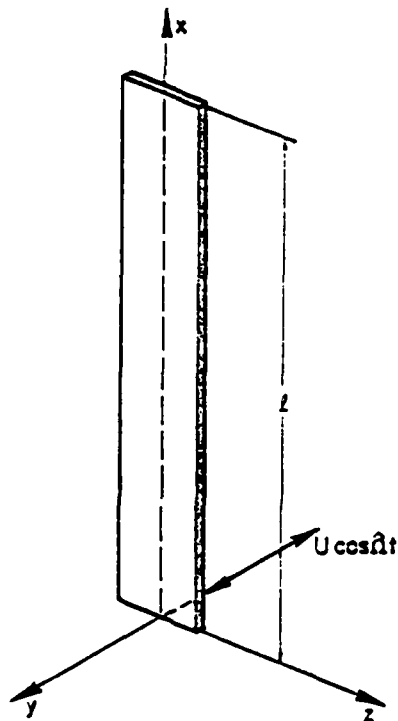
Figure 1: Geometry of the elastica system.
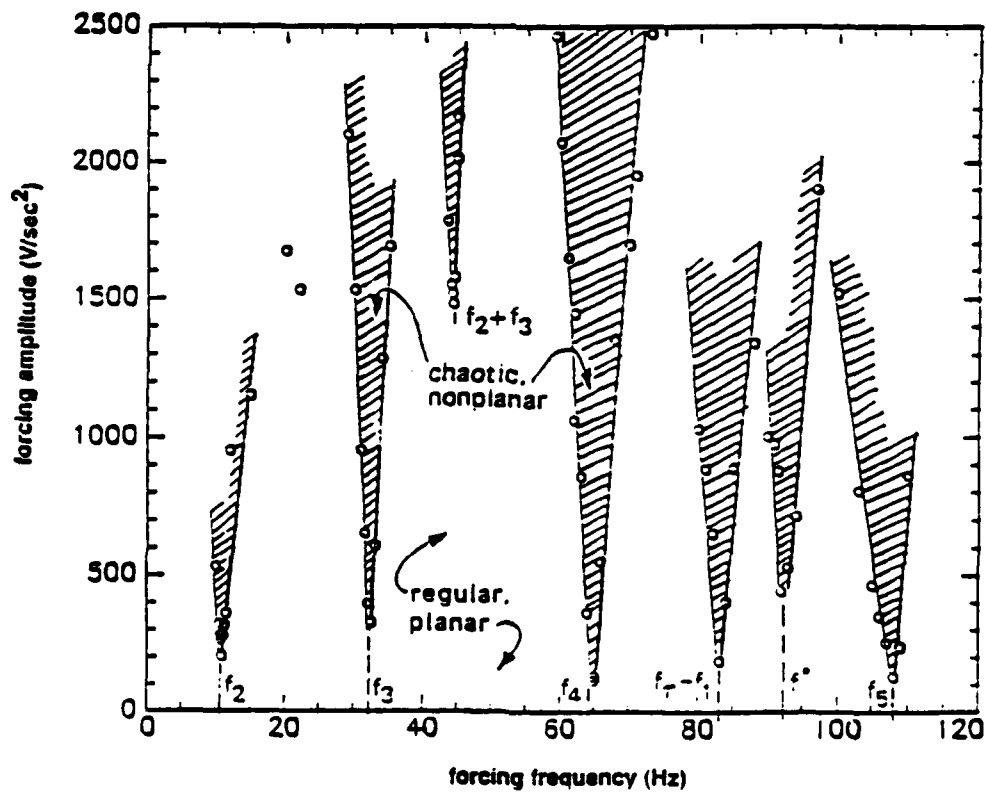
Figure 2: Stability boundaries for the elastica obtained by holding the forcing frequency fixed and increasing the forcing amplitude until planar motions lost stability.

17
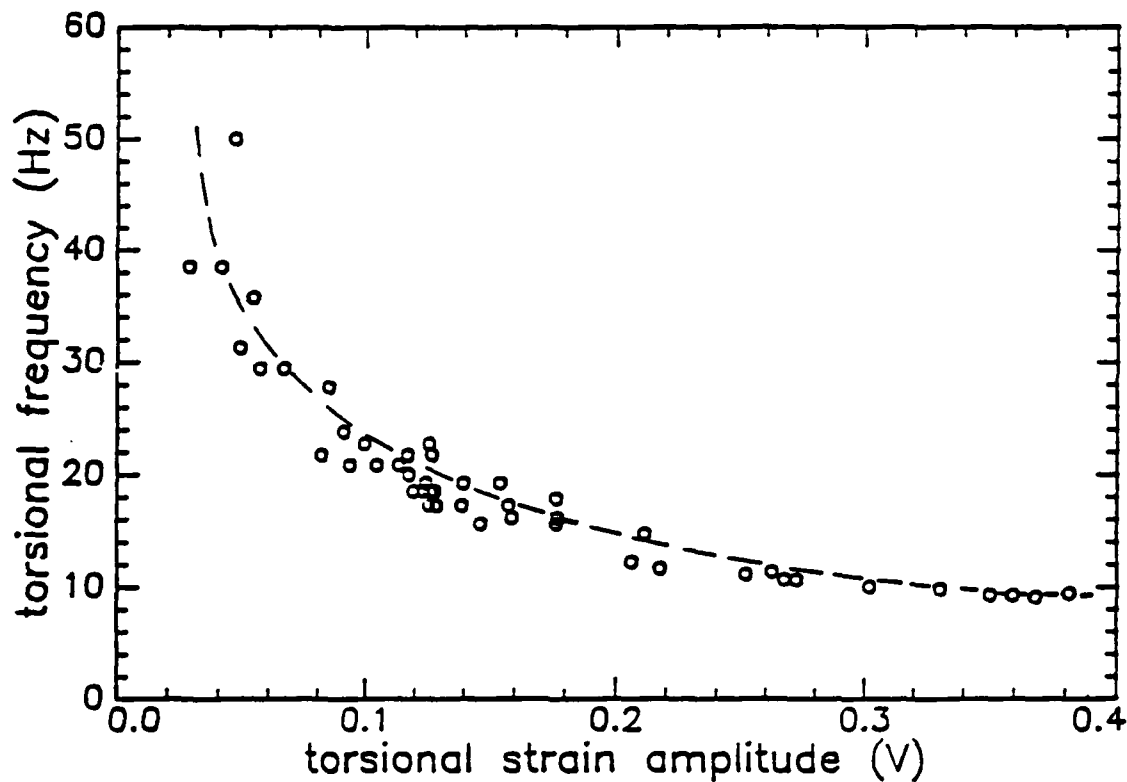
Figure 3: Experimental frequency-amplitude characterisitic for the family of nonlinear modes.
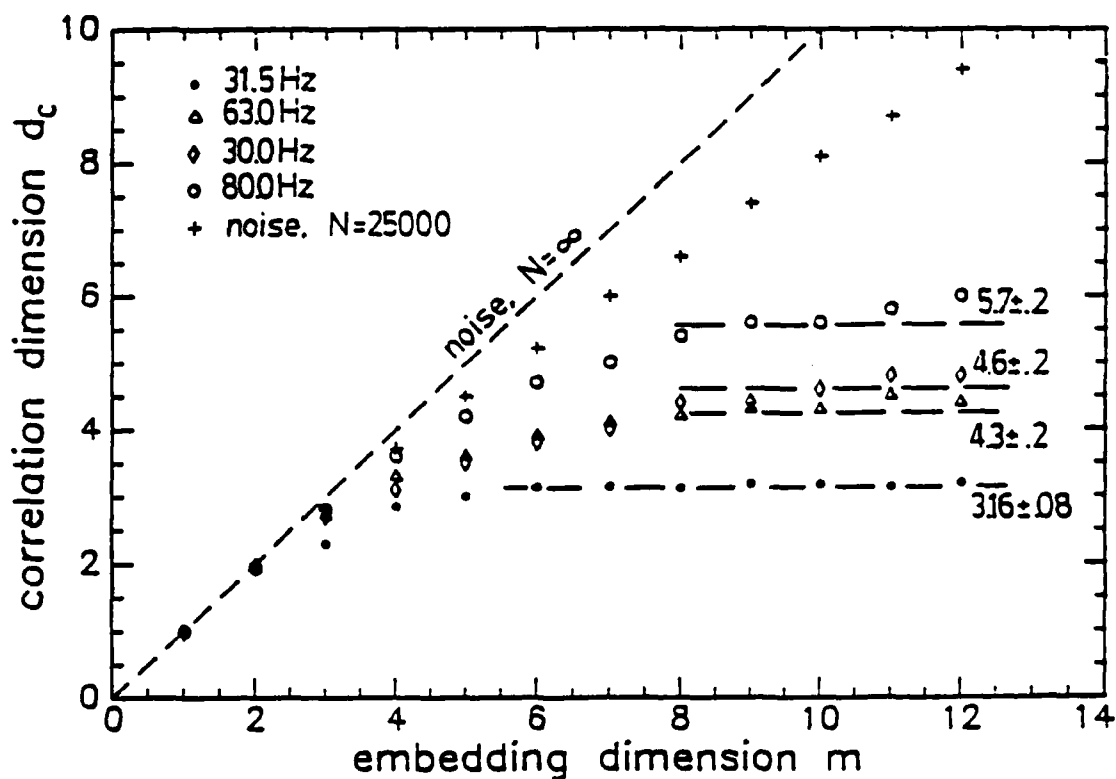
Figure 4: Summary of experimental fractal dimension results.
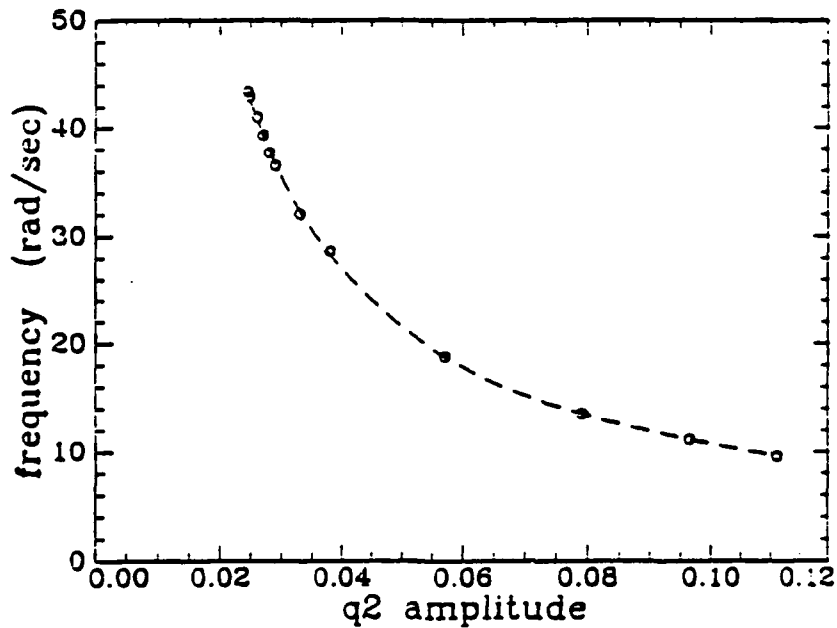
Figure 5: Frequency-amplitude characteristic for the nonlinear modes in the 2 mode model.
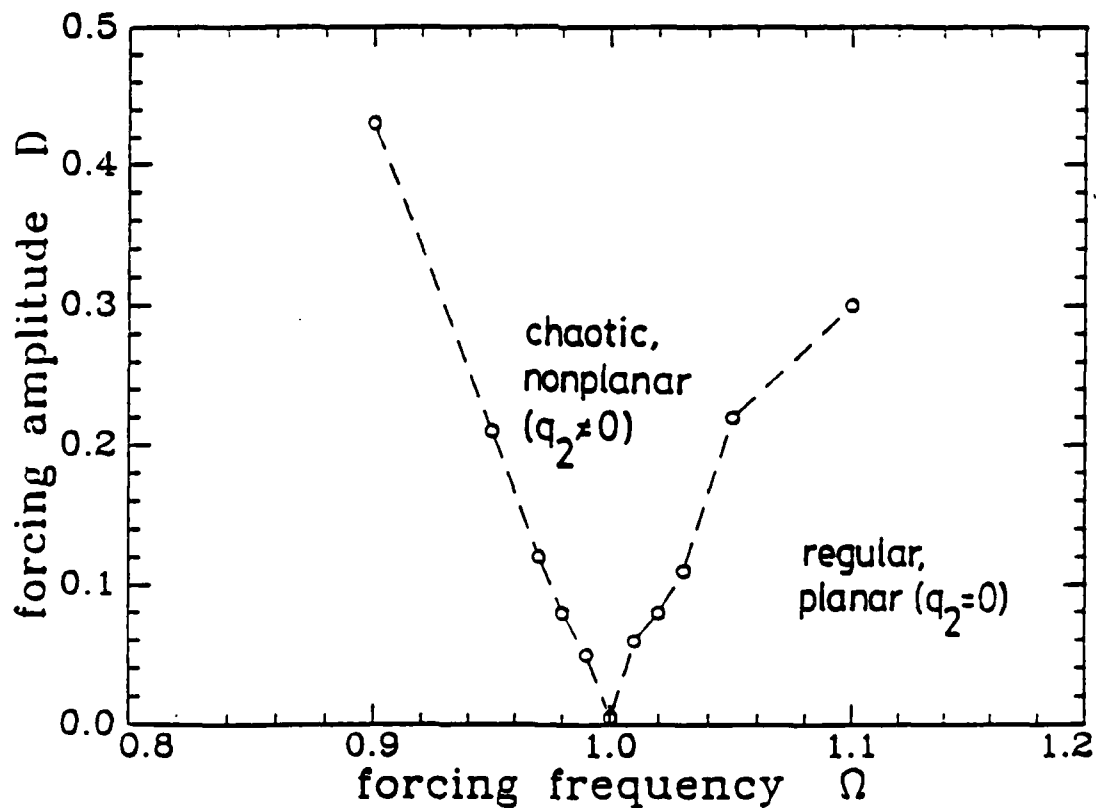
Figure 6: Stability diagram for the 2 mode model.

Project Title:
Autocorrelation on Symbol Dynamics for a Chaotic Dry-Friction Oscillator

Faculty Leader:
Professor Francis C. Moon
Mechanical and Aerospace Engineering

Graduate Research Assistant:
Brian F. Feeny
Theoretical and Applied Mechanics

Now at:
Institut für Robotik
ETH Zürich
Rämistrasse 101
8092 Zürich
Switzerland

Executive Summary:

An autocorrelation function based on symbol dynamics is applied to a chaotic dry-friction oscillator to estimate the largest Lyapunov exponent. The friction problem is well suited for symbol dynamics since two distinct states of motion can be identified: sticking and slipping. In addition, the dynamics of the oscillator can be reduced to a non-invertible one-dimensional map, which has been studied in terms of binary symbol sequences. The study is done for an experimental oscillator and for a numerical model. The numerical result is compared to the Lyapunov exponent estimated from the continuous flow.

Introduction

Experimentalists often wish to quantitatively characterize chaotic motion by calculating the Lyapunov spectrum. However, it is computationally difficult to estimate Lyapunov exponents directly from time series data, especially in the presence of experimental noise. Singh and Joseph [1] proposed the use of symbol dynamics to obtain an autocorrelation and an estimate of the largest Lyapunov exponent. Thus, a binary sequence of yes-no information can be used to quantitively characterize the dynamics. In this paper we report the successful use of this technique on the chaotic dynamics of a dry-friction oscillator.

The modeling of friction in dynamical systems has a long history which goes back to the ancient egyptians. In 1931, Den Hartog [2] solved the equations of a harmonic oscillator with Coulomb friction for periodic motion. Shaw [3] has used modern techniques to extend those results to include a stability analysis, and found period-two motion and beating phenomena. Grabec [4] modeled friction in cutting tools, and found self-excited chaos in a four-dimensional phase space. In diploma theses under K. Popp, of the University of Hannover, F.R.G., Ahlborn [5] and Jahnke [6] observed quasiperiodicity and chaos in a self-excited continuum and a harmonically driven self-excited friction oscillator.

In this letter, we present results for a one-degree-of-freedom oscillator with dry friction dependent on both displacement and velocity. This can occur, for example, if displacement induces elastic deformation which, in turn, causes changes in the normal load at the friction surface. The nondimensionalized equation of motion is

$$\ddot{x} + 2\zeta\dot{x} + x + n(x)f(\dot{x}) = a\cos(\Omega t), \tag{1}$$

where $f(\dot{x})$ represents the friction coefficient and $n(x)$ represents the normal load. We let

the normal load vary linearly with displacement, and, for physical consistency, we restrict the normal load to be nonnegative, so that $n(x) = 1 + kx$ for $x > -1/k$, and $n(x) = 0$ for $x < -1/k$. Often, the friction is modeled by a Coulomb law, which includes a static coefficient of friction μ_s, and a dynamic coefficient of friction μ_d. If $\mu_s = \mu_d = \mu$, the friction law may be written as

$$f(\dot{x}) = \mu \operatorname{sign}(\dot{x}). \tag{2}$$

One might try to approximate a Coulomb law with a continuous function such as

$$f(\dot{x}) = (\mu_d + (\mu_s - \mu_d) \operatorname{sech}(\beta \dot{x})) \tanh(\alpha \dot{x}). \tag{3}$$

The *tanh* term represents the jump from positive friction to negative friction, and approaches a discontinuity as $\alpha \to \infty$. The *sech* term represents the transition from μ_s to μ_d.

The numerical solution for the continuous case is performed using a standard fifth order Runge-Kutta code with stepsize adjuster. The numerical solution for the discontinuous case (not studied in this note) requires a special algorithm which follows that of ref. [3]. A three-dimensional representation of a numerical solution of the continuous equation of motion is shown in Figure 1. In this plot we can see the stick-slip motion (described in [2] and [3]). The sticking region is plotted with small dots, and the slipping motion is plotted with large dots. Also, on the upper right portion of the portrait, we can see trajectories from the inside of the attractor stretching above the sticking region and folding back onto the outside of the attractor. This stretching and folding is typical of chaotic one-dimensional maps and two-dimensional horseshoe maps. A similarly shaped attractor was found from the experimental dry-friction oscillator described below.

Description of Experiment

The experiment consisted of a mass attached to the end of a cantilevered elastic beam. A diagram is shown in Figure 2. The mass had titanium plates on both sides, providing surfaces for sliding friction. Spring-loaded titanium pads rested against the titanium plates. The titanium plates were not parallel in the direction of sliding, thus a displacement of the mass caused a change in the force on the spring-loaded pads. Hence a change in displacement caused a change in normal load and friction. The elastic beam, mass and pressure pads were fixed to a common frame which was excited harmonically by an elecromagnetic shaker. Strain gages attached to the elastic beam were used to sense the displacement of the mass relative to the oscillating frame.

Discussion of Results

An experimental Poincaré section is shown in Figure 3a. It represents a slice of the three-dimensional phase portrait of Figure 1 parallel to the x-$\dot{x}$ axes, perpendicular to the Ωt axis [7]. The standard autocorrelation of the experimental strain signal is shown in Figure 4. It consists of a rapid decay into a small oscillation, suggesting that the signal is uncorrelated, although the influence of the harmonic driver is present. The autocorrelation of a periodic signal would be periodic, with no component of decay.

Notice that the Poincaré map appears to be confined to a one-dimensional object embedded in two-dimensional phase space. By defining a coordinate s along the Poincaré map as shown in Figure 3a, we can obtain a return map as shown in Figure 3b. The return map (Figure 3b) resembles a tent map. The tent map is well known to be chaotic, and the

23

dynamics of similar maps have been studied in terms of binary symbol sequences[8].

The Poincaré section in Figure 3a is located near the axes labeled in Figure 1. Note that it cuts through the sticking region. The sharp, horizontal part of the Poincaré plot is in the sticking region, and the fuzzy part is in slipping motion. This suggests a natural use of symbol dynamics for the motion, namely sticking or slipping. By considering whether the motion is sticking or slipping at each pass through the Poincaré section, we can construct a binary symbol sequence.

Singh and Joseph [1] have proposed a technique of extracting quantitative information from a binary symbol sequence. First it is necessary to represent the symbol sequence $u(k)$ as a string of 1's and -1's. These values are chosen so that the expected mean of a random sequence of equally likely symbols is zero. As the trajectory passes through the Poincaré section for the kth time, if it is not sticking, we set $u(k) = 1$. If it is sticking, we set $u(k) = -1$. An autocorrelation on such a symbol sequence is defined as

$$r(n) = \frac{1}{N} \sum_{k=1}^{N} u(k+n)u(k), \quad n = 0, 1, 2, \ldots, \qquad N \gg n. \tag{4}$$

If the sequence is chaotic, the autocorrelation should have the property $r(n) \to 0$ as $n \to \infty$.

If the sequence becomes uncorrelated, an estimate of the largest Lyapunov exponent can be obtained using the binary autocorrelation function. The largest Lyapunov exponent can be defined as

$$\lambda = \frac{1}{N} \sum_{i=1}^{N} \log_2 \frac{d(n)}{d_o(n-1)}, \tag{5}$$

where $d_o(n-1)$ is the starting distance between two trajectories, and $d(n)$ is the distance between them after one iteration. Since the binary sequence is uncorrelated, we can estimate $d_o(n-1)$ as the expected value of the distance $\bar{d}_o(n-1)$ between two randomly

24

chosen points in the same symbol region. In our example, we measure the distance using coordinate s on the Poincaré plot. Two points chosen from the sticking region have an expected distance $\bar{d}_o(n-1) = 1/3$. Two points from the nonsticking region also have an expected distance $\bar{d}_o(n-1) = 1/3$. If $u(n-1)$ and $u(n)$ are in the same region, their iterates will either stay in that region, be in different regions, or both be in the other region. One defines[1]

$$\alpha = \log_2 \frac{\bar{d}(n)}{\bar{d}_o(n-1)}, \tag{6}$$

where $\bar{d}(n)$ is the expected distance of two points, each chosen from separate regions. For our problem, $\bar{d}(n) = 1$ and $\alpha = \log_2 3$. Replacing $d_o(n-1)$ and $d(n)$ in (5) with their expected values defines the macroscopic Lyapunov exponent, λ_m, which is rewritten via a derivation in ref. [1] as

$$\lambda = \frac{\alpha}{2}(1 - r(1)^2), \tag{7}$$

Application of equations (4), (6) and (7) to a symbol sequence derived from the tent map yields a rapidly decaying autocorrelation and a Lyapunov exponent $\lambda_t = 0.787516$ for a string of 100000 symbols, and an exponent of $\lambda_t = 0.787705$ for a string of 2048 symbols, compared to its exact value, calculated using log_2, $\lambda_{te} = 1$. Application to the logistic map yields a rapidly decaying autocorrelation and a Lyapunov exponent of $\lambda_l = 0.791578$ for 100000 symbols, and $\lambda_l = 0.791116$ for 2048 symbols, compared to its exact value of $\lambda_{le} = 1$.

The binary autocorrelation function for an experimental sequence of length 2048 was obtained using (4) as shown in Figure 5a. Applying equations (6) and (7), the resulting Lyapunov exponent is $\lambda_{exp} = 0.79055$. Using equations (4), (6) and (7) on numerical

smooth-law data (2048 symbols) yields the autocorrelation in Figure 5b, and a Lyapunov exponent of $\lambda_{s_1} = 0.79219$. The largest Lyapunov exponent of the flow can be estimated numerically[7], and can be related to that of the Poincaré map via $\lambda_{flow} = \frac{\lambda}{T}$, where T is the driving period. This calculation of exponent for the Poincaré map from the equations of motion gave $\lambda_{s_2} = 0.77$.

Conclusions

Binary symbol dynamics were used to describe the stick-slip motion of a dry-friction oscillator. Sticking and slipping motion were used as the states in the binary sequence. It was shown that the dynamics of the dry-friction oscillator is reducible to a one-dimensional map, well suited for symbol dynamics. The proposed method in ref. [1] produced a binary autocorrelation function which was used to estimate the order of magnitude of the largest Lyapunov exponent. This estimate was done for experimental and numerical data. The implication is that for limited information, i.e. a series of 'yes' and 'no' information, quantitative information of the dynamics can be easily obtained.

References

[1] P. Singh and D. D. Joseph, Phys. Lett. A 135 (1989) 247-253.

[2] J. P. Den Hartog, Trans. of the ASME 53 (1930) 107-115.

[3] S. W. Shaw, J. Sound Vibr. 108(2) (1986) 305-325.

[4] I. Grabec, Phys. Lett. A 117(8) (1986) 384-386.

[5] D. Ahlborn, Wechselwirkungen von nichtlinearen Reibkräften mit linearen Kontinua

(Diplomarbeit am Institut für Mechanik B, Universität Hannover, 1987).

[6] M. Jahnke, Nichtlineare Dynamik eines Reibschwingers (Diplomarbeit am Institut für Mechanik B, Universität Hannover, 1987).

[7] F. C. Moon, Chaotic Vibrations (Wiley-Interscience, New York, 1987).

[8] J. Guckenheimer and P. Holmes, Nonlinear Oscillations, Dynamical Systems and Bifurcations of Vector Fields, Applied Mathematical Sciences No. 42 (Springer-Verlag, New York, 1983).

Figure Captions

Figure 1. Three-dimensional phase portrait of the numerical solution using a continuous friction law with parameters $\mu_s = 1$, $\mu_d = 0.7$, $\zeta = 0.015$, $\alpha = 50$, $\beta = 5$, $\Omega = 1.3$, and $a = 1.45$.

Figure 2. Schematic of experiment.

Figure 3. (a) Experimental Poincaré section, (b) Return map of Poincaré section.

Figure 4. Standard autocorrelation function for experimental time series.

Figure 5. Binary autocorrelation function for (a) symbol sequence from experimental data, (b) symbol sequence from numerical simulation.

SLIPPING

STICKING

SLIPPING

SLIPPING
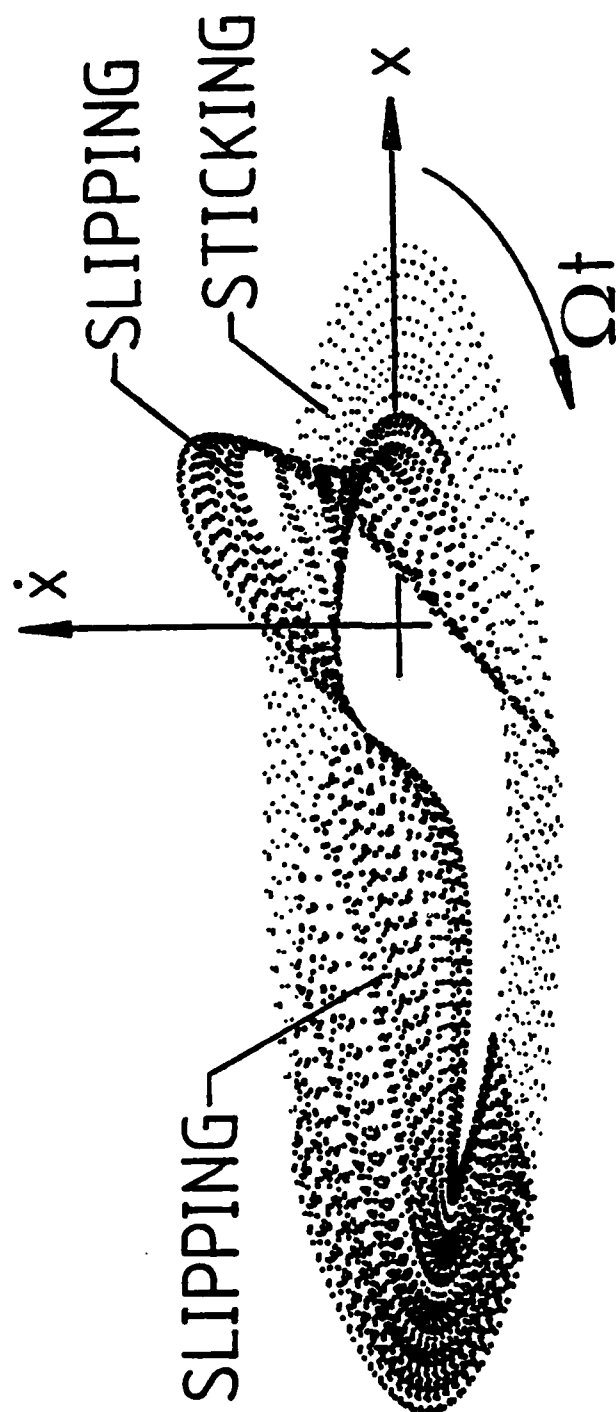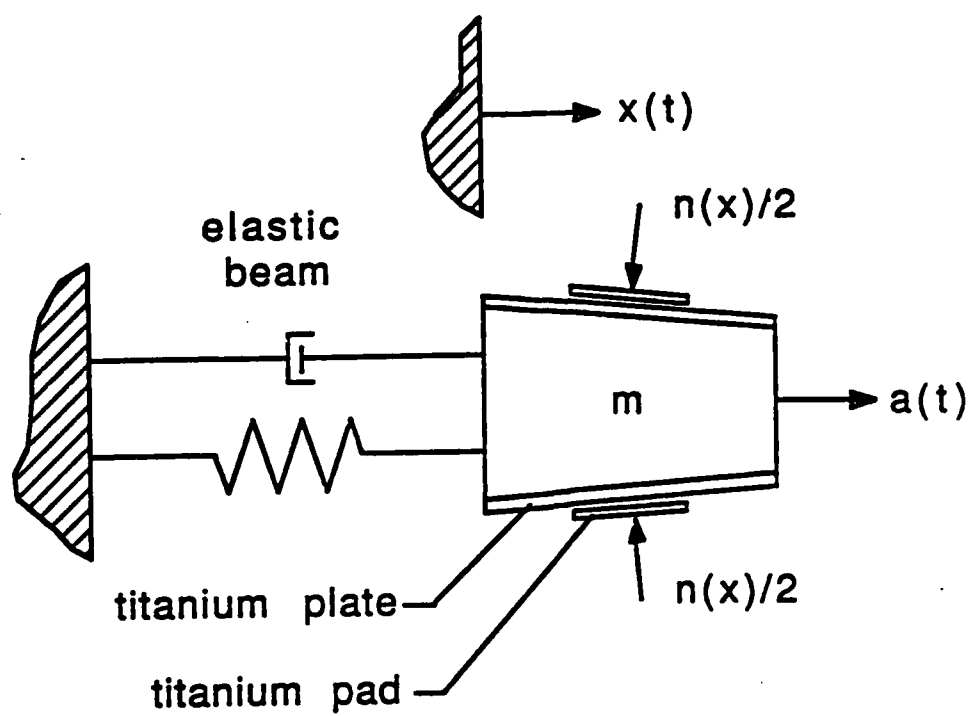
x

$\dot{x}$

Ωt

Figure 1
(Feeny, Moon)

28

elastic beam

x(t)

n(x)/2

m

a(t)

titanium plate
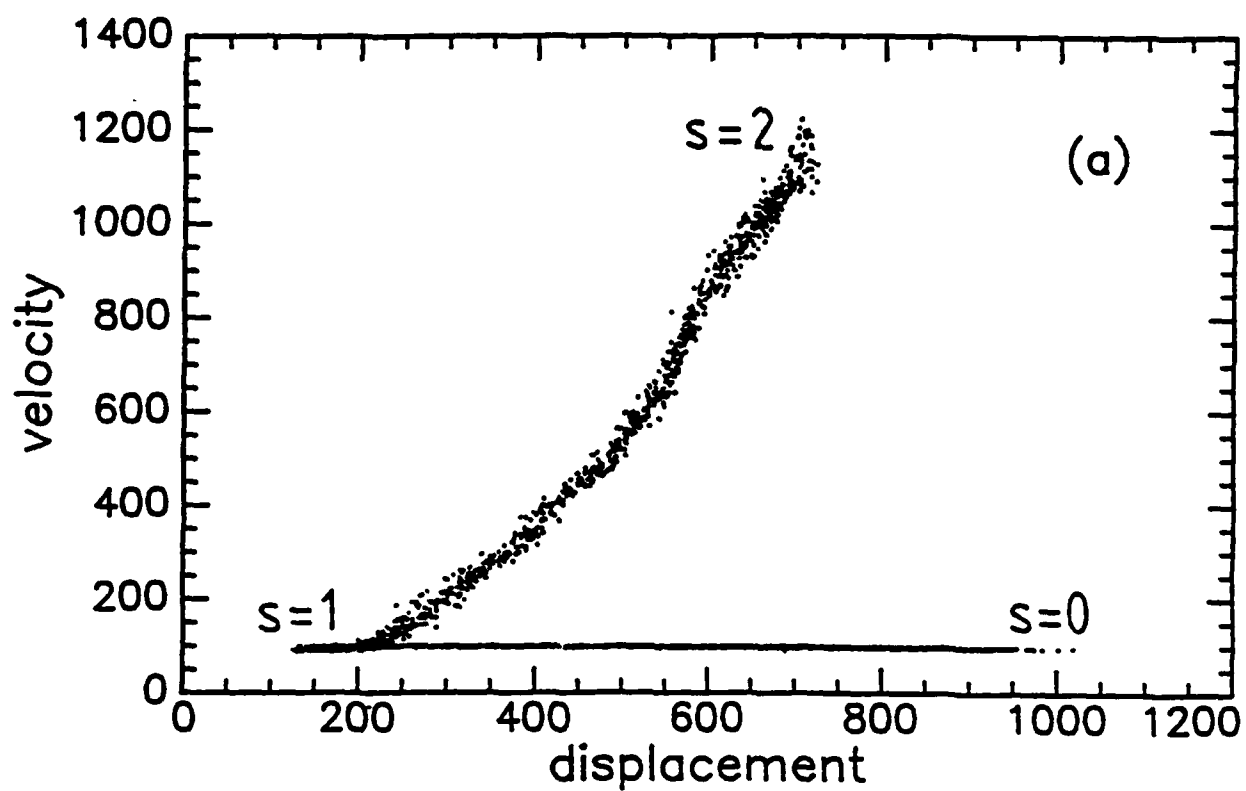
titanium pad
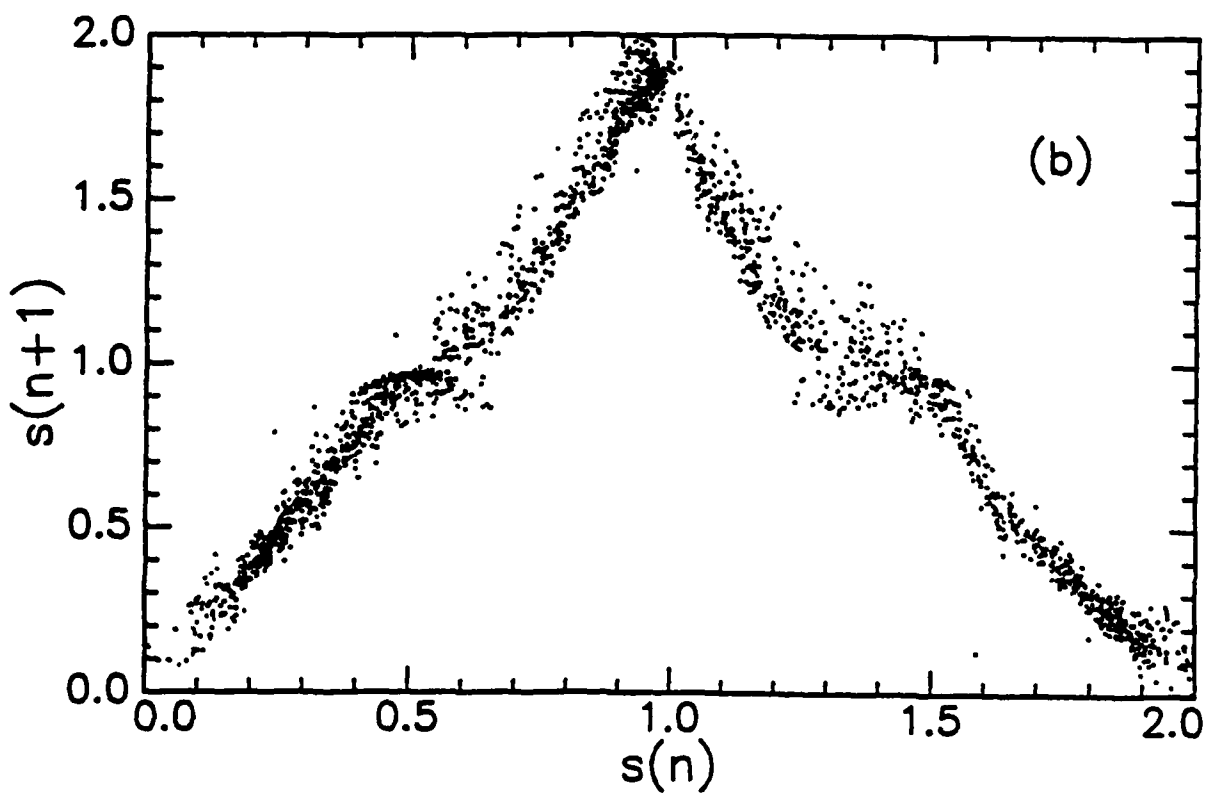
n(x)/2

Figure 2
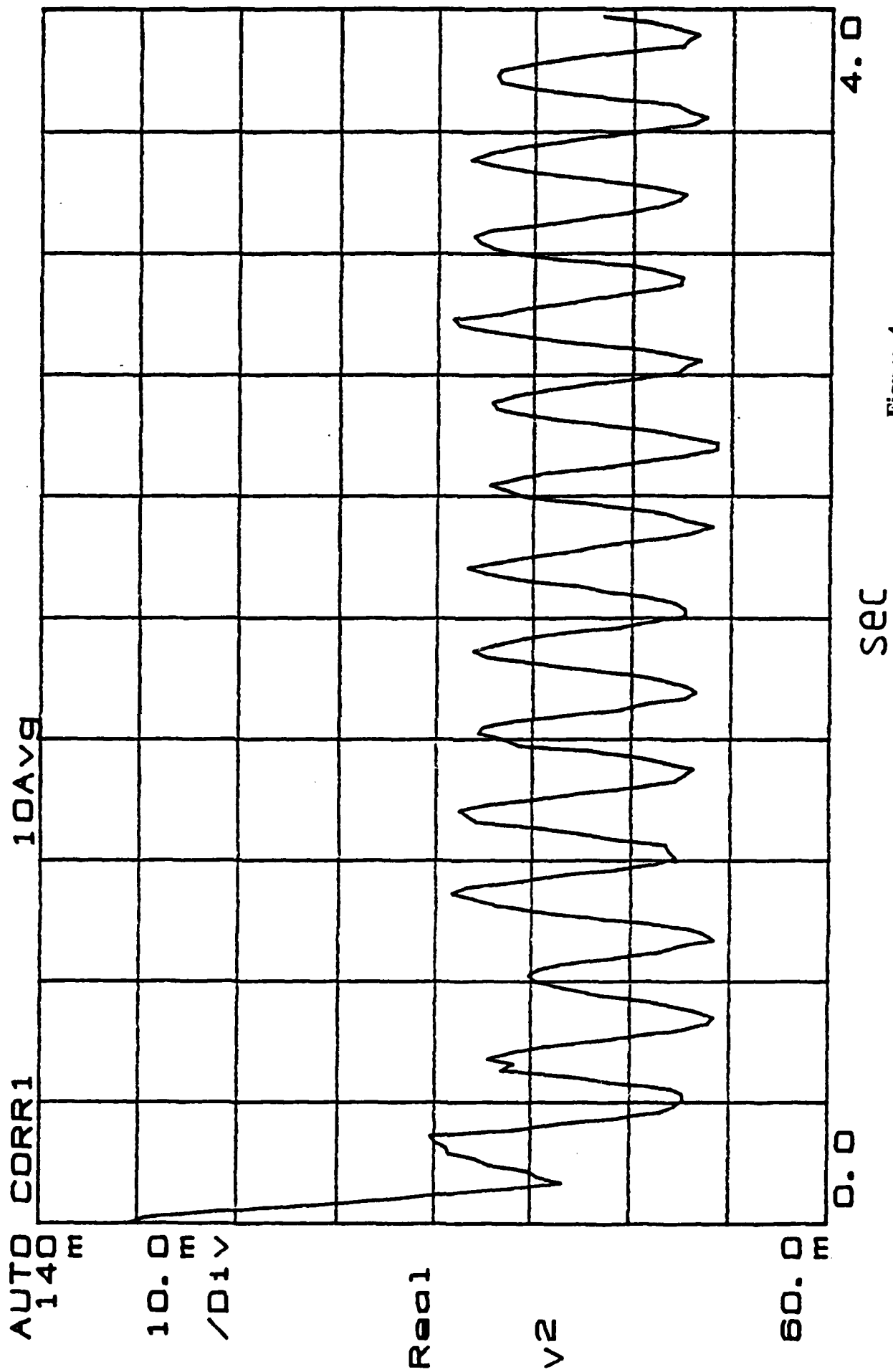**(Feeny,Moon)**

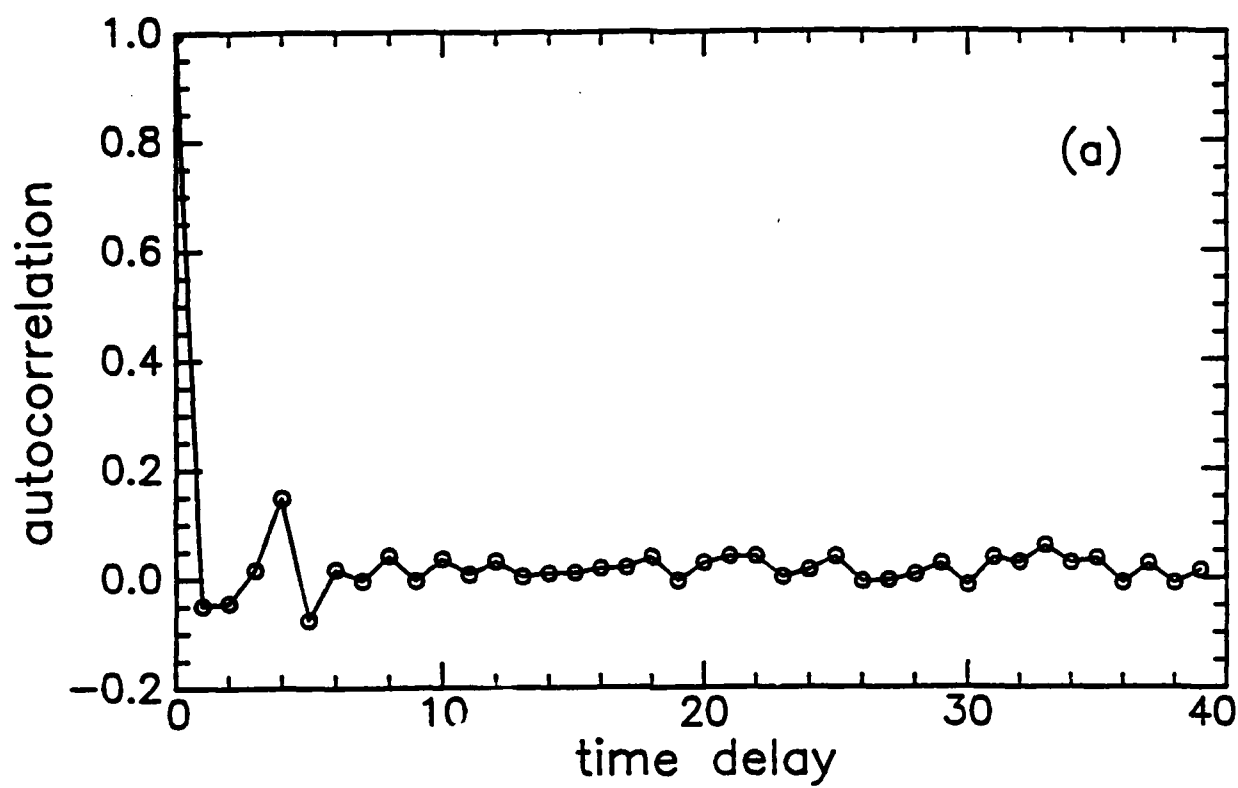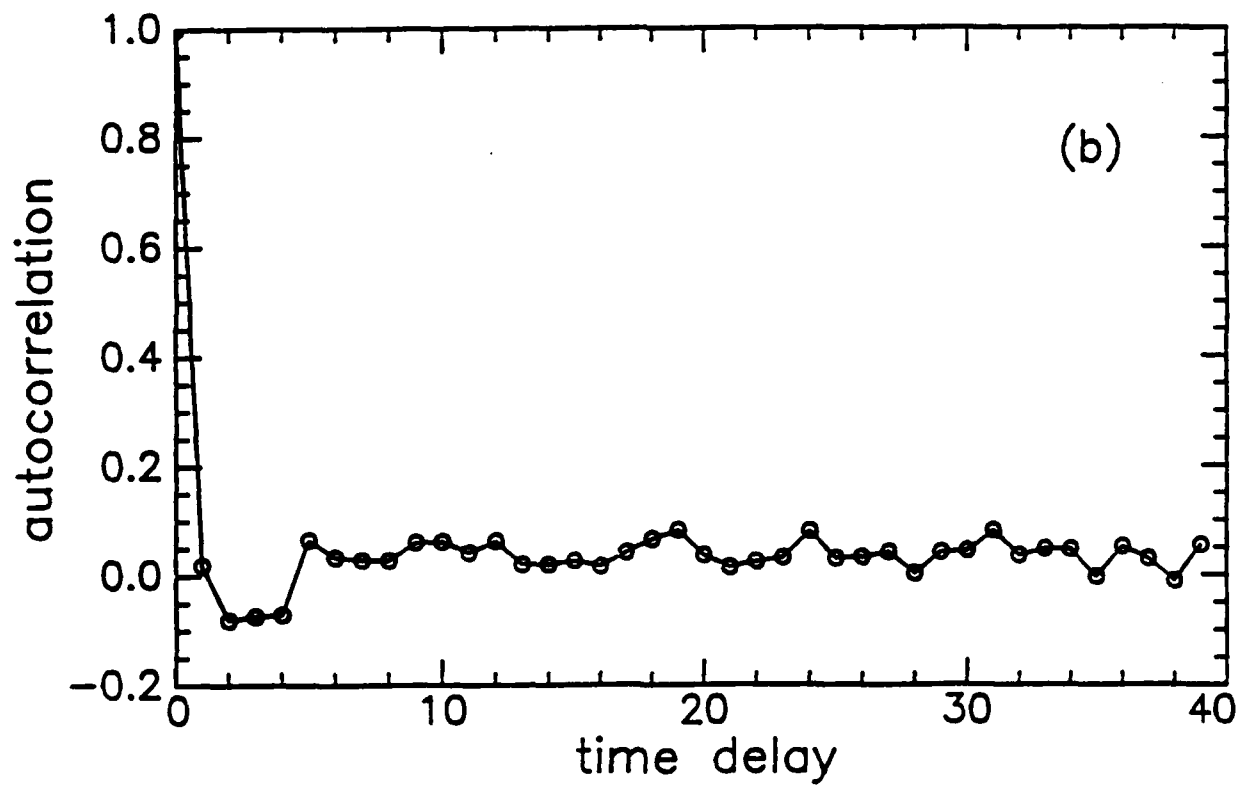**Figure 3**
(Feeny,Moon)

30

Figure 4
(Feeny,Moon)

Figure 5
(Feeny,Moon)

Project Title:
Experimental Study of Chaotic Vibrations in a Pin-Jointed Space Truss Structure

Faculty Leader:
Professor Francis C. Moon
Mechanical and Aerospace Engineering

Graduate Research Assistant:
G.X. Li
Department of Theoretical and Applied Mechanics

Now at:
Department of Mechanical Engineering
McGill University
817 Sherbrooke St. W.
Monreal, P.Q., Canada H3A 2K6

Summary:

In this paper the dynamics of a pin-jointed space truss structure is studied. Experimental results demonstrated that the response of the truss, under sinusoidal excitation, exhibited broad band chaotic-like vibrations. It is believed that very small gaps in the joints create nonlinearities that lead to the chaos. When a tension cable was added to place the structure under compressive loads, the level of chaos was reduced. Numerical simulation of the truss dynamics including small gaps in the truss joints also showed similar chaotic behavior.

Introduction

It was our suspicion that small amounts of play in the joints could lead to chaotic dynamics in the response of the structure under periodic excitation. Chaotic dynamics in actual space structures might make it difficult to design active control system to damp out transient dynamics.

A second goal of this study was to see if internal stresses applied through a tension cable could reduce the pin-related nonlinearities and eliminate the chaotic dynamics.

The results of both studies lead us to believe that pin connected trusses can behave quite chaotically under periodic forcing and that internal compressive loads may partially quench this chaotic behavior under low enough forcing. Numerical simulation for trusses having loose joints was also carried out to verify some of our experimental results.

The Structure

The structure which was tested in our laboratory is a 3.5 meter long 3-D truss with 16 bays, built with aluminum rods. The aluminum rods have a diameter of 0.476 cm (3/16 in), and have yield and ultimate stresses of 324 and 468 x 10^6 N/m^2, respectively. The

Young's modulus is 73.0×10^9 N/m^2 (10.6×10^6psi), and the density is 2.77 gram/cm^3 (0.1 lbs/in^3). The structure is shown in Fig. 1, where the diagonal members on the front side were not drawn for the purpose of clarity. The cross-section of the structure is triangular consisting of three equal-length rods of 22.2 cm (8.75 in). The bay length is also 22.2 cm. All parts of the structure were made of aluminum, and the total mass was approximately 2.3 kg. Hung with rubber bands, the first six natural frequencies of our truss had frequencies from 0.3 to 4.0 Hz, which is relatively small compared with the first experimental bending natural frequency of 44 Hz. Thus we refer to our truss as a free-free structure.

One effect of the nonlinear joints is that the measured natural frequencies were rarely the same in different measurements. In most cases, the first bending frequencies varied in the range of 42 to 45 Hz in experiments.

Chaotic Oscillations of the Structure

The forced dynamic response of the truss was studied by applying a sinusoidal force and measuring the output signals with the use of the accelerometer. The accelerometer was mounted close to a joint at one of the two ends. The driving frequency was in the range of 25 ~ 75 Hz, which was in the neighborhood of the first "natural" frequency of 43 Hz.

Unlike an ideal linear truss, which has a periodic output when forced by a periodic input, the response of the truss was often random-like for relatively small forcing. This strangeness of the response was indicated in the broadband power spectrum of the output signal as shown in Fig. 3(b). If the forcing amplitude was sufficiently small, the broadband power spectrum of the response would disappear, and many clear spikes (peaks) emerged indicating different mode frequencies and their combinations. Fig. 3(a) shows the power spectrum for the forcing signal (which was directly measured from the shaker with the use of an accelerometer), which had one principal frequency and several superharmonic components.

In this study, we define a broad band response of a system under periodic forcing to be *chaotic*. This criterion is for experimental convenience. Mathematically one should show that the largest Lyapunov exponent for the vibration output is positive in order to label the motion chaotic (see Ref. 3, Chapter 5). However, experimental measurement by Lyapunov exponents has not been reliably developed. Thus, we rely on the FFT signal to define chaos. The appearance of chaotic dynamics of the truss once again suggests that the nonlinearities associated with the pin truss joints complicate the dynamics of the system.

Connections of the Truss with the Shaker

In the dynamical testing, we found that when the structural response became chaotic (with broadband spectrum), the chaos was also fed back to the shaker. The signal from the

---

†For a similar truss structure with *welded joints*, the first natural frequency from simulation is approximately 4% higher than the value from experimental testing. This error becomes bigger for the higher modes.

armature of the shaker, measured by another accelerometer, was contaminated; the spectrum of this signal also contained many narrow-banded peaks. In our experiments, the truss was originally connected to the shaker with a rigid steel rod. Obviously, when the motion of the truss was chaotic, the motion of the armature became chaotic too.

To study the dynamics of the truss alone, we designed a decoupling device to isolate the chaos of the truss. The objective of such a device was to supply a force to the truss at the same time separating the motion of the truss from that of the shaker.

Effects of Cable Tensions

We have seen that the dynamics of the truss was complicated because of the nonlinear pin joints. To control the dynamical response, a steel cable was added to the truss in the direction along the longerons, in hopes of bringing back the dynamics of the truss into the linear regime, at least to reduce the level of chaos.

To this end, two triangular thin aluminum plates (0.3175 cm thick) were attached to each end of the truss (see Fig. 1,4). Then a tension cable was connected to the two centers of the two plates. The total length of the cable can be adjusted by some special screw-nuts. A full wheatstone bridge was designed to measure the tension forces in the cable. A schematic configuration after the addition of the plates and the cable is also shown in Fig. 1.

The first natural frequency of the steel cable is given by the formula

$$f = \frac{1}{2L}\sqrt{\frac{T}{\rho}} \; ,$$

where $L \approx 3.556$ m is the length of the cable, $\rho = 7.33 \times 10^{-3}$ kg/m is the mass density, and T is the tension it carries. The typical load of the cable will be in the range of $0 \sim 25$ kg, which corresponds to the fundamental frequencies of the cable in $0 \sim 25$ Hz. It is seen that these frequencies are below the natural frequencies of the truss. In experiments, the interactions between the truss and the cable were weak, and the cable tension was considered to be constant in each experiment.

Fig. 5 demonstrates the power spectra for the responses of the truss for different cable tensions. In Fig. 8, the driving frequency was 45 Hz. When the cable tension was set to be 13.0 kg, we observed a periodic output of the truss for certain input forcing, the output signal only contained a few clear peaks in the frequency domain (see Fig. 5(a)). To see the effects of the cable tension, we gradually reduced the tension to 3.0 kg and waited for some time to let the vibration settle down, the spectrum became broadbanded as shown in Fig. 5(b). Generally the more the T was reduced, the more broad the power spectrum was. In some case, the level of the power spectrum was also increased even for fixed input forcing level.

Inspired by the results in Fig. 5, we tried to find criteria for chaos, in the frequency domain, for different cable tensions. In general, the power spectrum of an output signal contained many peaks, like the one in Fig. 8(a), before the onset of chaos. For each fixed frequency, we gradually increased the driving amplitude until the spectrum of the response of the truss became broadbanded, like the one in Fig. 5(b). When this transition occurred,

we recorded the forcing amplitude. Repeating the above procedure for different driving frequencies and different cable tensions, we obtained chaos criteria for the truss, as shown in Fig. 6. The horizontal axis represents the driving frequency, and the vertical axis is the acceleration of the shaker, which is proportional to the driving force applied to the truss. It is clear in the figure that when the cable tension is increased, the forcing amplitude is also increased for the onset of chaotic responses.

These results hold out the promise that the nonlinear effects of pin joints or deployable truss elements may be reduced if initial compression in the truss is applied with tension cables.

Conclusions and Future Work

The experimental study on the pin-jointed truss has shown that the dynamics of the structure could be extremely complicated by the nonlinear joints. The modal frequencies of the truss were considerably lower than the ones for the linear truss. The dynamic response was clearly chaotic indicated by its broadband spectra. By adding a tension cable along the longeron direction of the truss, the degree of chaos was lowered.

Numerical simulations for our 16-bay truss were also carried out by including the small gaps of the joints in our mathematical model. The preliminary simulation results indeed tell us that the dynamics of the truss is complicated by the looseness of the joints. More extensive and complete simulations are still needed to fully understand the system dynamics.

Some theoretical analyses for interpreting the experimental results have been reported. A bilinear, periodically forced, one-degree-of-freedom oscillator has been shown to yield chaotic motions via a period-bifurcation sequence[8]. Another system, which also yields chaotic motions when the feedback is strong enough, is a trilinear oscillator[9]. A preliminary study for a single degree of freedom oscillator having trilinear stiffness, as shown in Fig. 7, is being carried out, and period-doubling bifurcation sequence and thus chaos has been observed[10]. The result can be employed to understand the dynamics of our laboratory truss.

This study clearly shows that the practical construction of truss type structures in space may bring in nonlinearities in the properties of the joints. The observation of chaotic behavior in such structures suggests that linear methods of theoretical and experimental analysis may not be useful, and that the new tools of nonlinear vibration may be needed to understand the dynamics of real structures in space.

References

[1]Ikegami, R., Church, S.M., Keinholz, D.A., and Fowler, B.L., "Experimental Characterization of Deployable Trusses and Joints," presented at the Workshop on Structural Dynamics and Control Interaction of Flexible Structures, Marshall Space Flight Center, Huntsville, Alabama, April 1986.

[2]Natori, M., Iwasaki, "Adaptive Planar Truss Structures and Their Vibration Characteristics," presented at the Workshop on Structural Dynamics and Control Interaction of Flexible Structures, Marshall Space Flight Center, Huntsville, Alabama, April 1986.

[3]Moon, F.C., *Chaotic Vibrations*, John Wiley & Sons, New York, 1987.

[4]Ross, C.T.F., *Finite Element Methods in Structural Mechanics*, John Wiley & Sons, New York, 1885.

[5]Chapman, J.M., Shaw, F.H., and Russell, W.C., "Dynamics of Trusses Having Nonlinear Joints," presented at the Workshop on Structural Dynamics and Control Interaction of Flexible Structures, Marshall Space Flight Center, Huntsville, Alabama, April 1986.

[6]Matsumoto, T., Chua, I.O., and Tanka, S., "The Double Scroll," *IEEE Trans. Circuits Syst.* CAS-32 (8), pp.798-818, 1985.

[7]Ih, C.C., Wang, J.J., and Lin, Y., "Control and Simulation of Space-Station Vibrations," Jet Propulsion Laboratory, Pasadena, California, 1987.

[8]Shaw, S.W. and Holmes, P.J., "Periodically Forced Linear Oscillator with Impacts: Chaos and Long-Period Motions," *Physics Review Letters*, Vol. 51, 1983.

[9]Golnaraghi, M.F., *Chaotic Dynamics and Control of Nonlinear and Flexible Arm Robotic Devices*, Ph.D Thesis, Ithaca, New York, 1988.

[10]Li, G.X., Rand, R.H., and Moon, F.C., "Bifurcations and chaos in a zero-stiffness impact oscillator," to be published in *International Journal of Nonlinear Mechanics*.

Figure Captions

Figure 1.   (a) The experimental truss structure; (b) the cable tensioned truss hung from the ceiling by two soft rubberbands.

Figure 2.   Sketch of a typical nonlinear joint.

Figure 3.   Typical power spectra for the input and output signals; note that the power spectrum for the system response under periodic input is broadband.

Figure 4.   The experimental setup for the dynamic tests.

Figure 5.   Power spectra demonstrating the effects of cable tensions.

Figure 6.   Criteria for chaos in the forcing frequency and amplitude plane.

Figure 7.   (a) A pin-jointed rod member in the truss; (b) an idealized model; (c) the force-displacement curve.

(a)

(b)

The tension cable

Figure 1
(Moon, Li)

0.75"

1.25"

Cotter pin
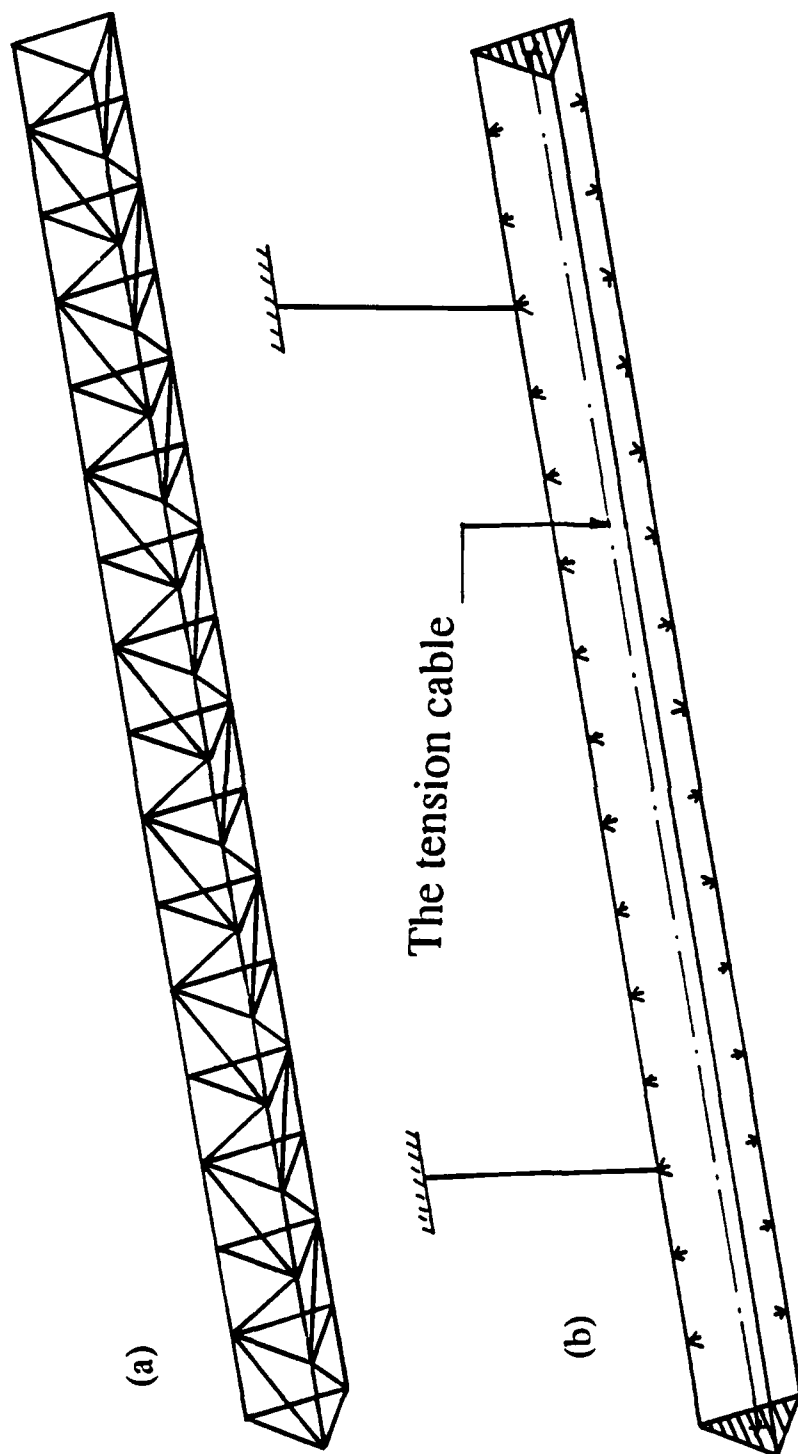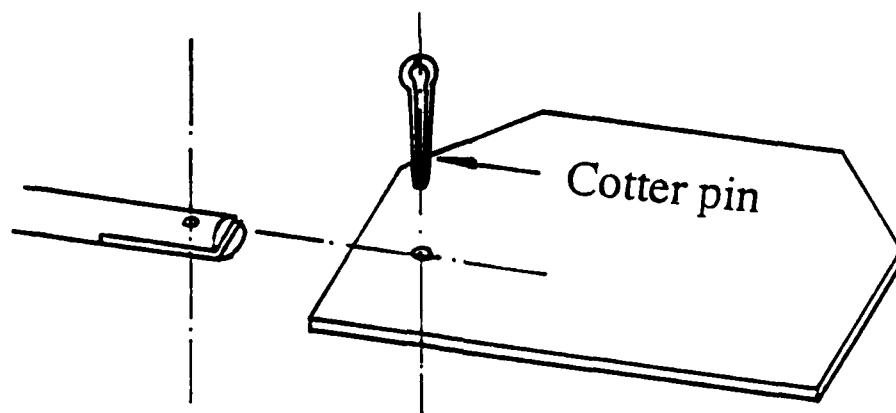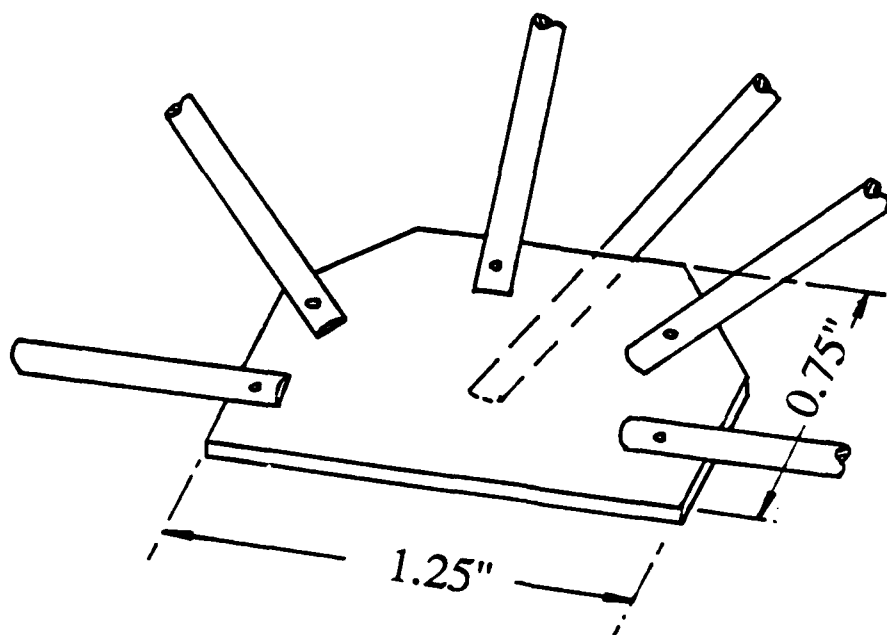
Figure 2
(Moon,LI)

Figure 3
(Moon,Li)

Accelerometer · The truss

Decoupling device

m_s · The shaker

$F_s = F_0 \sin \omega t$
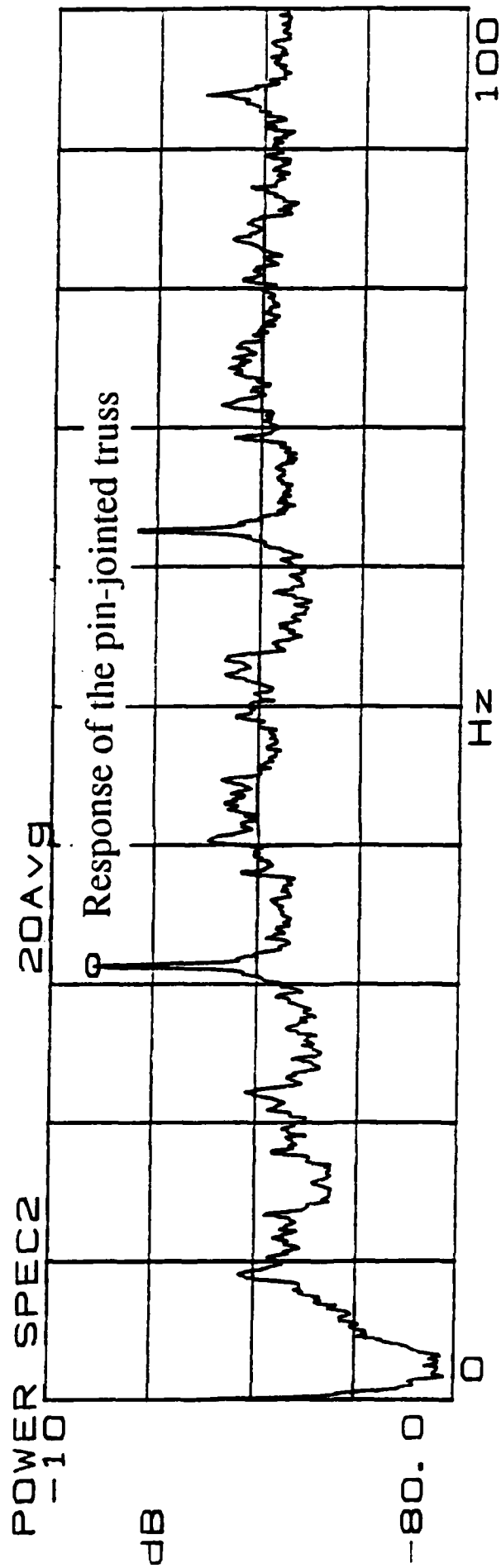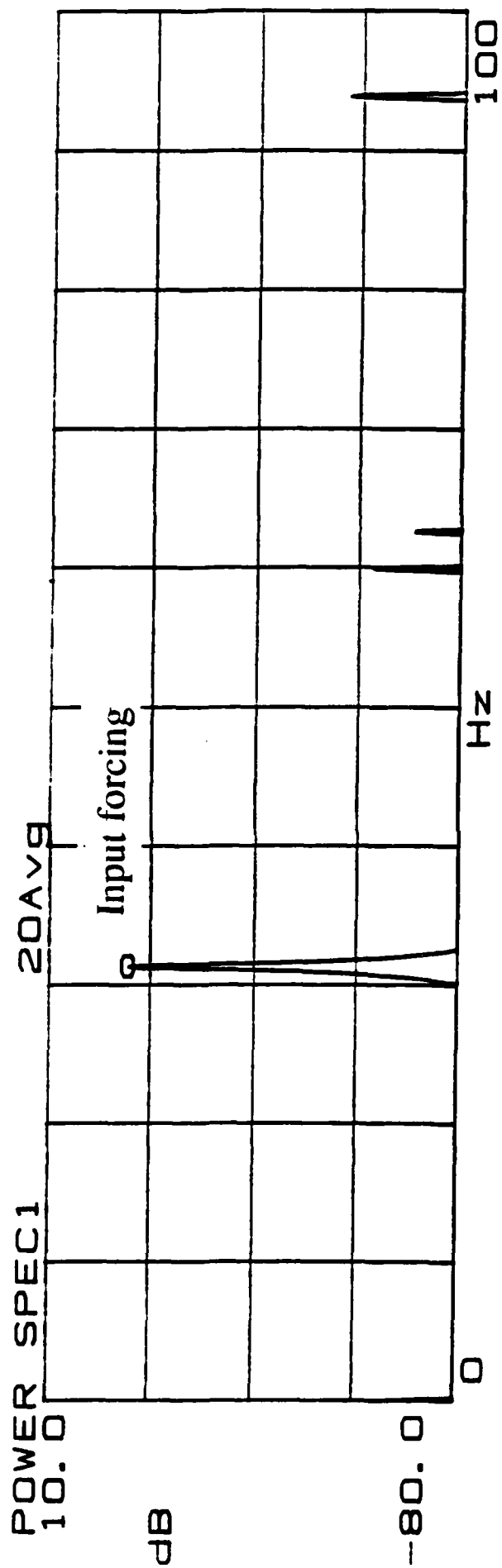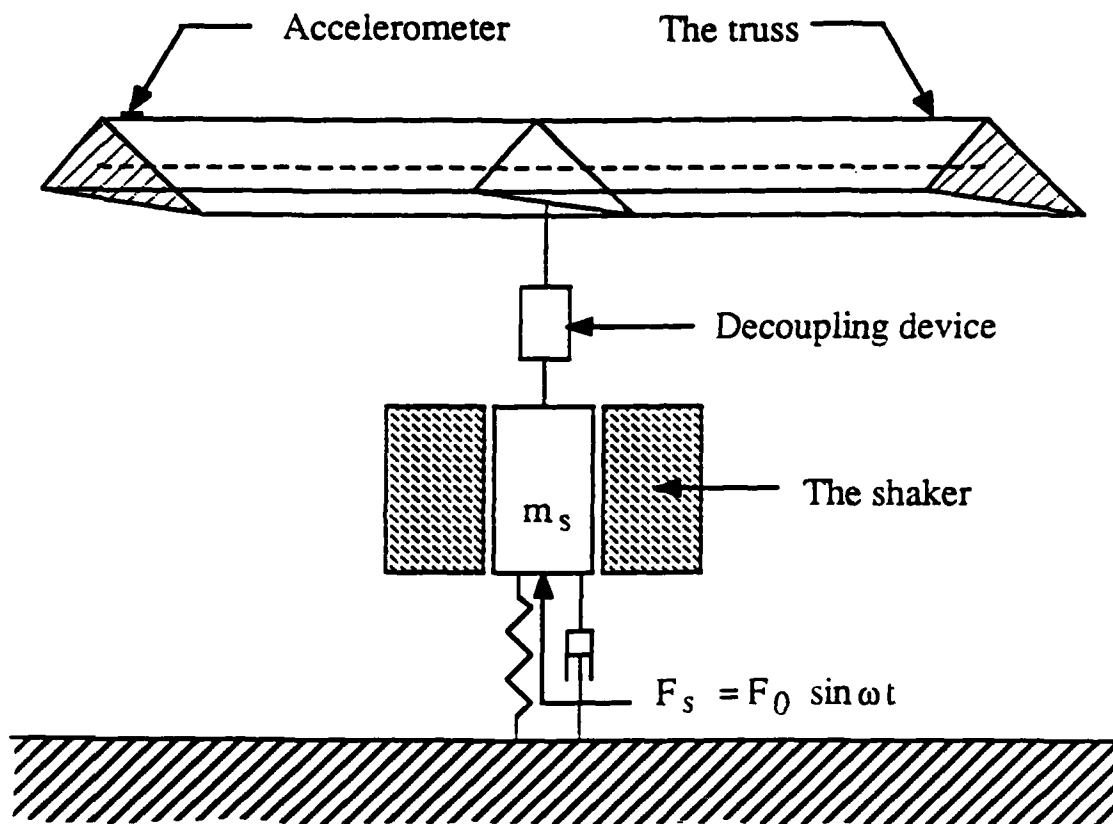
Figure 4
(Moon,Li)

Figure 5
(Moon,Li)

POWER SPEC2   10Avg

-20.0

dB

(a) T = 13.0 kg, f = 45 Hz

-80.0

20   Hz   332.5

POWER SPEC2   10Avg

-20.0

dB

(b) T = 3.0 kg, f = 45 Hz

-80.0

20   Hz   332.5

Figure 6
(Moon,Li)

43

(a)

(b)

x_1 $k = EA/L$ $2d$ x_2

(c)

$F(u)$

k

$- d$

d $u = x_2 - x_1$

Figure 7
(Moon,Li)

44
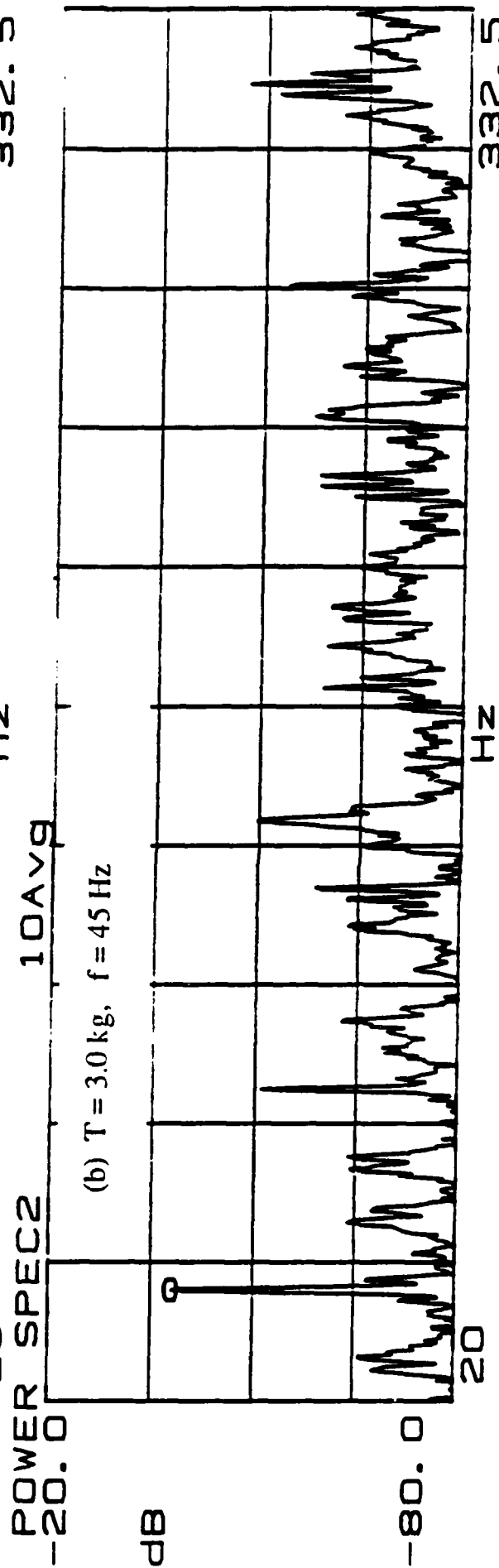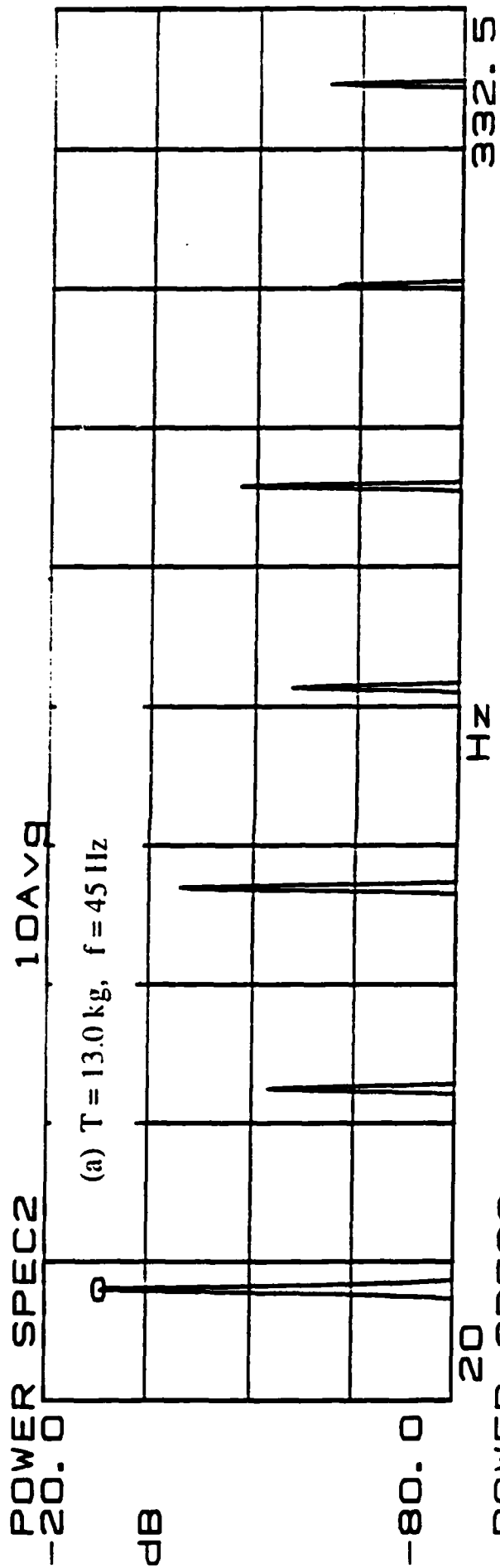
Project Title:
Chaotic Dynamics of a Buckled Truss Structure

Project Leader:
Professor Francis C. Moon
Department of Mechanical & Aerospace Engineering

Graduate Research Assistant:
Matthew A. Davies
Department of Mechanical & Aerospace Engineering

Project Summary:

Recent demands in the aerospace industry have lead to the development of large flexible structures designed for deployment in space. Since space structures carry essentially no gravitational load. They can be built much lighter than their ground based counterparts and due to the high cost of transporting material into space minimizing the mass of a space structure is a major design criterion. Unfortunately this often tends to make them quite susceptible to dynamic vibration.

One of the classical ways a structure can fail is through buckling. The most common form of buckling occurs when a column member loaded axially in compression becomes unstable and fails in bending, bowing out at the center and collapsing in a rather dramatic manner. Such failure is often sudden and catastrophic since buckling occurs immediately upon the attainment of some critical compressive load in the column with little or no forewarning. In a space structure where dynamic loads become more prominent one must not overlook the additional possibility of failure due to dynamic buckling.

In this paper we investigate the problem of dynamic buckling in large structures. We show conclusive evidence from experiments that such behavior is highly non-linear in nature and cannot be predicted by classical linear structural analysis and modeling techniques. Period doubling and chaotic vibrations common to many non-linear problems are observed and discussed. We also discuss possible metho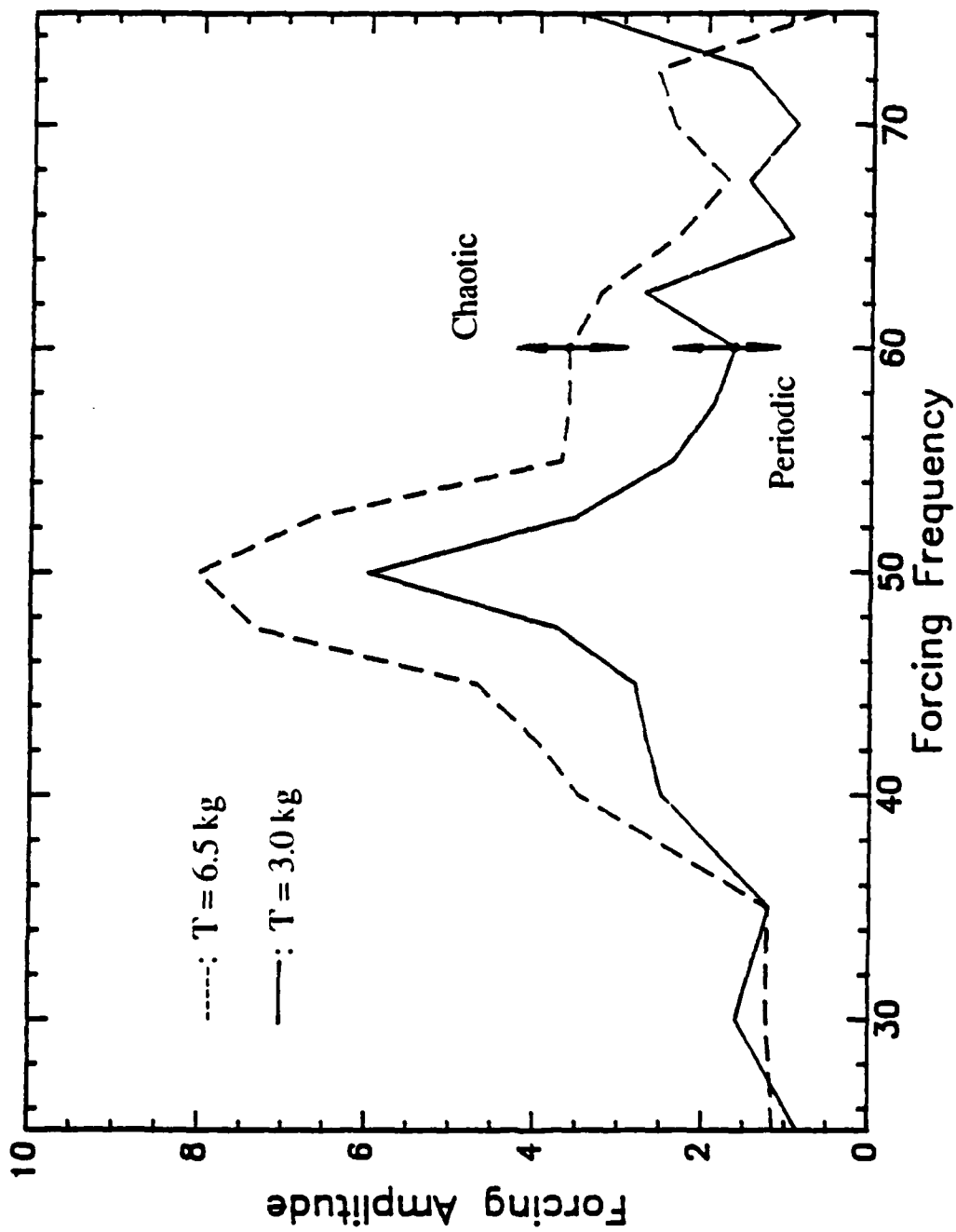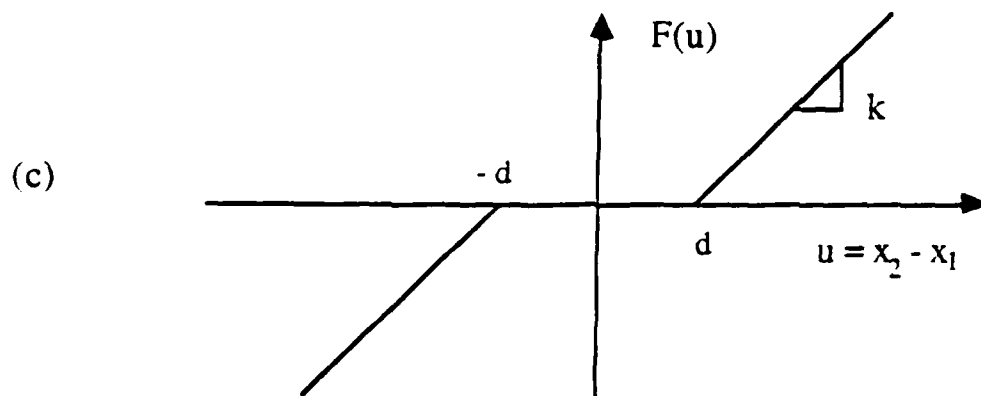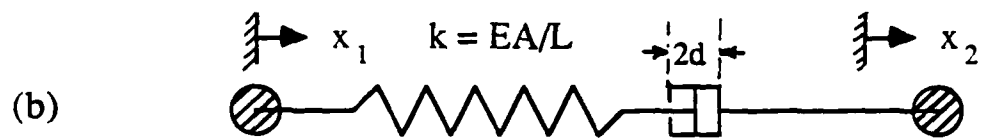ds of modelling structural members which buckle dynamically and present some preliminary results from one possible model.

Experiment

The main focus of our first dynamic buckling experiment is a three meter aluminum truss diagrammed in Fig. 1. The truss consists of 23 identical bays. One of the horizontal members in the center bay was removed and replace by a spring steel member 4.75 inches long, 1 inch wide and 0.005 inches in thickness. This member, although matching the stiffness of the other truss members in tension, is quite susceptible to buckling in compression. Hence, the structure is still quite resistant to loads in one direction while being relatively unable to resist loads in the other (see Fig. 2). The entire structure, configured in this manner, was then suspended from the laboratory ceiling using gum rubber strips in order to simulate a free floating environment. Harmonic excitation was then applied to the truss using a 100 lb electromagnetic shaker table. The dynamic response of the truss was recorded and analyzed.

Dynamic response of the truss was measured by strain gages placed directly upon the spring steel buckling member. The signal from these gages, after sufficient

amplification and filtering, was differentiated electronically and then both the signal and its derivative were monitored and recorded using a Nicolet Model 206 Digital Oscilloscope. In this way we were able to produce phase planes and Poincaré maps of the data in real time. Also, using an HP3562A Signal Analyzer we were also able to produce power spectra, autocorrelations, and probability density functions from the strain data.

Experimental Results

Five different types of data were collected during the experiments. These were: (1) phase planes (strain vs its derivative), (2) Poincaré maps, (3) power spectra, (4) probability density functions and (5) autocorrelations (correlation of the data to itself). A *Wavetek Model 180LF* signal generator was used to provide harmonic input to the shaker and thus to the structure at the desired frequency. As the amplitude of the excitation was varied, different types of dynamic behavior were observed. Increasing the amplitude of excitation while keeping the frequency constant caused the initial period one motion to become unstable and undergo a bifurcation to period two motion. This type of dynamic behavior is distinguished by the existence of a component of the motion at half the frequency of the driver. Further increases in amplitude from these levels lead to other period doublings to period 4 and period 8 type motions. Finally, slight increases in amplitude from the period 8 levels lead to unpredictable or chaotic motions. This type of behavior indicates a typical progression of period doubling now known to be a trademark of many nonlinear systems. Such a progression can be best summarized by a bifurcation diagram. A bifurcation diagram is a plot of sampled values of the system output (in this case strain) versus some controlled system parameter (in this case driver amplitude), where the sampling rate of the system output is the period of the driving signal. Using a *Masscomp Data Acquisition System* we were able to create an experimental bifurcation diagram of truss behavior. The *bifurcation diagram for varied amplitude at a frequency of 13.87 Hz is shown in figure 3.* The phase plane plots of the different types of motion have been superimposed on the bifurcation diagram in order to further illustrate the motion.

As can be seen in Fig. 3 chaotic motion ensues after the period doubling sequence. Figs. 4a-e show the character of such motions. In the double plots the upper plot is the system response while the lower is the driver. Chaotic motion persists for a narrow range of amplitudes after which a very large period two motion appears. Unfortunately this motion is so large that its destructive effects on the truss prevent further investigation of its characteristics. Also shown in Fig. 4f is a Poincaré map of chaotic motion seen at a driving frequency of 5.8 Hz.

Model for Dynamic Buckling

We model the buckling member in the truss as an elastica. An elastica is a thin strip of incompressible material whose major mode of deformation is buckling. In the elastica problem deformations are allowed to be quite large but strains are assumed to remain small. Consider the elastica shown in Fig. 5. This problem can be solved most easily by considering it as a combination of two symmetric parts. The equation of deformation for the elastica can be shown to be

$$EI \frac{d^2\theta}{ds^2} = -P \sin \theta \tag{1}$$

46

This equation, it will be noted, is the same as the equation of motion for a pendulum. This similarity was first noted by Kirchoff and is hence known as Kirchoff's analogy.

Equation (1) may be solved analytically resulting in elliptic integral expressions for the load P and displacement x as functions of the tip angle α. Plotting the end load P versus motion of the end of the beam x - l results in the force displacement curve shown in Fig. 6. Since the elastica is assumed incompressible no deformation can occur until critical load is achieved. After critical load buckling occurs and the beam undergoes large deformations for relatively small increases in load. The load deformation curve does, however, appear to be linear over a large range of deformation. This suggests that although the overall behavior of our buckling member is nonlinear the nonlinearity is concentrated at the instant of buckling and the behavior elsewhere is linear.

The final step in this portion of the analysis is to piece together beam behavior between the tension-compression and the buckling states. To accomplish this we relax the inextensibility restriction on our elastica and examine it's behavior. Coupling elastic extension-compression behavior with the elastica behavior strongly suggests that we are justified in using the bilinear stiffness curve shown in Fig. 7 to represent our buckling member where the buckled beam stiffness is assumed to be nearly zero.

Simple Non-linear Oscillator Model

We begin our analysis of the dynamic structural buckling problem by examining a simple one dimensional oscillator. This system contains a non-linear spring element with the force-displacement curve shown in Fig. 7. The oscillator is shown in Fig. 8.

In (14) τ represents the time, z is the displacement of the mass relative to the cart, z is the critical displacement at which buckling occurs, z is the sinusoidal displacement of the cart, m is the mass of the oscillator, $k(z)$ is the non-linear spring (buckling member) stiffness and c is a linear damping coefficient. A similar system to this was studied by Holmes and Shaw (J. Sound & Vibra. **90** (1983) 129-155) in which they allowed the stiffness k_2 to become infinite while keeping k_1 non-zero. Here, as previously noted we wish to study the case where k_1 remains finite and $k_2 = 0$.

The equations of motion for this system are simply given by:

$$m \frac{d^2z}{d\tau^2} + c \frac{dz}{d\tau} + H(z) = - mA \, \Omega^2 \cos (\Omega\tau)$$

(2)

$$H(z) = \begin{cases} kz & z \geq z_0 \\ k z_0 & z < z_0 \end{cases}$$

The term $H(z)$ represents the restoring force of the nonlinear spring. For $z > z_0$ this increases linearly with distance from the $z = 0$ point. Thus, for sufficiently small driving amplitudes it is possible for the system to oscillate in an entirely linear manner about the origin. However, if the driving amplitude is increased so that at some time during the motion z becomes less than z the restoring force abruptly changes. At this point instead of increasing linearly with distance from the origin it remains constant. This corresponds to the transition to a buckled state in the nonlinear spring.

These equations really are quite nice because they are easily solvable in each of the two regions of linear behavior $z > z_0$ and $z < z_0$. The difficulty arises only at the point $z = z_0$ where the two solutions must be matched together. In analyzing these equations we first solve them explicitly in the two regions and then use a computer program to perform a matching procedure at $z = z_0$.

Numerical Results From the Model

Equation (2) was nondimensionalized and solved numerically. The parameters in this system are x, the nondimensional position, y, the nondimensional velocity, β, the non-dimensional driver amplitude, w, the non-dimensional driver frequency, x_0, the critical x value, and δ, the non-dimensional damping ratio. Many simulations were done for various values of the parameters, and phase plane and Poincaré map data were produced. For parameter values of w = 1.05, $x_0 = 0.002$, and $\delta = 0.02$ varying β from 0.002 to 0.0045 gave the results shown in Figs. 9a and b, 10a and b and 11a and b. Fig. 11 shows motion which appears to be chaotic as indicated by the space filling nature of the phase plane motion and the fractal Poincaré map.

Conclusion

We have seen from this research that the problem of dynamic buckling in structures is highly nonlinear. Experimentally, the presence of period doubling sequences and chaotic motions have been demonstrated. The existence of these motions at different amplitudes was illustrated by means of an experimentally generated bifurcation diagram. The experimental results lead to the development of a bilinear model for buckling which was justified on the basis of a modified elastica analysis. Preliminary results of this model were presented which showed the presence of period doubling and probably chaotic motions as well. Further simulations are necessary to verify or disprove the validity of this model.

Clearly, the motions of a structure containing a buckling member can be quite complex. Thus, it seems that one should exercise caution in the design of large structures and be aware that such motion can exist if one of the members is made to thin. Overlooking such a structural anomaly could be detrimental to other structural systems, active controllers, for example, which rely on the motions of the structure remaining linear.

REPLACED MEMBER
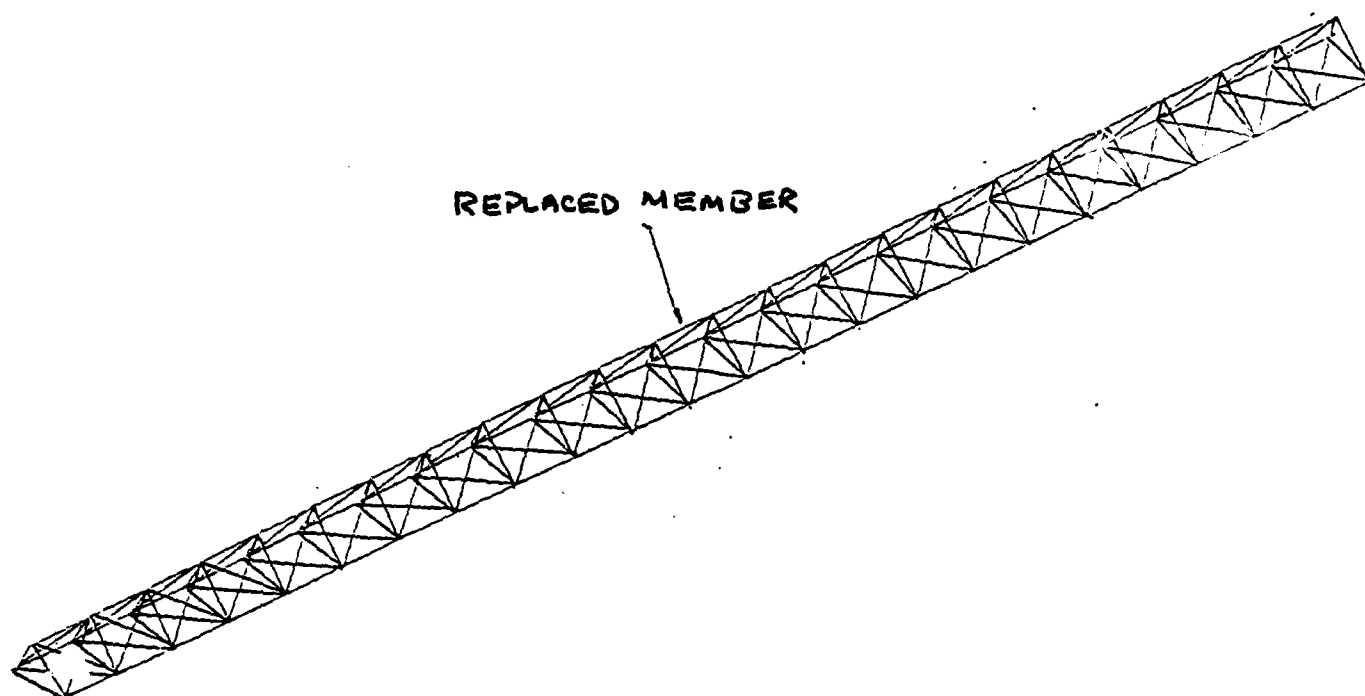
Figure 1.   Three meter aluminum truss.

BUCKING MEMBER

P
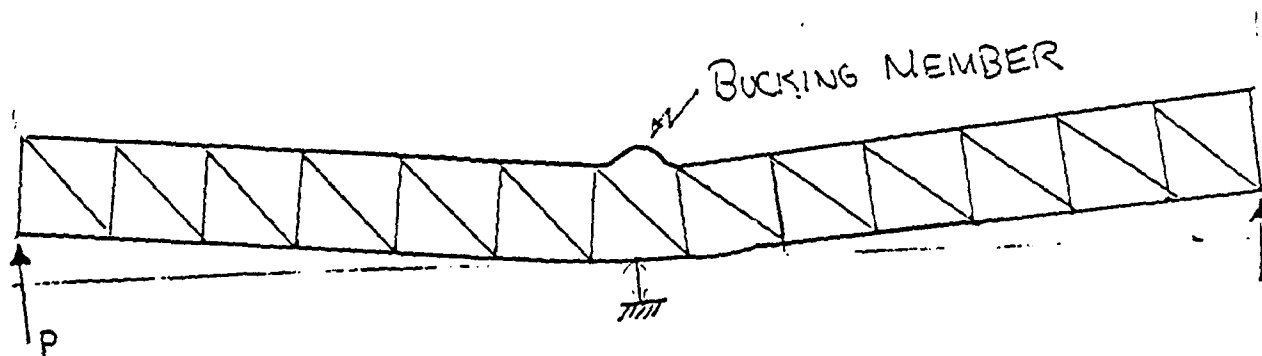
Figure 2.   Buckled truss under load.

49
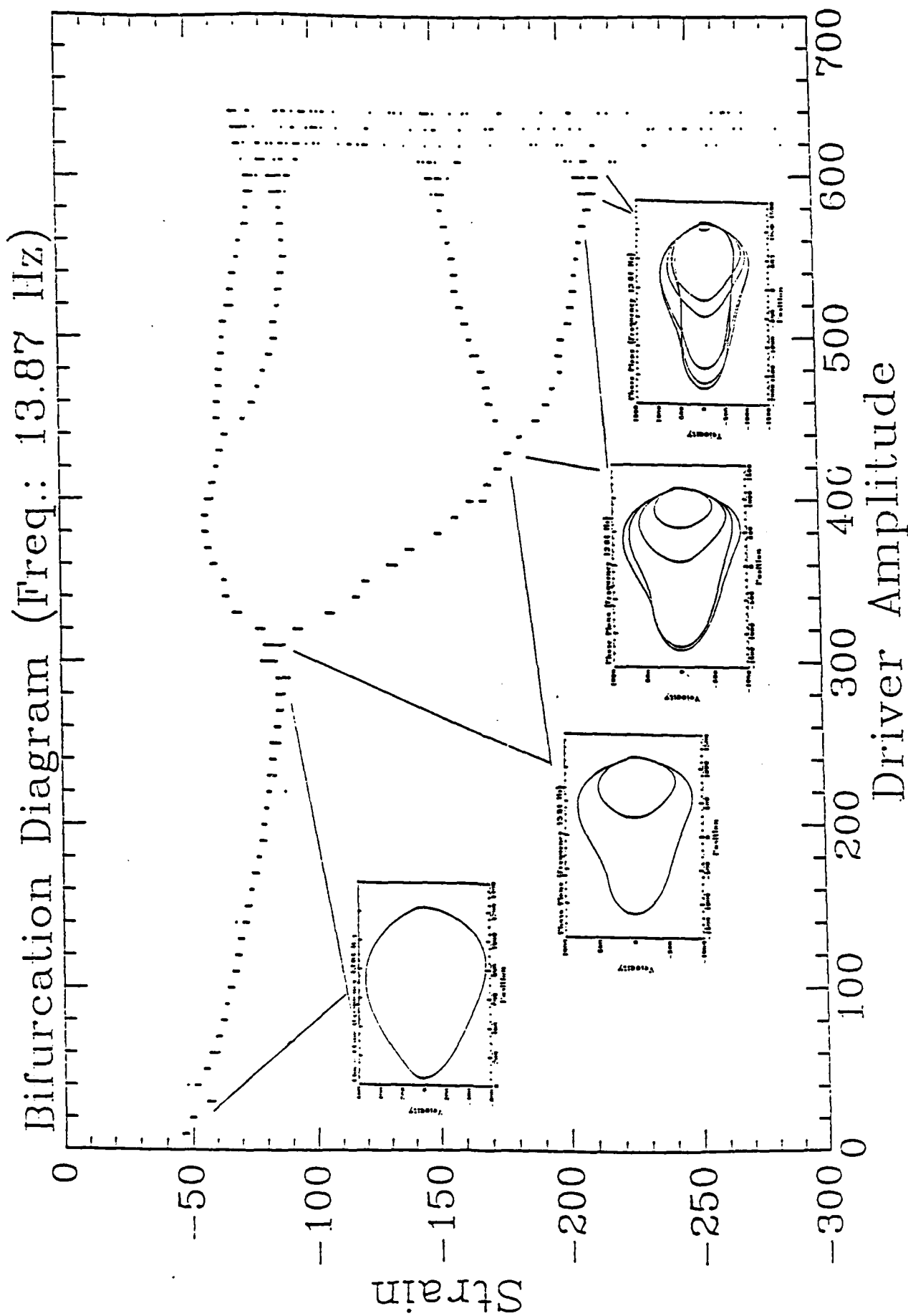
Figure 3. Bifurcation diagram varying driver amplitude and measuring strain.
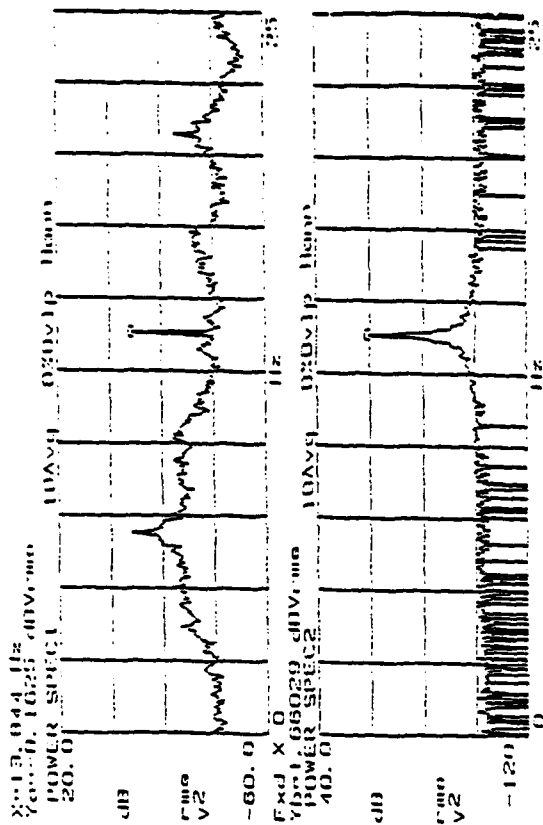
Figure 4b.   Power spectrum.

Figure 4d.   Probability density function.

Figure 4a.   Phase plane.

Figure 4c.   Autocorrelation.

51

Poincare Map (Frequency 13.84 Hz)

Figure 4e.

Poincare Map (Frequency: 5.781 Hz)
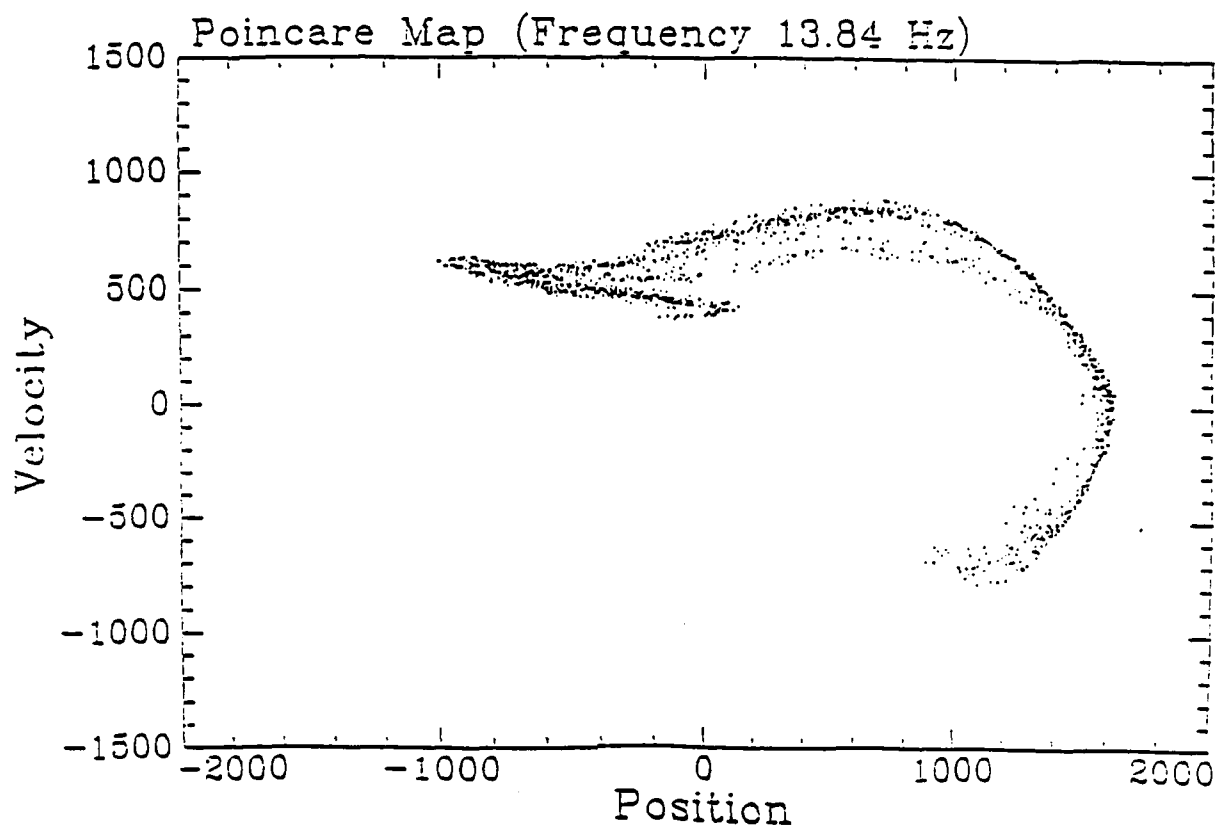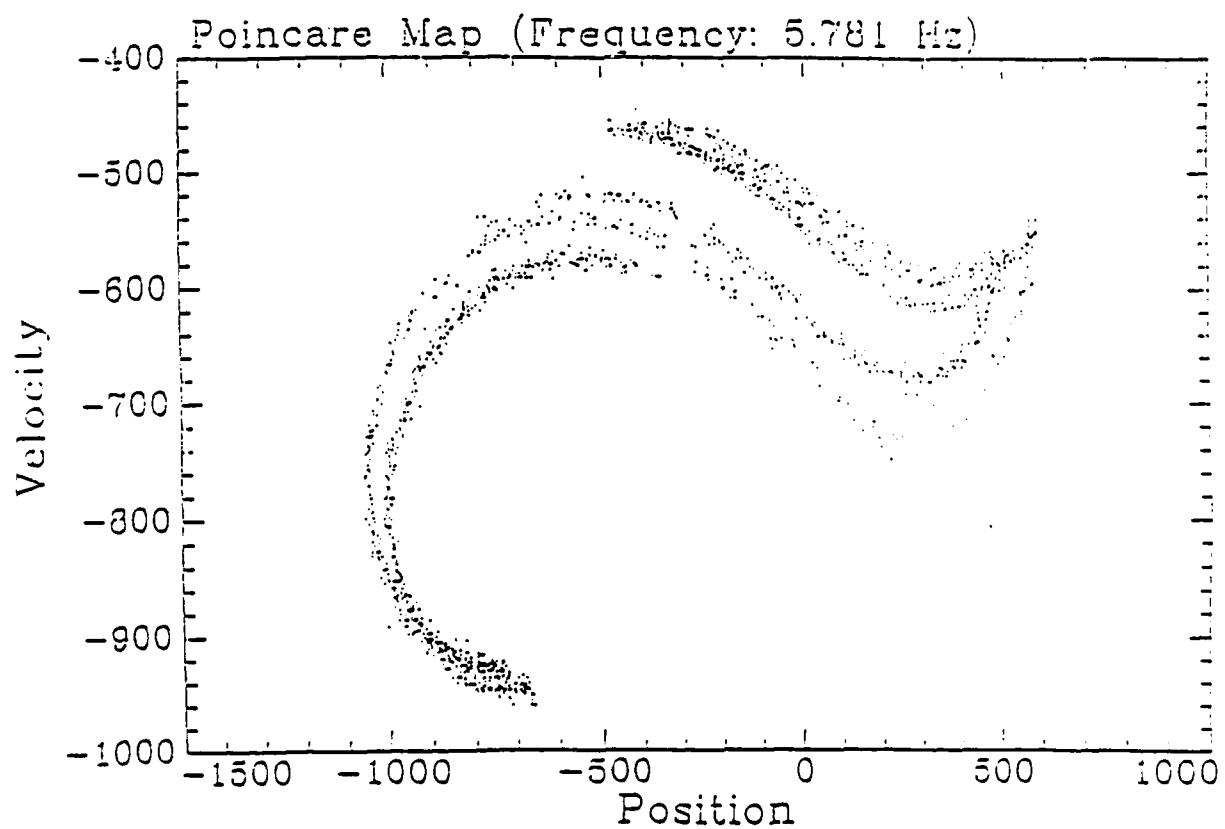
Figure 4f.

□ ≡ Portion Shown in figure 12

Original length: $2l$

Deformed length: $2x$
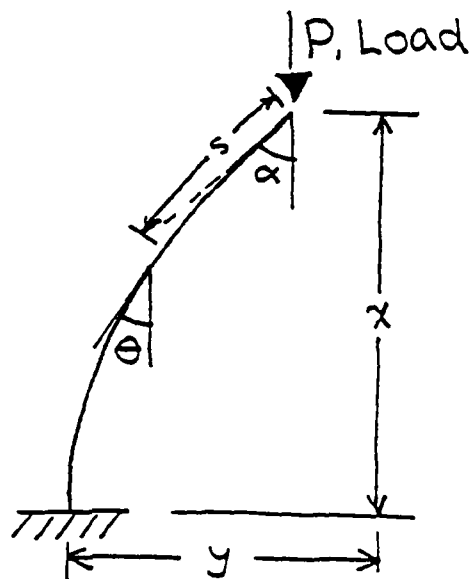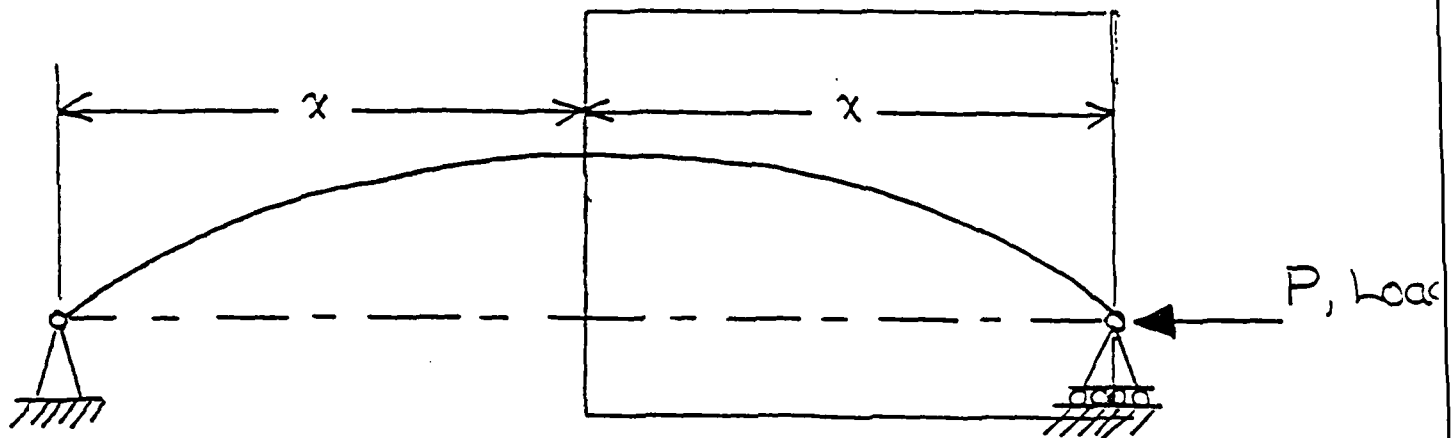
Original length: l
Deformed length: x
Coordinate along Elastica: s

Figure 5. Elastica, symmetric problem.
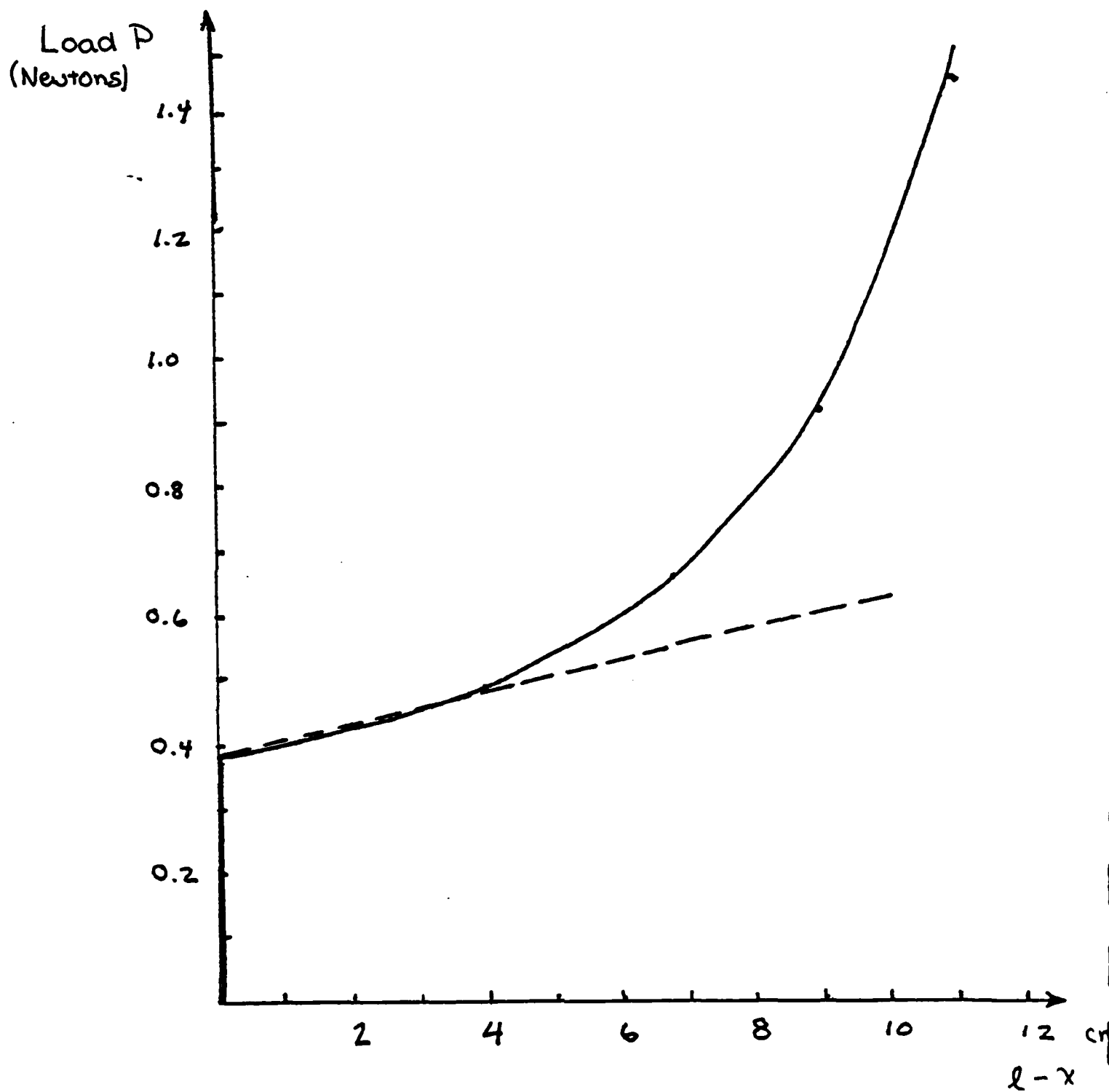
Figure 6.   Load vs. displacement curve.   Dotted curve shows linear range.
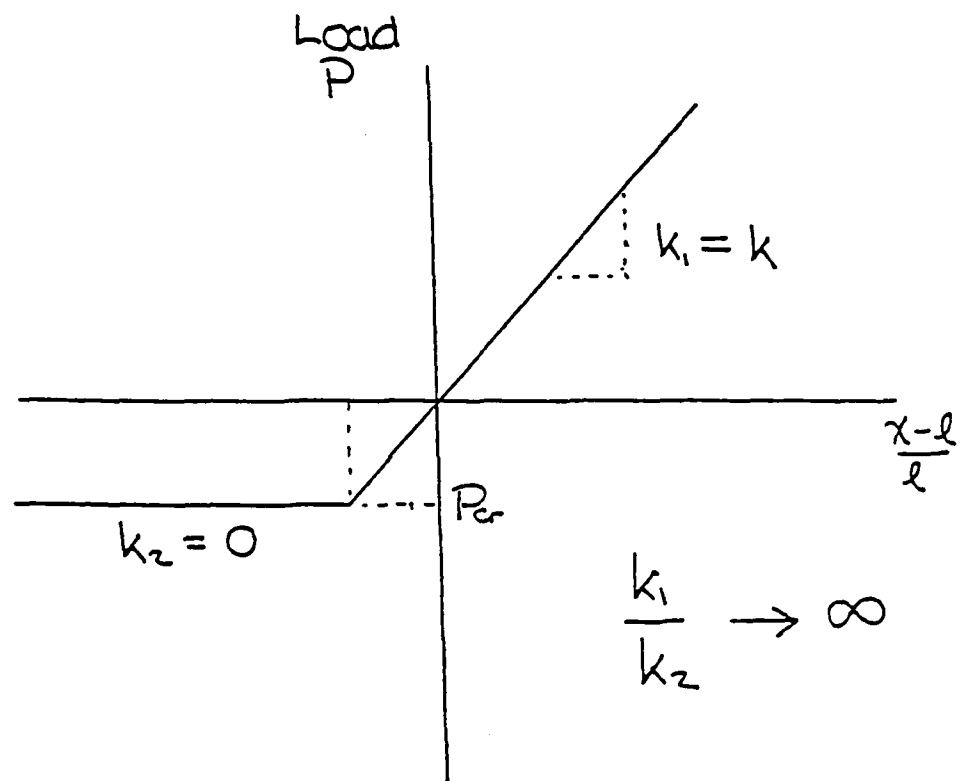
Figure 7.   Bilinear stiffness curve.
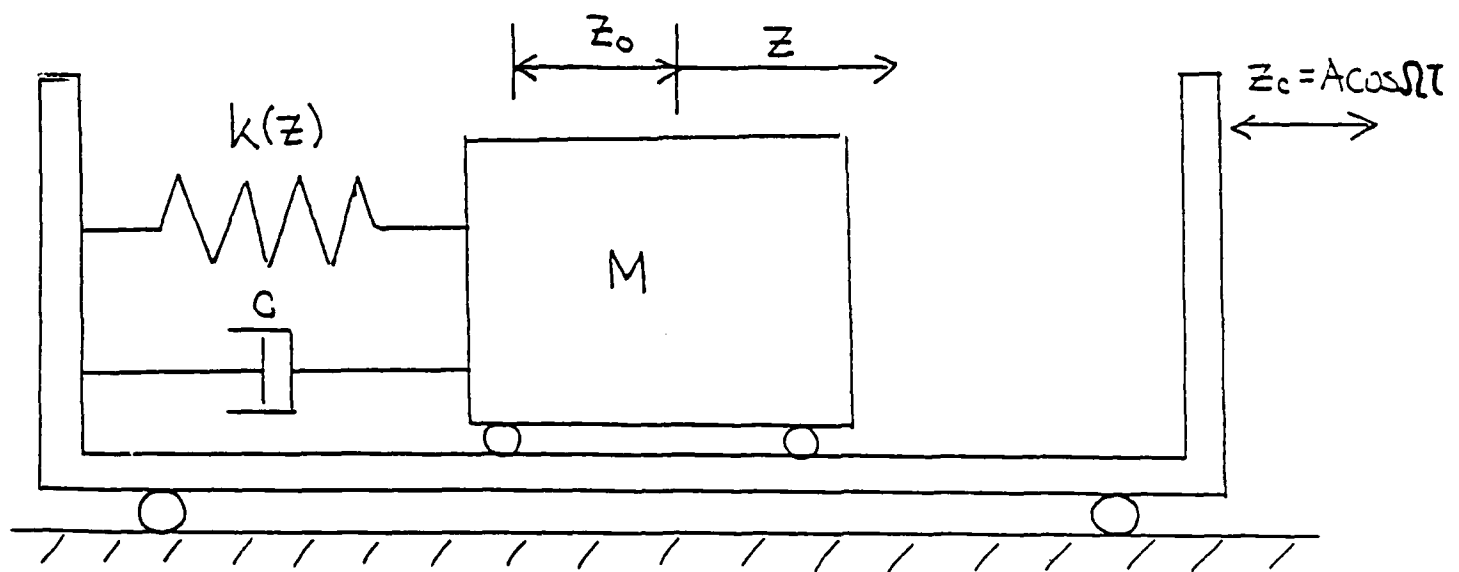
Figure 8.   Nonlinear oscillator.
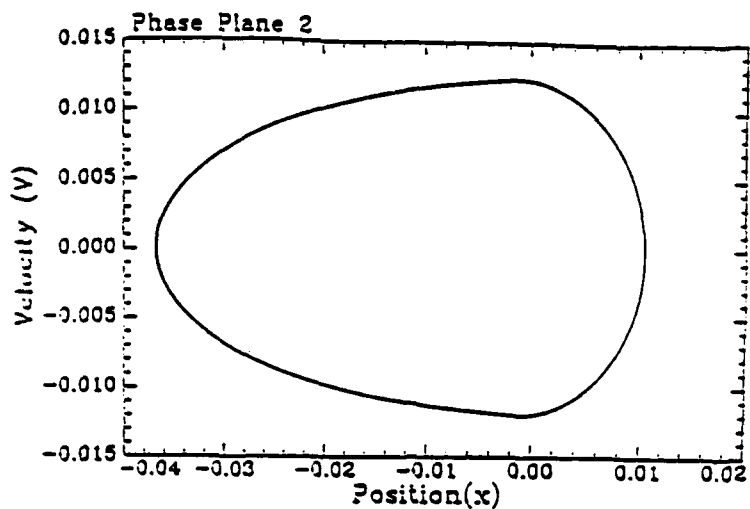
Figure 9a.
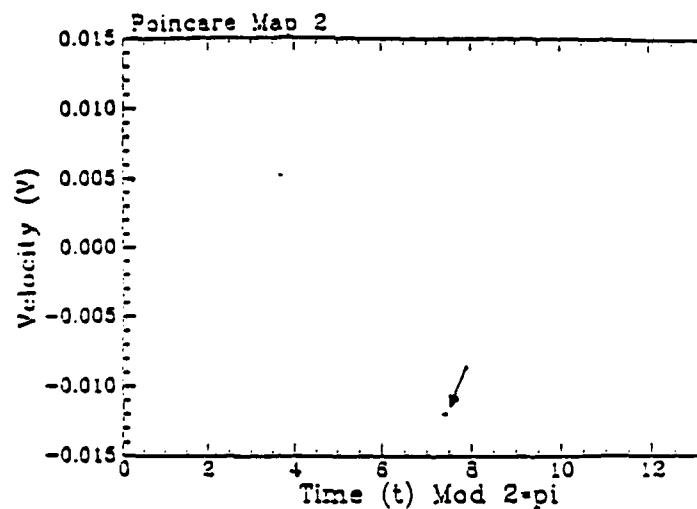
Figure 9b.
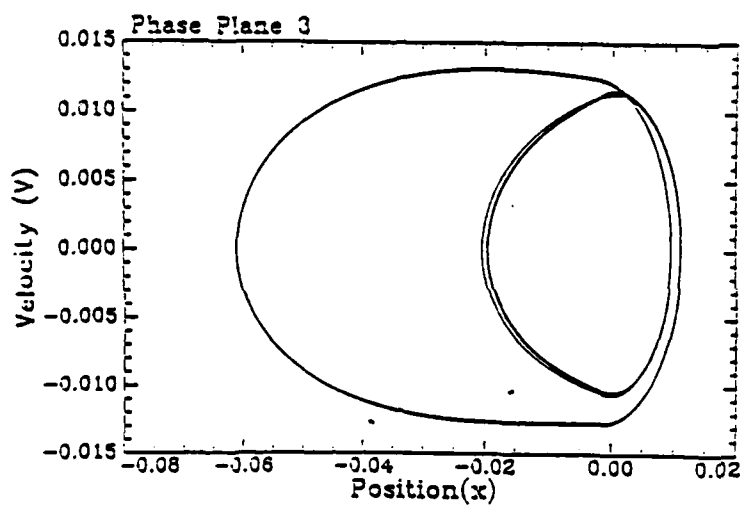
Figure 10a.
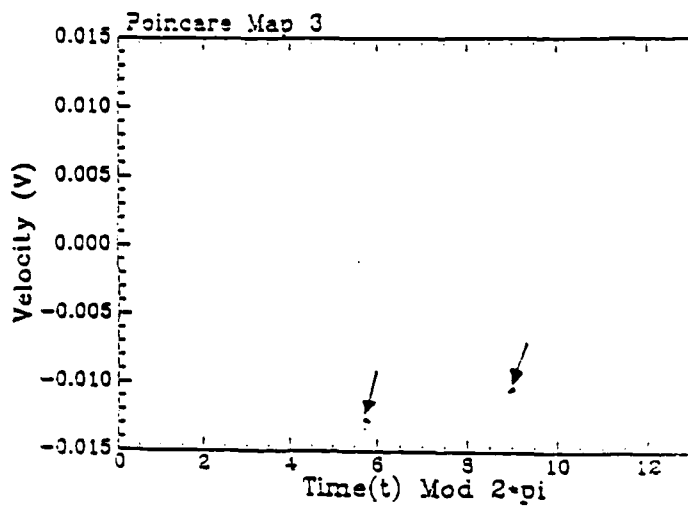
Figure 10b.
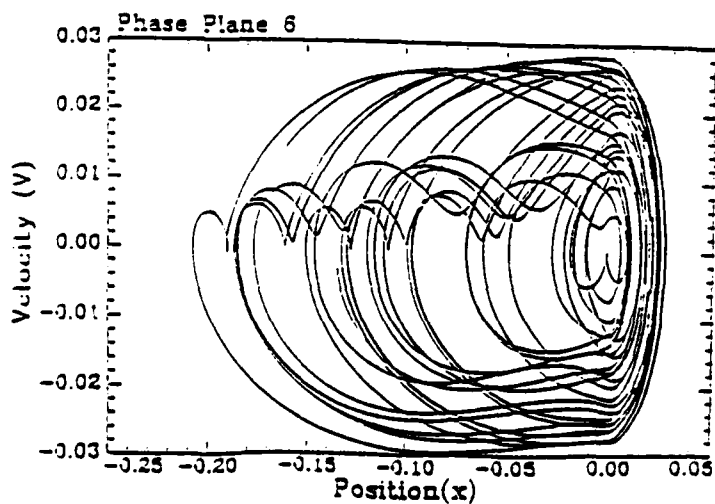
Figure 11a.
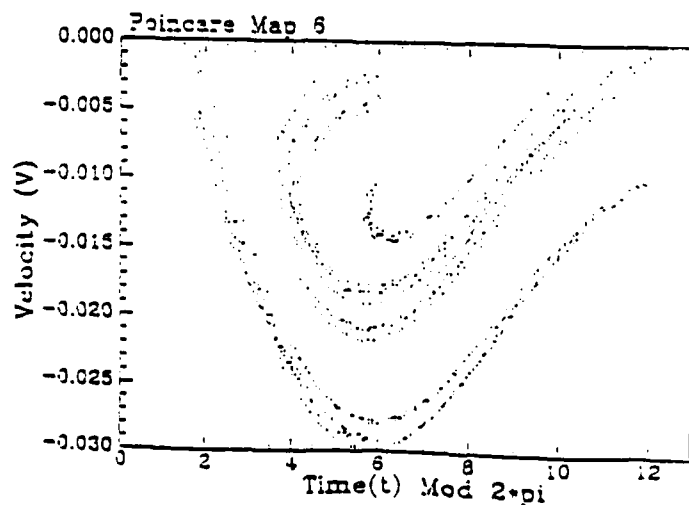
Figure 11b.

PROJECT SUMMARY

Project Title:
Computer Simulation of Control of Nonlinear Structural Dynamics

Faculty Leader:
John F. Abel, Civil and Environmental Engineering and Program of
Computer Graphics

Graduate Research Assistant:
Brian H. Aubert, Civil and Environmental Engineering and the Program
of Computer Graphics

Executive Summary:

Research software which can effectively model and numerically analyze
certain nonlinear behaviors of actively controlled space structures has
been implemented. Interactive computer graphics are used to aid the
interpretation of the complex results of the nonlinear dynamic analyses.
Modularity of the application code has been emphasized to facilitate
addition of different types of control strategies, different element types,
or alternative nonlinear analysis models. Computational environment
dependencies of both the analysis and display capabilities of the code have
been minimized, with the result that the software has been successfully
used on several different hardware and operating system configurations.
The current dynamic analysis capabilities include both geometric
nonlinearity and a bounding surface material nonlinearity model. The
simulations of active control methods which have been implemented can
include such physical realities as observation lag and saturation of the
control signal. Examples illustrate some of the capabilities that have
been implemented in this research software.

Project Description:

An effort has been undertaken at the Program of Computer Graphics at
Cornell University to develop software tools for research on the nonlinear
dynamic analysis of actively-controlled structures. The work builds on an
existing foundation of software developed for evaluating the nonlinear
performance of building structures subject to strong ground motion[1]. The
motivation for the work has been fueled by a desire to have a numerical
simulation capability to explore issues related to the placement and
performance of both new and existing control strategies for flexible space
structures. One new control strategy which has been examined using these
tools is an open-loop, optimal nonlinear method known as differential
dynamic programming (DDP)[2,3]. The primary reason for using DDP to obtain
active control solutions is that it includes the possibility of

nonlinearities in either the response of the controlled structure or in the controller itself. Many common strategies attempt to control nonlinear structures by using controls based on linear models of the structure. Another reason for examining DDP is to determine if the optimal nonlinear control solutions it produces can be used to find new control laws which may be applicable to more widely used closed-loop control strategies.

The focus of the research has been on control of very flexible space structures although many of the software capabilities could be used for analysis and design of actively controlled terrestrial structures. The control of space structures poses a significantly more difficult task than the control of normal building structures. Space structures are designed for low gravity environments. Because the mass penalty associated with placing material in orbit limits member weight and since the structures experience little dead load, structural members are relatively flexible. Space structures typically exhibit lower levels of passive damping than terrestrial structures, primarily due to the lack of a connection to a large energy sink such as the ground. The small amount of passive damping coupled with the inherent flexibility means that even impulsive dynamic excitation may result in long duration transient responses. In some instances the persistent dynamic responses may adversely affect the mission of the space structure and require the use of damping provided by active controls.

Use of controls to provide active damping increases the number of factors which must be considered as parts of the system design. In a large three-dimensional structure there are a daunting number of possible control locations for even a single active controller, and the optimum location may even be non-intuitive. With multiple controls, even relatively small structures provide a large number combinations of possible control locations[4]. Some control strategies (e.g., collocated velocity feedback) require only limited, local measurements of the dynamic structural response, while other methods require a more complete set of measurements. It is unlikely that a sufficient number of sensors will be put in place to provide a complete set of measurements of the dynamic state of the structure, so optimal sensor placement of a subset is also an issue which must be considered. Control systems which are to be implemented must be be designed to perform robustly in the face of failure of some of the limited number of controls or sensors. The control system should not be sensitive to the differences between the actual structure and the analytical model[5]. The performance of the control system must also be evaluated in conjunction with control effects such as observation lag and control saturation which are known to degrade control performance.

With an effective, comprehensive, and accurate software platform to test and compare proposed structural and control configurations, the time required to obtain a robust and efficient control can be significantly reduced. In many cases, such a simulator is used as an adjunct to other research and design tools, e.g., optimizers for control and sensor placement[4].

Implementation

The guiding principle of the software development has been to produce modular code which may be readily expanded in capability and which is easily portable across a number of hardware configurations. The application code is primarily written in ANSI standard C with the graphics display based on the X Window system. A limited number of modules written in FORTRAN are used to perform the computationally intensive sections of the analyses. By the choice of relatively common industry standards and by the avoidance of machine specific calls, the portability of the code has been enhanced. The modularity of the code should allow developers to easily insert new methods of control, controller models, element types, time integration algorithms, or equation solvers. The code has been successfully run on Digital machines operating under both VMS and ULTRIX and on Hewlett-Packard machines operating under HPux.

The current implementation consists of two programs, a general purpose modeller/visualization program named BASYS, and a batch analysis program named ABREAST for the nonlinear time integration. Future planned development in BASYS will allow the use of that program to interactively visualize and track the progress of the analyses rather than waiting for the results from batch jobs. BASYS uses a radial edge data representation[6] to store the structural data in a topology-based hierarchy of structural models. This topological representation allows rational access to the structural data while providing a framework in which the model can be rapidly modified, displayed, and manipulated. Object oriented programming concepts and data access provided by queries are also used to maximize the modularity of the code.

BASYS provides two basic means of visualization of the dynamic response of the models. The first is to provide an animated view of the dynamic response of the structure. If the desired response is a view of an interactively selected vibration mode, the eigenvector of the structure is dynamically displayed so the qualitative aspects of the mode shape can be evaluated. In the case of a transient analysis, the results from a selected time interval can be animated with selected force quantities displayed as color contours on the moving model. The second provision for visualization is to allow the analyst to create and display x-y plots of interactively selected response information.

ABREAST is general-purpose transient dynamic analysis tool which includes a subspace iteration algorithm to calculate the solution of the open-loop eigenvalue problem, the central difference explicit time integration algorithm, and the Newmark-β implicit time integration algorithm. The current version is primarily geared towards frame structures consisting of either truss or beam-column elements. A nine noded Lagrangian shell element is also available to model panels.

Structures which undergo large displacements and rotations need to be analyzed including the effects of geometric nonlinearity. The geometric

nonlinear capabilities of the analysis are based on an updated Lagrangian method and a geometric stiffness matrix[7]. The method assumes large displacements, large rotations, and small strains. The material nonlinearity is provided by a bounding surface plasticity model in three-dimensional force space. The bounding surface approach assumes that a concentrated plastic hinge can form at the member ends due to the interaction of the axial thrust with both the major and minor bending moments of the member. This material model[8] has been shown to accurately model such complex nonlinear behavior as kinematic hardening, cyclic loading, and the Bauschinger effect. Inclusion of both the geometric and material nonlinear effects allow the analyst to effectively track the three-dimensional behavior of large structures subject to dynamically applied loads. In ABREAST dynamic loading can be specified by (a) values calculated by a specific control method, (b) use of acceleration records, (c) load histories of specific design loads, and/or (d) a set of initial conditions may be used.

The three types of active control methods which have been implemented are open-loop load history, closed-loop collocated velocity feedback, and closed-loop constant gains feedback. To increase the realism of the simulation of controls, control saturation, observation lag, and control lag have been introduced into the current implementation. Control saturation occurs when the demanded control is larger than what the control element is capable of delivering. In this case only the maximum control force can be delivered. Observation lag is a consequence of the finite time needed to collect the state measurements of the structure. Control forces which are based on the measured observations are in error by the amount of difference between the most recent observation state and the actual current state of the structure. Control lag results from the fact that control elements typically cannot instantaneously respond to changes in force level demanded by the the control signal.

In addition, closed-loop controls may exhibit unexpected behavior in the nonlinear regime in that controls which are based on linear models may develop both observation and control spillover problems when applied to a more realistic nonlinear structural model. The analyst must use judgment both in the selection of an active control type and in interpretation of the results from an actively damped, nonlinear dynamic analysis due to the presence of these types of control-structure interaction (CSI). While the lags and the control saturation which are available are a first step toward modelling CSI, there is significantly more work which can be done. As a start, accurate prediction of the effects of CSI may require a more sophisticated model of the inner control loop dynamics of the control system itself.

The batch analysis currently runs on a single fast processor and the performance is acceptable for small to medium size problems. However there is always a desire to be able to expand the size and complexity of the analyses which can be undertaken. One option to reduce the clock time needed for a large analysis is parallel processing. Work is underway to

implement a parallel version of the explicit central difference algorithm of ABREAST. The central difference algorithm is amenable to parallelization since the solution proceeds on a degree-of-freedom level and does not require assembly of the global stiffness matrix. With a substructure on each processor, the central difference method can provide solutions which require a minimum amount of information to be exchanged between adjacent processors, thereby reducing the interprocess communication. The parallel version is being implemented as a multiple instruction, multiple data (MIMD) method using distributed memory. Synchronization needed between steps is provided by ISIS, a parallel application management tool under development at Cornell University. Care is being taken to provide a layer between the actual message passing routines and the application code to ensure that alternative methods can be easily substituted.

The interactive tools necessary for the analyst to manually partition the model into substructures have been implemented in BASYS. An automatic substructuring algorithm which attempts to minimize the amount of interprocess communication while providing load balancing between the processors has been tentatively selected for implementation[9].

Numerical Examples

As part of experimental research on active control of large flexible space structures[10], a three-dimensional frame has been built in the George Winter Structural Laboratory. This so-called "Cornell 10-meter frame," shown in Figure 1, consists of eleven bays with dimensions of 83.8 cm x 83.8 cm x 45.7 cm. The structure is suspended from four upper (fixed) nodes. The frame has been carefully fabricated from aluminum. The lateral tip displacement in the weak-axis direction for a statically applied tip load corresponds to a flexibility of 0.3 cm/N. The frame is designed to be representative of proposed space structures which are planned for use in a zero-gravity environment. In the model of the idealized structure, the members are aluminum tube stock with a modulus of elasticity of 68.9 GPa. The members are prismatic and have an outside diameter of 1.37 cm and a wall thickness of 0.22 cm. The structural members are modeled with linear beam-column finite elements, connected at moment-resisting joints. The masses have been lumped at the nodes. The translational mass at each node averages 2.15 kg. The rotational mass at the interior nodes is 33.4 $kg-cm^2/radian$ and is 19.6 $kg-cm^2/radian$ at the four bottom nodes. Table 1 shows a comparison between some of the experimentally measured natural frequencies of the structure and those calculated from a calibrated simulation model.

A set of initial conditions corresponding to a lateral tip displacement of 10 cm in the weak-axis direction has been used as a starting point for an actively controlled analysis. The initial conditions, obtained from a static analysis, produce a primarily two-dimensional excitation in the weak axis direction of the actual frame. However, due to the small differences between the front and back Vierendeel

trusses, there is a small torsional component of the structural response.

The frame uses a single linear motor placed above the structure as a controller of weak-axis motion. Two tendons, symmetrically placed with one on each side of the weak-axis frame, run between the linear motor and the bottom of the structure. The lines of action of the tendons lie in a plane midway between the two Vierendeel trusses. The tendons are offset from the structure by stiff standoffs, and a small roller is used at the end of each standoff to reduce frictional losses in the control tendons. Figure 2 is an elevation view of the structure with the tendons shown as dashed lines and standoffs shown as bold lines. Since the tendons can only provide tensile forces, the saturation limit for compressive forces has been set to zero. The controlled analysis included a 0.01 s observation lag. The control law is constant feedback gains based on a limited set of velocity observations. In the model, the four weak-axis velocities at each level of the structure are averaged and used with the appropriate entry of the constant feedback gain matrix to obtain the control forces.

The inherent passive damping of the structure has been assumed to be zero. The analysis has been done using a Newmark-β implicit time integration method. The lateral tip displacement results from a geometrically nonlinear analysis are plotted versus the uncontrolled response in Figure 3. Since the displacements and rotations resulting from this analysis are relatively small, the primary difference between a linear and geometrically nonlinear analysis is a small increase in the high frequency responses of the controlled nonlinear structure.

Additional numerical examples of the capabilities of the software are available[3,5,11].

Closure

A research platform for numerical evaluation of the performance of actively controlled structures subject to dynamic loading has been put in place. The software has been used as a numerical testbed by an interdisciplinary research group with interests in active control of flexible space structures and in CSI. The current capabilities of the software have allowed exploration of a new optimal nonlinear control strategy and have provided a means with which to investigate relevant active control issues in the design and laboratory testing of the Cornell 10-meter frame. Work is ongoing to implement a parallel version of some of the analysis capabilities. Extensions of the research into the subject of control of manuverable and deployable structures has also been begun.

References

(1) Srivastav S., and Abel J., "3-D Modelling of Buildings for Nonlinear Seismic Analysis," to appear in the Proceedings of Eurodyn 90, European Conference on Structural Dynamics, held June, 1990.
(2) Liao L-Z., Shoemaker C., "Convergence in Unconstrained Discrete-Time

Differential Dynamic Programming", <u>IEEE Transactions on
Automatic Control</u>, to appear.

(3) Shoemaker C., Liao L-Z., Aubert B., and Abel J., "Optimal Nonlinear
Control With Geometrically Nonlinear Finite Element Analysis for Flexible
Structures", <u>Computational Mechanics</u>, Atluri A. and Yagawa G.
(editors), Springer-Verlag, 1988, pp. 64.i.1-4.

(4) Lu J., Thorp J., Aubert B., Larson L., "Optimal Tendon Placement of
Tendon Control Systems for Large Flexible Space Structures," <u>Journal of
Guidance, Control and Dynamics</u>, submitted for publication, February,
1990.

(5) Aubert B., Abel J., Lu J., and Thorp J., "Effects of Structural
Imperfections on Constant-Feedback-Gain Control of a Spatial Structure,"
<u>Computing Systems in Engineering</u>, to appear.

(6) Weiler K., "The Radial-Edge Structure: A Topological Representation
for Non-Manifold Geometric Boundary Representations," <u>Geometric
Modelling for CAD Applications</u>, North Holland, 1988, pp. 3-36.

(7) Argyris J., Hilpert O., Malejannakis G., and Scharpf D., "On the
Geometrical Stiffness of a Beam in Space," <u>Computer Methods in Applied
Mechanics and Engineering</u>, Vol. 20, 1979, pp. 105-131.

(8) Hilmy S., and Abel J., "A Strain-Hardening Concentrated Plasticity
Model for Nonlinear Analysis of Steel Buildings," <u>NUMETA 85 Numerical
Methods in Engineering: Theory and Applications</u>, Proceedings of the
International Conference on Numerical Methods in Engineering, Swansea,
U.K., Vol. 1, Middleton J., and Pande G. (editors), A. A. Balkema, Boston,
1985, pp. 305-314.

(9) Farhat C., "A Simple and Efficient Automatic FEM Domain Decomposer,"
<u>Computers & Structures</u>, Vol. 28, No. 5, 1988, pp. 579-602.

(10) Larson L., "Experimental Program for Active Control of Flexible Space
Structures," M.S. thesis, Cornell University, Ithaca, NY, August, 1990.

(11) Aubert B., "Numerical Simulation of the Transient Nonlinear Dynamics
of Actively Controlled Space Structures," Ph.D. thesis, Cornell University,
Ithaca, NY, expected completion, January, 1991.

Published Papers and Reports

Aubert B., Abel J., "Computer Simulation of Control of Nonlinear Structural
Dynamics," to appear in the Proceedings of the 3rd Air Force/NASA Symposium
on Recent Advances in Multidisciplinary Analysis and Optimization, held
Sept., 1990.

Aubert B., Abel J., Lu J., and Thorp J., "Effects of Structural
Imperfections on Constant-Feedback-Gain Control of a Spatial Structure,"
<u>Computing Systems in Engineering</u>, to appear.

Aubert B., "Numerical Simulation of the Transient Nonlinear Dynamics
of Actively Controlled Space Structures," Ph.D. thesis, Cornell University,
Ithaca, NY, expected completion, January, 1991.

Table 1. Experimental frequencies (Hz) vs. theoretical frequencies, Cornell 10 m frame.

Mode	Mode Type	Exp. Frequency	Theo. Freqency	% Error
1	WB	0.6641	0.6614	-0.40
2	WB	1.9920	2.0040	+0.60
3	T	2.2270	2.3906	+7.34
4	WB	3.5160	3.4573	-1.67
5	SB	3.7096	3.9690	+6.99
6	WB	5.3130	4.9697	-6.46
7	WB	6.4450	6.3172	-1.98
8	T	7.1480	7.0756	-1.01
9	WB	7.7730	7.8245	+0.66
10	T	8.7890	8.5854	-2.31
11	WB	9.1020	9.1617	+0.65
12	T	9.6880	9.5274	-1.66
13	T	10.6200	10.1415	-4.50
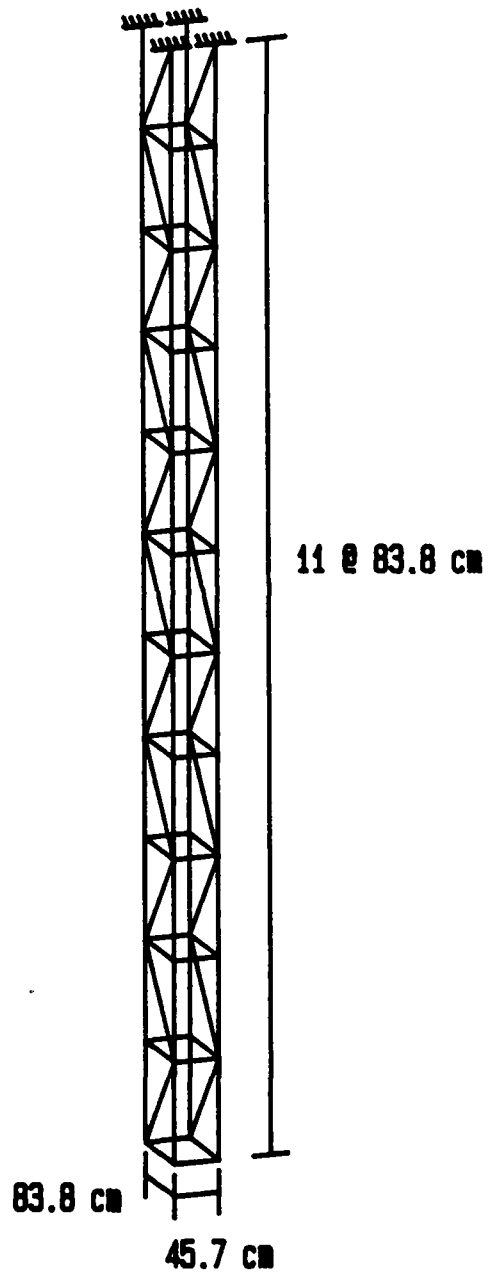
Figure 1. Experimental 10 m frame built at Cornell.

Figure 2. Elevation view of the tendon control used on the 10 m frame.
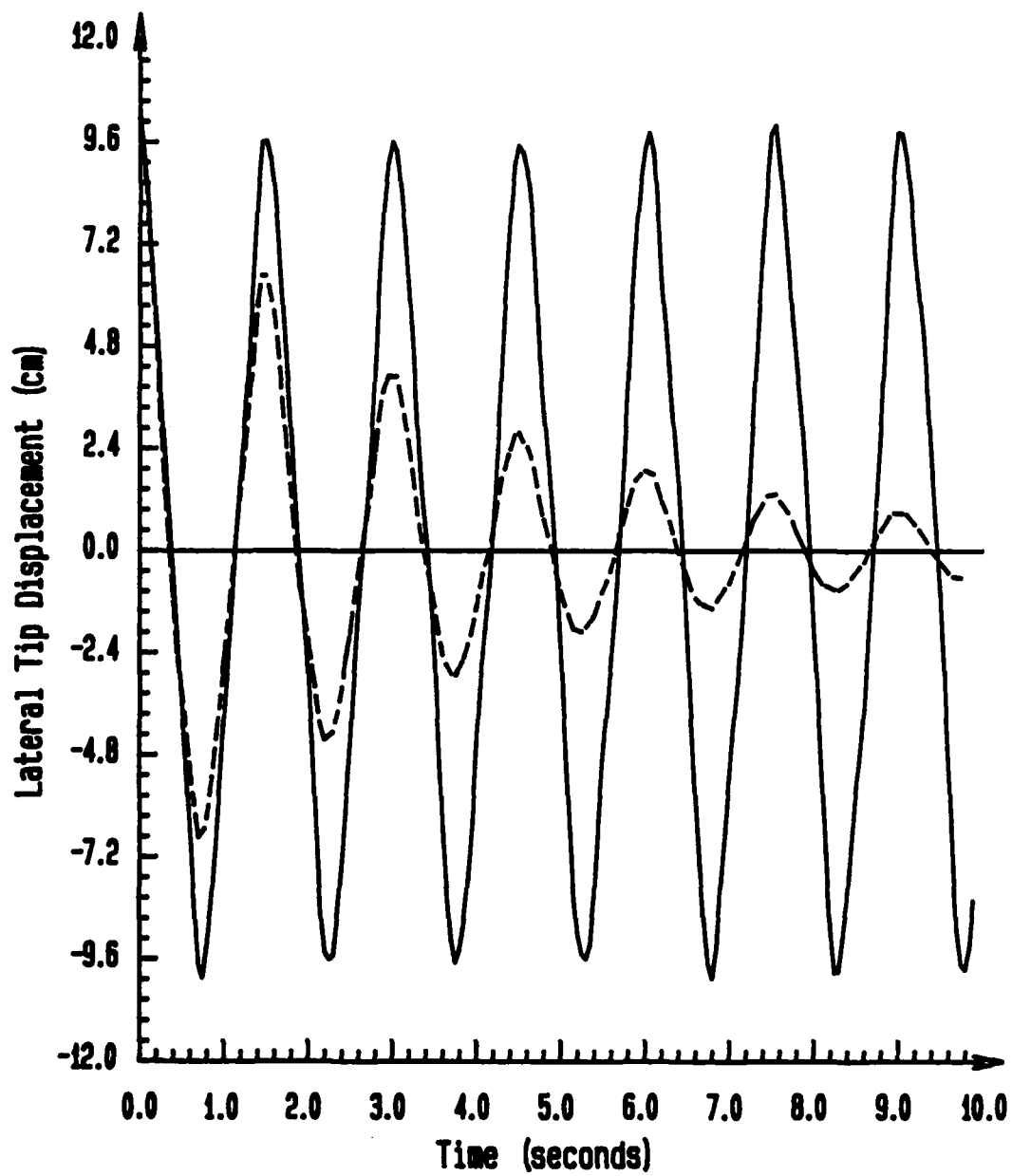
Figure 3. Controlled vs. uncontrolled lateral tip
displacement.

67

PROJECT SUMMARY

Project Title:
Effects of Structural Imperfections on Constant–Feedback–Gain Control of a Spatial Structure

Faculty Leader:
John F. Abel, Civil and Environmental Engineering and Program of Computer Graphics

Graduate Research Assistant:
Brian H. Aubert, Civil and Environmental Engineering and the Program of Computer Graphics

Other Participants:
Professor James S. Thorp, Electrical Engineering
Jin Lu, Graduate Research Assistant, Electrical Engineering

Executive Summary:

The numerical sensitivity of a constant-feedback-gains controller to random structural imperfections is examined using the results of a series of finite element analyses. The basic finite element model, which uses linear beam-column elements, is a 2-D simplification of a large (10 meter long) 3-D frame currently undergoing testing at Cornell University. The cross-sectional properties, nodal coordinates, and masses of the models were randomly varied within four different ranges of maximum imperfection. Twenty transient dynamic analyses were run for each range of structural perturbation. Each analysis used a different random distribution of imperfections. The results of the finite element analyses show that the optimal control configuration, found by dynamic programming, exhibited unacceptable sensitivity to small perturbations of the structural model. A second, nearly optimal, control configuration was found to be more robust with respect to structural imperfections.

Project Description:

A tendon based active control system for a large 3-D structure is being implemented at Cornell University. The tendon forces in the system are calculated by using constant feedback gains in conjunction with a limited set of the state observations of the structure. Tendon based control systems have been previously explored[1-4]. The choice of a tendon based active control system was motivated by the fact that an effective amount of active damping could be provided for several natural modes of a large multi-degree-of-freedom system by using a limited set of actuators

and sensors. In addition, the particular experimental structure undergoing testing allowed the selection of an optimal control configuration by a dynamic programming method[5]. However, by basing the non-collocated, constant-feedback-gains controller on an incomplete set of state observations of the structure, the stability of the closed-loop system in the face of unmodeled structural perturbations cannot be implicitly guaranteed.

Variations between the responses of the modeled and actual structure can be caused by such things as neglecting small geometric or material nonlinearities, not modelling actual joint flexibility, or not accounting for the differences between the finite element model and the real structure due to the presence of fabrication imperfections. While it is possible to develop a sufficiently sophisticated finite element model to represent the system behavior accurately, the increase in the computational cost of the control optimization becomes prohibitive. It is preferable to develop a robust control strategy that performs adequately in the presence of the unmodeled perturbations of the actual structure. In an effort to determine whether the initial optimal control configuration is sufficiently robust, a set of four ranges of fabrication imperfections has been selected. Results from transient dynamic analyses with random distributions of imperfections in the selected ranges have been examined to determine the effects on the closed-loop control performance. The primary goal of the analyses is to expose any weaknesses of the control strategy prior to the first physical control test of the experimental structure.

Structural Model Description

As part of ongoing research on active control of large flexible space structures, a 3-D frame has been built in the George Winter Structural Laboratory. The 3-D frame, shown in Figure 1, consists of eleven bays with dimensions of 83.8 cm x 83.8 cm x 45.7 cm. The structure is suspended from four upper (fixed) nodes. The frame has been carefully fabricated from aluminum. The lateral tip displacement in the weak-axis direction for a statically applied tip load corresponds to a flexibility of 0.3 cm/N. The frame is designed to be representative of proposed space structures which are planned for use in a zero-gravity environment. The flexibility of the frame may require use of geometrically nonlinear analyses for later testing in which the second order effects will be more significant. Masses have been added at the nodes of the frame in order to bring more of the flexural periods of the structure within the frequency response limits of the active control actuator. The joints of the experimental structure are fabricated to provide moment resistance at the member ends. In a finite element simulation, where each beam-column is modeled with a single finite element, the frame has a state vector dimension of 528, consisting of 264 nodal displacements and 264 nodal velocities. The initial experimental testing of the behavior of the controlled 3-D structure includes excitation solely in the weak axis direction. For the initial analysis of the structure, to reduce the computational expense associated with both the control and finite element calculations, a 2-D simplification of the actual 3-D frame

69

has been used. A 2-D model of the frame using a single element between nodes has a state vector dimension of 132. The 2-D model used is shown in Figure 2. Later experimental testing of the structure which may include torsional and strong axis excitation will require the use of a 3-D analysis model.

The 2-D model is a Vierendeel truss consisting of eleven 83.8 cm x 45.7 cm bays suspended from two fixed upper nodes. In the model of the idealized structure, the members are aluminum tube stock with a modulus of elasticity of 68.9 GPa. The members are prismatic and have an outside diameter of 1.37 cm and a wall thickness of 0.22 cm. The structural members are modeled with linear beam-column finite elements, connected at moment-resisting joints. The model mass matrix includes contributions from the members, the connections, and the nodal masses added to the structure to lengthen the structural periods. The masses have been lumped at the nodes[6]. The translational mass at each node is 1.81 kg. The rotational mass at the interior nodes is 33.4 kg-cm^2/radian and is 19.6 kg-cm^2/radian at the two bottom nodes.

To ensure a broad excitation of the natural structural frequencies, a step function has been selected as the load input. The loading is a lateral impact load, applied at a lower tip node with a 22.2 N magnitude. The load is constant for 1.1 seconds after which it is suddenly removed. Any inherent passive damping in the structural model is neglected, allowing the broad spectrum of excited modes to persist in the case of the uncontrolled simulations. The intent of using a step load function and neglecting any inherent passive damping is to bound from above the sensitivity of the model to small imperfections.

Active Control Description

Figure 3 shows the two control configurations used with the 2-D model of the structure. The control force is applied to the structure by rollers at the ends of stiff standoffs (shown as bold lines in Figure 3) at the nodes. The standoffs are much stiffer than the other members and do not significantly contribute to the structural response. Therefore, the standoffs are not explicitly modeled as structural elements. The control force is found by multiplying a set of constant feedback gains by a limited set of system state observations. The fifteen selected observations are the average horizontal velocities, one at each level, and the rotational velocities of the four lowest nodes. The control force is assumed to be uniform along the tendon. The tendon is represented by the dashed lines shown in Figure 3. The assumption of a constant control force means frictional losses along the length of the tendon are neglected. Applying the control force at a distance away from the controlled nodes allows both translational and rotational control forces to be applied to the nodes. For the model used in the control calculations, the control tendon is assumed to be capable of applying both tensile and compressive forces. In a real structure, compressive forces in a tendon are not possible. Instead, two tendons are used with the second tendon using a symmetric

configuration on the opposite side of the structure, as shown in Figure 4. The use of a single tension/compression control to model two tension-only controls is not exact. However, if a robust active control system is obtained, any small errors in the analytical model will not seriously degrade the controlled performance of the structure.

The control configurations used for the tendon based control system are obtained using a dynamic programming method[5]. The dynamic programming uses the standoff lengths as parameters. For fabrication reasons, the actual standoffs come in length increments of 7.6 cm with a maximum length of 22.8 cm. The standoffs can be chosen to extend to either side of either column line. The dynamic programming algorithm has a choice of fourteen different standoff lengths at each level of the 2-D model. The performance index of the dynamic programming algorithm is the amount of damping in the first mode as measured by the size of the corresponding entry in the modal control influence matrix. Initially, optimality of the control configuration is solely based on this performance index. For a structural model in which the mass and stiffness matrices are represented by [M] and [K], the modal control influence vector is the product of the matrix which diagonalizes $[M]^{-1}[K]$ and the control influence matrix. The non-zero entries in the control influence matrix, or vector in the case of one active controller, reflect the proportion of the control force which is applied to the individual degrees of freedom at the controlled nodes. The ratios between the entries of a column of the modal control influence matrix represent the ratios between the amount of active damping provided in those modes for a given set of constant feedback gains. The selection of the control configuration and the sensor locations allows the calculation of the constant feedback gains. The gains are calculated to provide effective active damping in the first ten natural vibration modes of the structure. One important point is that although the 2-D model of the structure appears to be like a cantilever beam, the control configurations imply that the actual first mode behavior of the structure is not that of a cantilever beam. Both of the control configurations are more complex than what would be expected to be necessary to control the first mode of a simple cantilever beam.

The second control configuration was tried after the first, optimal controller exhibited a lack of robustness in simulations with structural imperfections. The first control configuration is sensitive to structural imperfections because the second entry in the modal control influence vector is close to zero. The imperfections can cause the second entry, which corresponds to the second natural mode of the structure, to change sign. When this occurs, the first controller, rather than providing active damping, destabilizes the second mode of the structure. The second controller is selected from a group of nearly optimal (with respect to the first mode) controls which have been found by the dynamic programming algorithm. The second controller is nearly as effective at providing damping in the first mode and is anticipated to be less sensitive to structural imperfections since none of the first ten entries of control influence vector are close to zero and are essentially the same size.

71

Analysis Results

The finite element computations have been done with software developed for nonlinear, transient dynamic analysis of framed structures using one of a variety of direct time integration techniques. These analyses have been run linearly, using Newmark-β implicit time integration with the integration parameters chosen for unconditional stability. The time step is set to 0.005 seconds to ensure reasonable accuracy and to minimize the effects of numerical damping inherent in the solution algorithm. Trials have been run with a time step of 0.001 seconds and no perceptible difference is apparent in the responses of the model. The total time duration simulated by the analyses is 8.0 seconds, corresponding to approximately four fundamental periods of the structure. Beam-column elements are used to model the structural members. One finite element is used for each structural element.

Analyses have been run to examine the performance of the two control configurations and the associated constant feedback gains applied to the ideal structural model. A plot of lateral tip displacement of the idealized structure is shown in Figure 5. The response of the ideal structure with the two different control configurations is compared to the response of the uncontrolled structure. Both controls provide acceptable active damping of the excitation. The control forces for the two different configurations are shown in Figure 6. Although the first controller is optimal with respect to the first mode, the overall control force demand of the second controller is significantly less, indicating that it is more efficient in providing damping in the other controlled modes. Specifically, the second mode periodicity is clearly seen in Figure 6 in the trace of the control force of configuration 1. It is reasonable to expect that the near zero second entry in the modal control influence vector of the first control configuration will result in relatively large constant feedback gains and control forces associated with the second mode.

Four series of analyses with random distributions of structural imperfections have been run for each control configuration. Each series consists of twenty transient dynamic analyses for each control configuration. Three types of structural perturbations have been introduced in the model. The perturbed quantities are selected to attempt to simulate the model uncertainty caused by using nominal structure properties without first taking into account fabrication tolerances and variations in mass and stiffness properties of the actual structure. In order to simulate the variation between the nominal and real stiffness of the structural members, the cross-sectional area and moment of inertia values of the members are randomly varied in the range of ±10% in all four series of analyses. The mass variations between the model and the actual frame are expected to be less than the variations in stiffnesses, so a range of ±5% is used in all four series of analyses. To simulate the differences between the model and the real structure due to fabrication tolerances, four ranges of random nodal perturbations have been selected. The nodal coordinates are randomly varied in the ranges of ±0.0 cm, ±1.3

cm, ±2.5 cm, and ±5.1 cm. The random variation of the structural properties for each analysis is taken from a uniformly distributed sample within the range for the appropriate series. A uniform distribution is selected rather than a normal distribution to provide a more rigorous test of the numerical sensitivity of the control configurations. The ranges of imperfections are selected to encompass imperfections which might realistically be expected to occur in a physical model or prototype.

The results of transient dynamic analyses of the randomly perturbed structures are shown in Table 1. The percentage values listed represent the fraction of the simulations which exhibit a stable response. Instability was found to occur in the modes in which active damping is not provided and in a mode in which active damping is supposed to be present. The instability in a "controlled" mode occurs only in the case of the first control configuration. The majority of the unstable responses of the first controller are caused by the change of sign of the second entry of the modal control influence vector. A plot of a lateral tip displacement for this type of controller instability is shown in Figure 7. The remainder of the unstable responses of the first controller and all of the unstable responses of the second controller occur when a high mode, which is not initially supposed to be actively damped, becomes excited by the control forces. In the absence of small amounts of passive damping in the structure, the high frequency response continues to increase. A plot of lateral tip displacement for this type of controller instability is shown in Figure 8. From the values in Table 1, it is obvious that the first control configuration is unsatisfactory for even small perturbations while the second control configuration performs well in the first three ranges of perturbations. It should be noted that the stability results for the linear analyses of the perturbed models can also be obtained by examination of the closed-loop eigenvalues of the controlled system. The use of transient analyses to determine stability of the controlled structures is dictated by the desire to extend this research into geometrically nonlinear response which would not allow solution for the closed-loop eigenvalues.

The effects of the random imperfections on the open-loop eigenvalues of the models can be seen in Table 2. The results of eigenvalue analyses are shown for the first five natural vibration modes of the models. The tabulated values are the mean periods of the models in a given series and the values in parentheses are the standard deviations from the mean. The maximum difference between the ideal and imperfect simulations is 1.8% for the ±0.0 cm case, 3.5% for the ±1.3 cm case, 4.8% for the ±2.5 cm case, and 11.3% for the ±5.1 cm case. For the first three series of analyses, the small differences between the ideal and imperfect open-loop eigenvalues imply that a well formulated active control will be effective in providing damping. The performance of the second control configuration, indicated in Table 1, supports this.

The performance of the first control configuration is clearly inadequate in all four ranges of imperfections. The fact that the control, when acting on a system with unexpected structural imperfections,

73

destabilizes a low mode is not acceptable. The second control configuration performs as expected in the first two ranges of imperfections. The fact that the second control destabilizes high modes in the third and fourth ranges of imperfections is clearly not desirable. However, it performs more robustly than the first control and is more suitable for implementation on the actual experimental structure. The third and fourth ranges of imperfections also represent extreme levels of fabrication tolerances which may not be acceptable for well built structures.

Conclusions

Discrepancies between the idealized numerical models used to establish control configurations and the actual structure can degrade the performance of active controls. Numerical testing of a control strategy with perturbed numerical simulations can reveal some shortcomings of the active control prior to physical testing. By revealing the unexpected poor performance of the first control configuration, we were able to avoid some serious experimental difficulties. If the first control configuration had been experimentally implemented, valuable time would have been lost as the source of the problem may have been obscured by other possible experimental errors. It should be noted that while sensitivity analysis will not guarantee good experimental performance, it is a means by which some control weaknesses can be exposed. It is found that use of a performance index based solely on the damping provided to a single mode does not result in the most robust control. It has been demonstrated that optimality of the active control configuration must be based on both performance in providing active damping and on some measure of control robustness in the dynamic programming algorithm[5].

References

(1) Y. Murutso, H. Okubo, F. Terui, "Low-Authority Control of Large Space Structures by Using a Tendon Control System", Journal of Guidance, Control and Dynamics, Vol. 12, March-April, 1989, pp. 264-272.
(2) C. P. Pantelides, "Computer-Controlled Structures", Computers & Structures, Vol. 34, No. 5, 1990, pp 715-726.
(3) Roorda, J., "Experiments in Feedback Control of Structures", Structural Control, proceedings of the 1st IUTAM Symposium on Structural Control, Leipholz, H., (editor), North-Holland, Amsterdam, 1979, pp. 629-661.
(4) L.L. Chung, R.C. Lin, T.T. Soong, A.M. Reinhorn, "Experimental Study of Active Control of MDOF Structures Under Seismic Excitations", NCEER Technical Report 88-0025, July, 1988.
(5) J. Lu, J.S. Thorp, B.H. Aubert, L. Larson, "Optimal Tendon Placement of Tendon Control Systems for Large Flexible Space Structures", submitted to Journal of Guidance, Control and Dynamics, February, 1990.
(6) R.D. Cook, Concepts and Applications of Finite Element Analysis, John Wiley & Sons, New York, 1981.

Published Papers and Reports

Aubert B., Abel J., "Computer Simulation of Control of Nonlinear Structural Dynamics," to appear in the Proceedings of the 3rd Air Force/NASA Symposium on Recent Advances in Multidisciplinary Analysis and Optimization, held Sept., 1990.
Aubert B., Abel J., Lu J., and Thorp J., "Effects of Structural Imperfections on Constant-Feedback-Gain Control of a Spatial Structure," Computing Systems in Engineering, to appear.
Aubert B., "Numerical Simulation of the Transient Nonlinear Dynamics of Actively Controlled Space Structures," Ph.D. thesis, Cornell University, Ithaca, NY, expected completion, January, 1991.

Table 1. Results of transient dynamic analyses with the active controls applied to the perturbed structures.

Series	Range of Imperfection	% of Stable Control Trials	
		Configuration 1	Configuration 2
1	± 0.0 cm	85	100
2	± 1.3 cm	55	100
3	± 2.5 cm	15	95
4	± 5.1 cm	5	55

Table 2. Results of open-loop eigenvalue analyses, mean periods (seconds) and standard deviations (seconds).

Mode	Ideal T	Imperfect Analysis Series			
		1	2	3	4
1	2.0303	2.0093 (0.0067)	2.0097 (0.0230)	2.0189 (0.0459)	2.0578 (0.0952)
2	0.6699	0.6627 (0.0023)	0.6631 (0.0060)	0.6656 (0.0111)	0.6756 (0.0211)
3	0.3916	0.3877 (0.0014)	0.3874 (0.0027)	0.3875 (0.0051)	0.3871 (0.0101)
4	0.2753	0.2723 (0.0011)	0.2723 (0.0020)	0.2723 0.0034)	0.2721 (0.0063)
5	0.2106	0.2082 (0.0006)	0.2084 (0.0011)	0.2084 (0.0021)	0.2081 (0.0042)
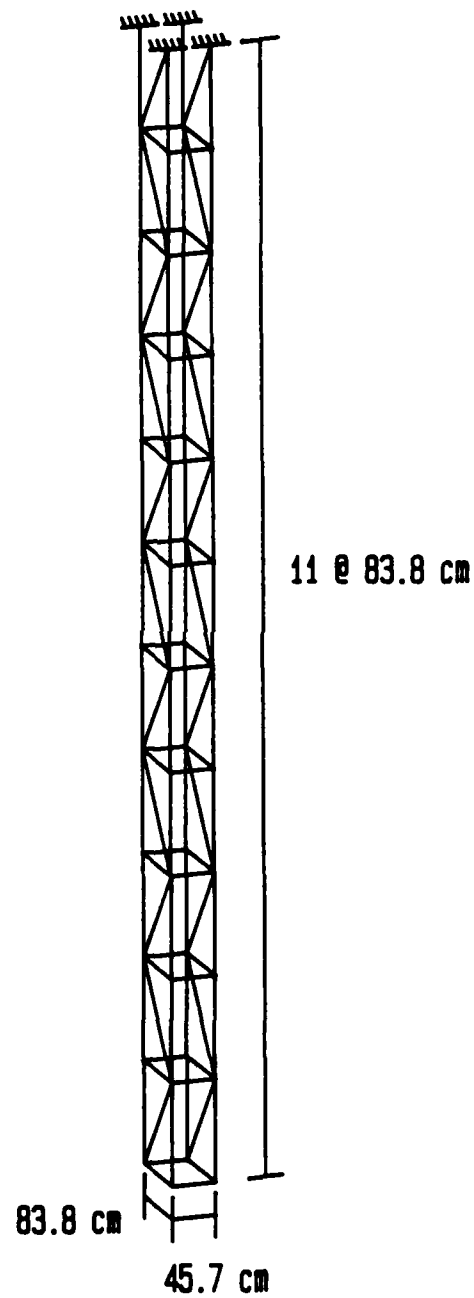
Figure 1.   3-D experimental structure.

11 @ 83.8 cm

45.7 cm
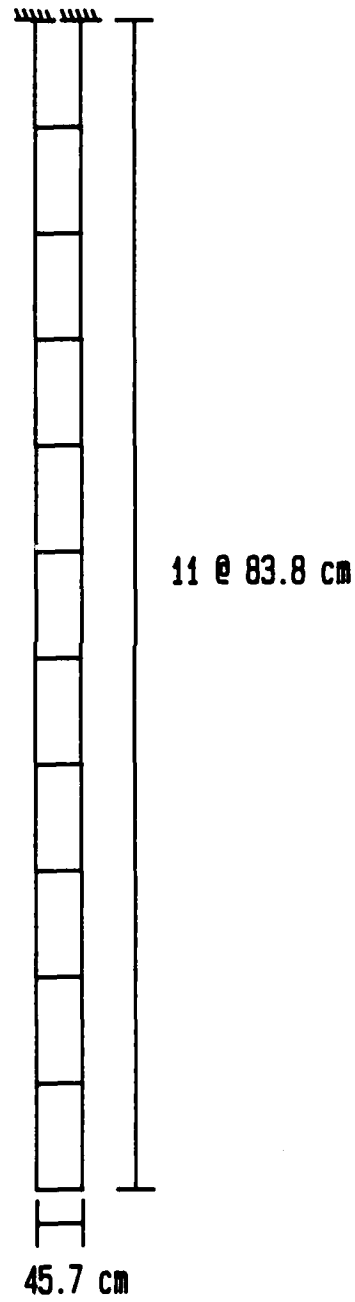
Figure 2. 2-D model of the experimental structure.
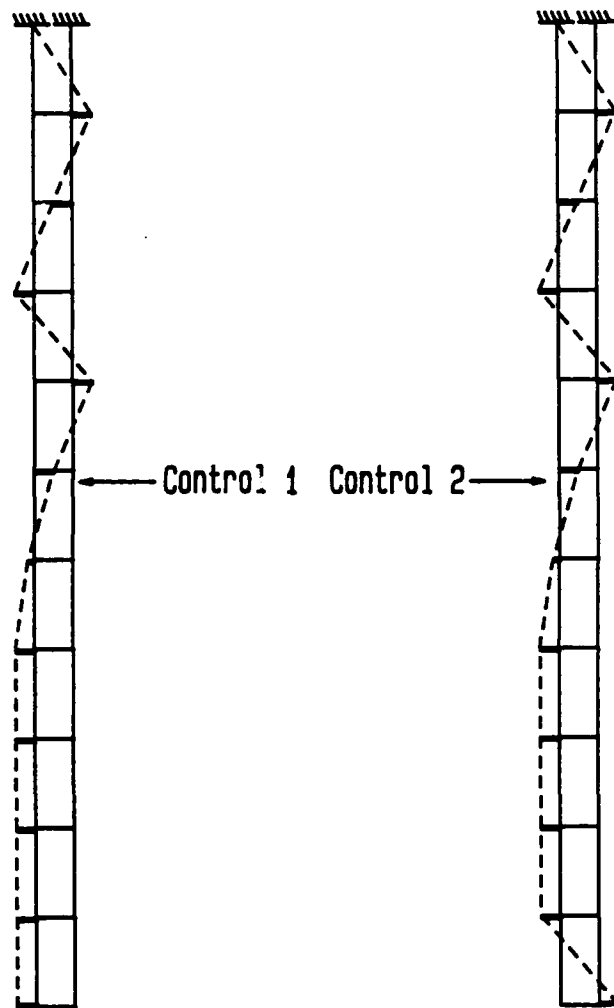
Figure 3.   2-D model with the two different control configurations.

Figure 4. Actual tendon configuration required for an experimental
structure with two tension-only controls.
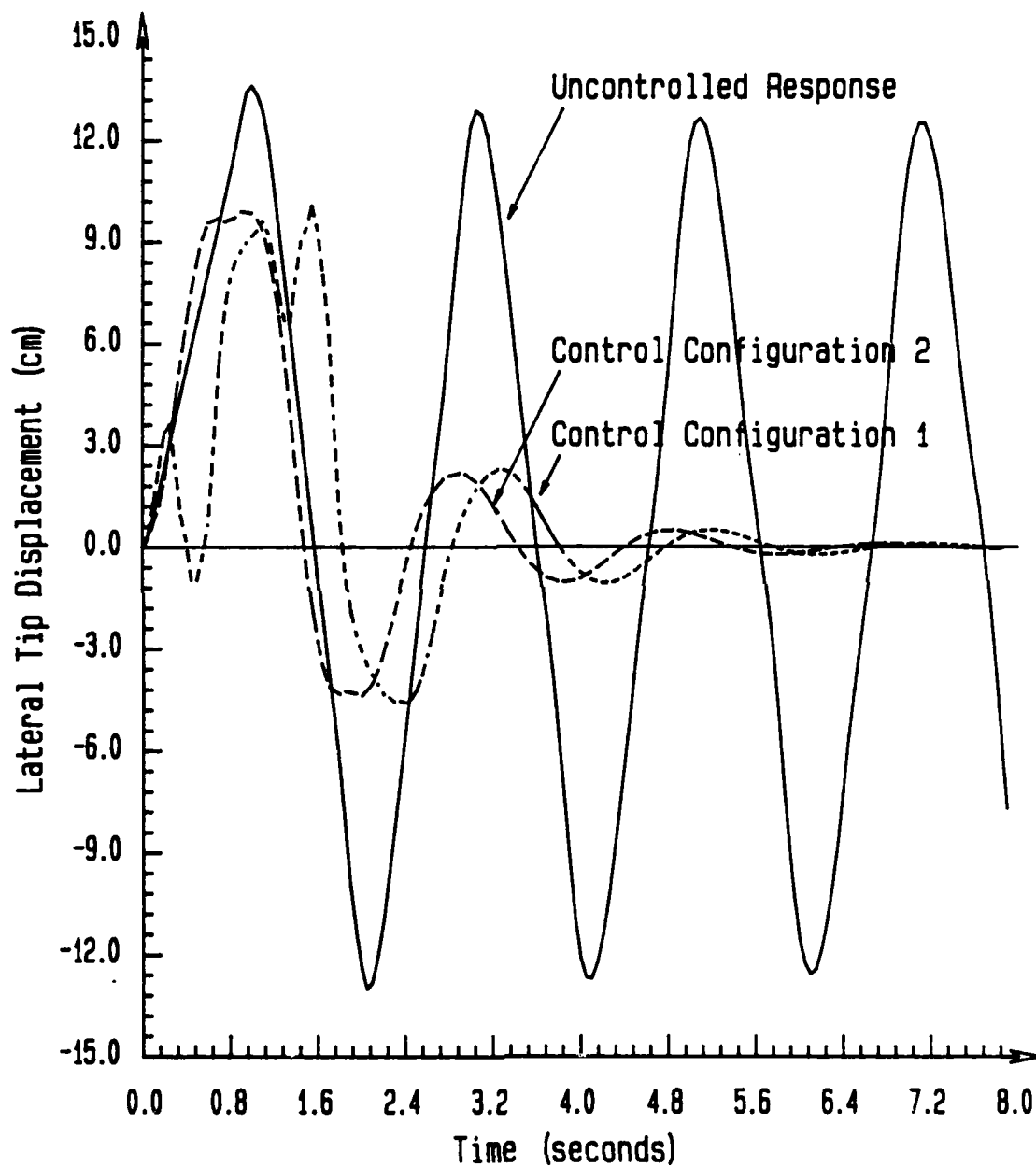
Figure 5. Uncontrolled versus controlled response of the idealized 2-D structure.
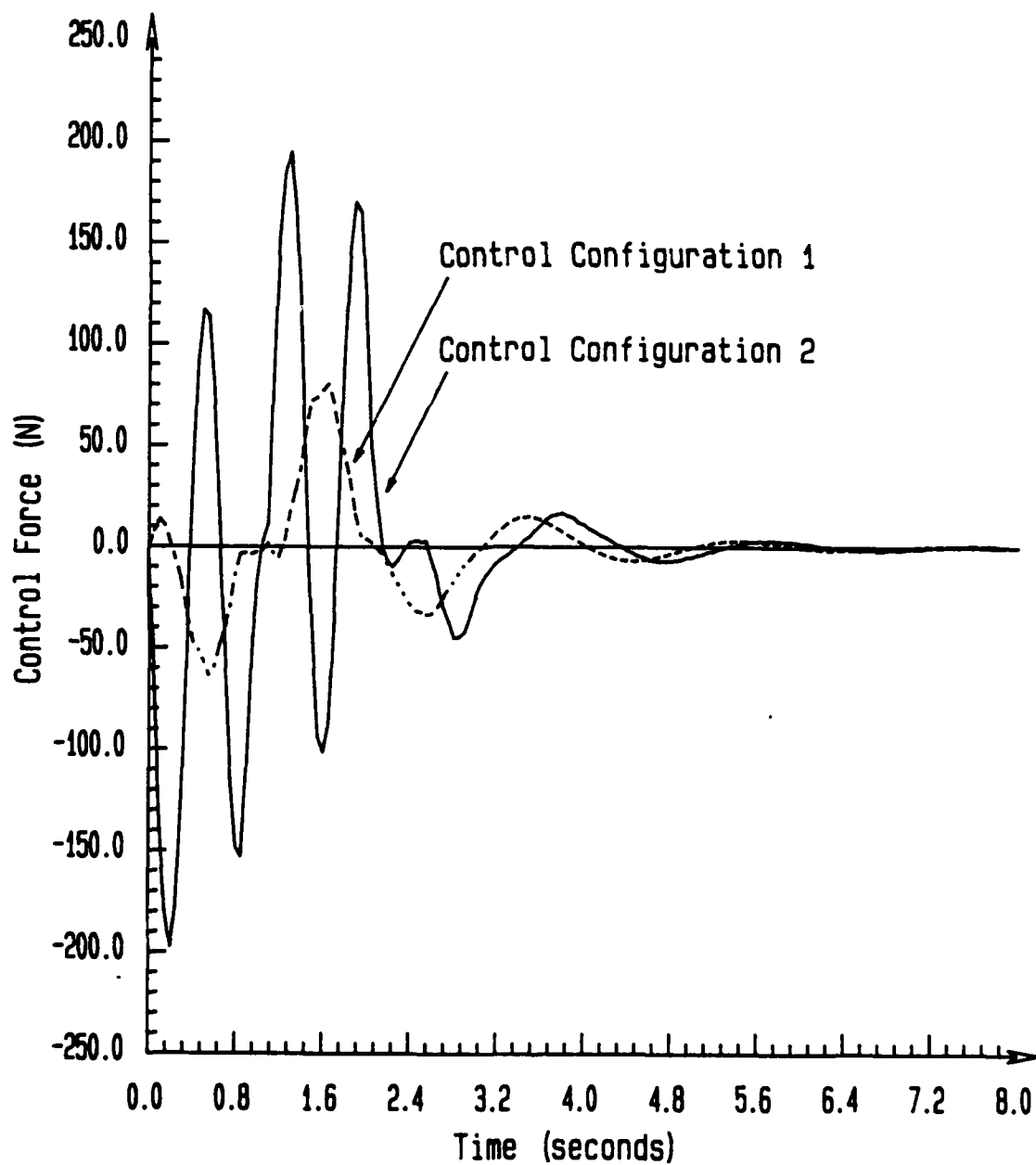
Figure 6. Control forces for the idealized structure, configuration
1 versus configuration 2.
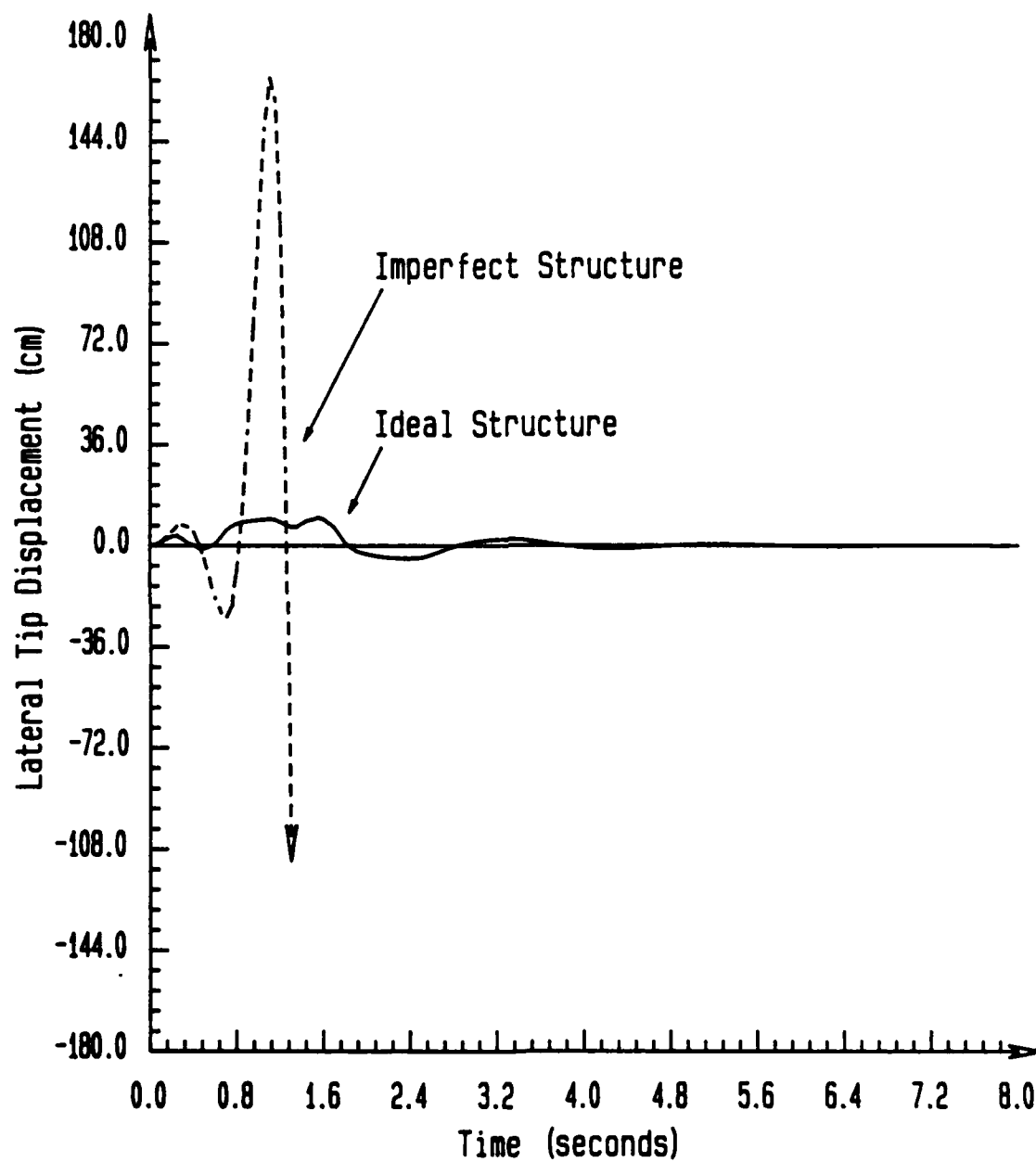
Figure 7. Typical destabilization of a low frequency mode for a
perturbed structure, control 1.
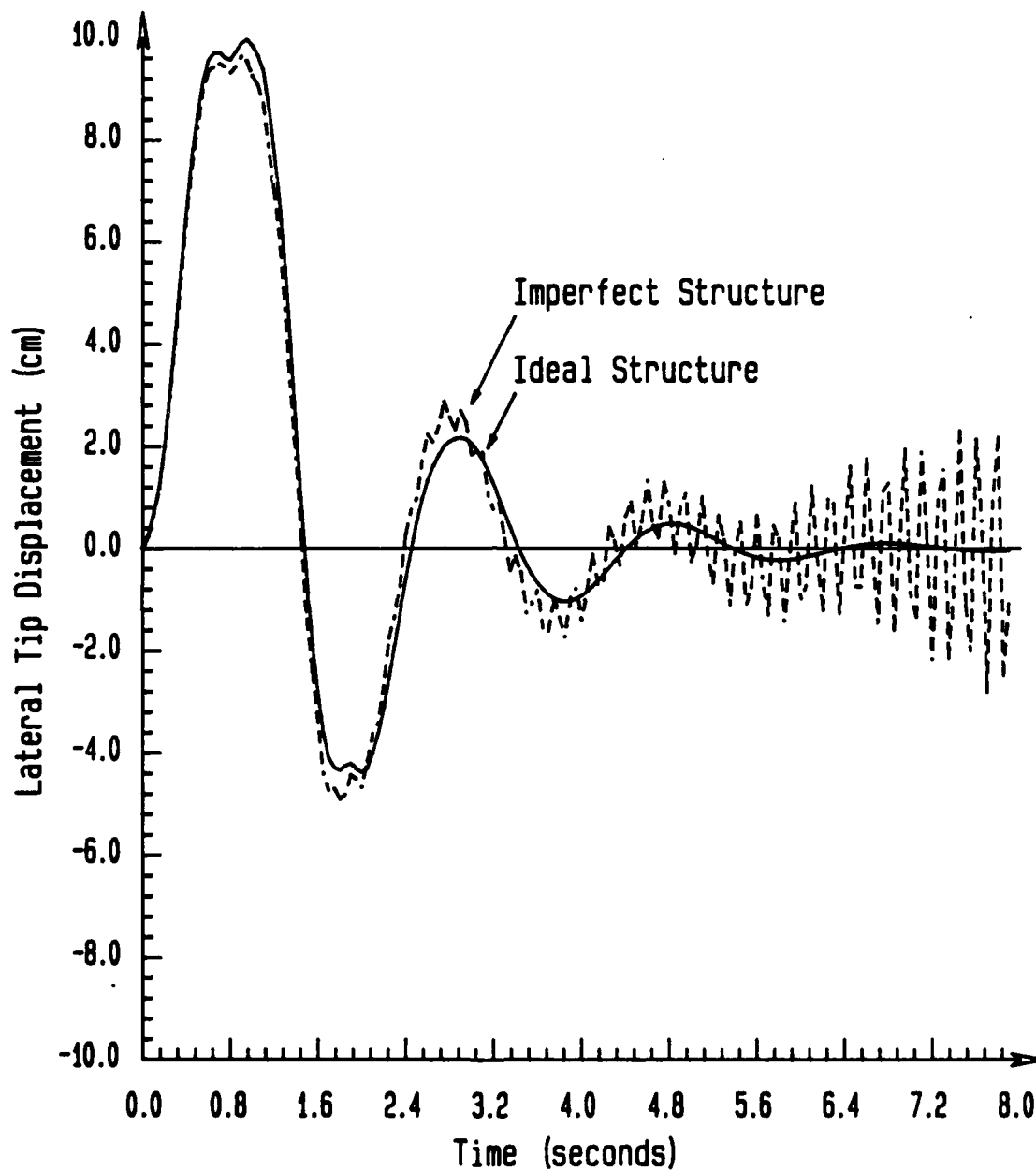
Figure 8. Typical destabilization of a high frequency mode for a
perturbed structure, control 2.

Project Summary:
Experiments on Co-located Feedback Vibration Suppression in a Space Frame Using New Magnetic Actuators[1]

Faculty Leader:
Professor Francis C. Moon
Mechanical and Aerospace Engineering

Graduate Research Assistant:
P.-Y. Chen
Mechanical and Aerospace Engineering

Now at:
Chung-Shan Institute of
  Science and Technology
P.O. Box 90008-15-3
Lung-Tang
Tauyuan, Taiwan, ROC

Summary:

A 6.5-meter long experimental space truss was built to implement the concept of co-located velocity feedback control with multiple channels using new magnetic actuators to damp out large motions. Non-local self-equilibrated internal control forces are applied to suppress the bending vibration of this experimental truss. The control forces are generated through new voice-coil type magnetic actuators with a high force-to-mass ratio manufactured to Cornell specifications by the MOOG Corporation, Aurora, New York. A moving magnet inside a solenoid is employed to pick up the corresponding velocity signal. This magnetic velocity sensor was designed as an integral pat of the actuator to achieve co-location of sensor and actuator force. In order to transmit the nonlocal torque-free control forces, an actuator mechanism was also invented. Unlike the conventional tendon control system, this actuator mechanism is not pre-stressed so that the truss members are not weakened. It is shown that there exist optimal damping ratios for the feedback gains. The experimentally measured damping ratios for the fundamental and second modes using this new actuator/control system were effectively increased up to 9.0% and 16.9%, respectively. Vibration amplitudes of several centimeters can be suppressed with this device.

Project Description:

In the vibration control of large flexible structures for space applications, the choice of actuators plays a key role. Theoreticians often place forces at different locations on the structure without a discussion as to how these forces can be realized. Two actuator concepts widely discussed in the literature are proof-mass [1,2] and gas-jet [3]. Both are what one could call local actuators. The gas-jet idea, however, does not guarantee the conservation of linear and angular momenta of the structure without the addition of other constraints, such as pair-wise control. In contrast to employing a ground-based actuator [4] or a gas-jet, a self-equilibrated internal force is an ideal candidate for the vibration control of a free structure. A number of actuator designs using

---

this concept are also discussed in the literature. They include piezoelectric implanted strutts [5,6], shape-memory alloy [7] and active strutts with hydraulic [8] or electro-magnetic [9] forces. When applied to truss-type structures, these designs can also be thought of as local actuators.

For low frequency vibration, structural deformation is usually not localized at one point, and the potential energy is distributed over the structure. Therefore, a nonlocal control force can perform in this situation more efficiently than a local force actuator. In order to create a nonlocal self-equilibrated internal control force, an actuator mechanism is required to transmit the control force. A tendon control system [10,12] is a typical example. Since a cable is quite flexible and cannot offer a compressive force, the identification and modelling of its dynamics is not straightforward and should receive further study.

A research program was conducted at Cornell to assess the potential for using non-local magnetic actuators in a co-located control system for active vibration suppression of a space truss. Extensive theoretical, numerical and experimental results are reported in the Ph.D. dissertation of the first author [13]. Only some of the experimental results are reported in this paper.

In this research, new magnetic actuators were developed to possess a fast response speed and a high force-to-mass ratio. A new actuator mechanism was also invented to transmit nonlocal torque-free control forces. The required velocity signal is directly measured from a moving magnet inside a solenoid. This velocity sensor was designed as an integral part of the actuators.

The design philosophy of the experimental space truss built in the laboratory was mainly based on two considerations: fundamental natural frequency and linearity. In order to make sure that the response time of the control system (actuators, sensors and feedback circuits) was short enough to control the structural vibration, the fundamental natural frequency of the experimental truss was designed to be around 10 Hz. Another design issue is the linearity of the structural characteristics. One important nonlinear effect that the design sought to prevent was buckling. This linear truss has been designed so that buckling would not occur, as long as the vibration amplitudes at both ends were less than 10 mm.

At this time, a systematic way to decide the optimal placement of actuators and sensors is still under research. However, based on engineering judgment, it seems that an actuator placed across a region with higher strain-energy density will have better performance characteristics. By a process of trial and error, in which the controllers spanned various numbers of bays along the edges or across the faces of the truss, the effective locations of actuators were investigated.

Experimental Set-up

A six-and-half-meter long experimental space truss with rigid joints, (Figure 1), was designed to evaluate the idea of a generalized co-located velocity feedback control using nonlocal actuators. Its cross section is an equilateral triangle measuring 180 mm along each edge, and the slenderness ratio is about 36. Due to the size limitation of the experimental truss in the laboratory, a lumped mass was added at each joint in order to meet the fundamental natural frequency requirement. The frequency thus attained was 10.4 Hz. It turns out that the total mass of this designed truss is about 9.0 Kg: one third is due to truss members, and the remainder is consisted of rigid joints. The truss members, made of Al-2024-T3, are circular rods with 4.8 mm diameter, while the rigid joints, made of Al-6061-T6, are cubic blocks with 31.8 mm edges. They were assembled together with a two-part epoxy to form a truss. In order to prevent each truss member from buckling, the number of bays in this truss was increased up to 24. Finally, in order to simulate a space environment, this truss was suspended by two soft rubber strips.

Based on this simple truss model, the first twenty-two lowest natural frequencies of the suspended truss are calculated and listed in Table I. A refined frame model, which includes the bending effect of truss members, was also adopted for comparison.

Actuators

A custom-ordered magnetic actuator was developed by the Moog Corporation in East Aurora, New York. It is a voice-coil type magnetic actuator, in which the magnetic field is about 8 K Gauss (Figure 2). Its coil was made of a 28 AWG wire. In the vibration control with one actuator, a prototype actuator, whose time constant, defined as the ratio of inductance to resistance, is about 0.6×10^{-3} sec, was used. While, in the second experiment, two new-version actuators, whose time constant is about 1.4×10^{-3} sec, were employed. These new-version actuators have larger output force per unit current and can produce 10.0 Kg force with 0.6 Kg mas. Some basic specifications of the second type of actuators is listed in Table II. All of these actuators were driven by TECHRON 5530 power supply amplifiers. These amplifiers, made by Crown International Inc. in Elkhart, Indiana, have 300 watt output power over a bandwidth of 20 KHz.

Sensors

In order to pick up the required velocity signal which was fed back into the actuators, two types of velocity sensors were considered. One was a commercial linear variable differential transformer (LVDT) [11] with a differentiator. This LVDT, made by the R.D.P. Electronics Ltd. in Wolverhampton, United Kingdom, has a useful bandwidth of 200 Hz. The displacement signal measured by it was fed into the differentiator to obtain the velocity signal indirectly. In this case, the actuator and sensor were arranged in a parallel configuration. The other is a home-made velocity sensor, in which the velocity signal was measured directly from a moving magnet inside a solenoid (Figure 2). The solenoid was made of a 40 AWG wire, and the moving magnet was a somarium-cobalt type magnet. The sensitivity of the velocity sensor used is listed in Table II. In this case, the actuator and the sensor were combined in a serial configuration, as shown in Figure 2.

Actuator Mechanism

Theoretically, the control force determined by the feedback law must be exerted between two remote joints. Because the torsional rigidity of each joint is very soft, a small moment at a joint can greatly degrade the control effort. In the vibration control with one actuator, the numerical simulations for control forces offset by 0 mm and 25 mm are compared. In this analysis, the refined frame model must be used to analyze the bending effect due to the moment created by the offset control force. In the case of 25 mm offset, the offset control force does damp out the relative motion of both ends of controller, but not the relative motion between two remote joints. Therefore, the soft torsional rigidity at each joint can make the offset control force useless. Therefore, as shown in Figure 3, an actuator mechanism was invented to create a torque-free control force. In this mechanism, the force applied between two joints is twice the force generated by the actuator, and the measured velocity at the sensor is also twice the relative velocity between two joints. Therefore, this mechanism also amplifies the feedback gain by a factor of four.

Control with Two Actuators

In this experiment, the actuator mechanisms spanned across five bays, as shown in Figure 1,3. The general bending vibration of the experimental truss was excited by an impact force at one end of the truss, and the acceleration response was measured at the other end. The transient

responses were recorded both for the structure without controller and for various feedback gain combinations in the two actuators. Their time histories and gains (G = 0, 2650, 5300, 10600, 15900 and 21200 Kg/sec) in both actuators are plotted in Figure 4. Many vibration modes are involved in these time histories. In order to focus on the fundamental and second modes, a band-pass digital filter with 20-30 Hz passing bandwidth was used to capture the symmetric and anti-symmetric bending vibration of the lowest mode, respectively. The filtered responses are plotted in Figure 5. For the structure without controller, the lightly damped response gives a 0.4% damping ratio. After the placement of the controller, the damping ratio of the truss increased to 1.5% and 3.6% for the first and second mode, respectively, due to the friction force between moving parts. The contour plots of the damping ratios for the fundamental and second modes versus the feedback gains g_1 and g_2 in two actuators are also plotted in Figure 6. For the fundamental mode, the damping ratio can be increased up to 9.0% for an optimal gain 15900 Kg/sec, in which the output voltage from the velocity sensors is amplified by a factor of 1500 before being fed back into the actuators. For the second mode, the damping ratio can be increased up to 15.9% for an optimal gain 5300 Kg/sec. In this experiment, when the output voltage from the velocity sensors was amplified by a factor of 3000, the controllers started to become unstable, and the oscillating frequency was above 2000 Hz. In this situation, the vibration amplitude of the truss is almost zero, but the output of the power supplies oscillates between two saturation levels. It indicates that the shielding problem of the electromagnetic interference between actuator and sensor is not completely solved yet. Fortunately, the optimal feedback gain had been passed, before the feedback loop began to oscillate.

Under the optimal feedback gain, the damping ratios of the fundamental and second modes for different input levels are plotted in Figure 7. Their performances are quite consistent for different input levels.

Finally, another test was conducted to suppress the single-frequency vibration of the experimental truss, which was excited by a 10 Hz sinusoidal force. (In this case, initially, two actuators are connected to a signal generator to excite the truss at 10 Hz frequency. Then, by switching back to the feedback loop, they are also used to suppress the 10 Hz vibration of the truss. By adjusting the magnitude of the output voltage of the signal generator, the displacement amplitudes of the truss vibration at both ends were driven up to 10 mm. By using the optimal feedback gain, the damping ratios of the free and controlled decays for different displacement amplitude are shown in Figure 8. The damping ratios of free and controlled decays are around 0.5% and 7.2%, respectively.

Numerical Simulation with Two Actuators

For the numerical simulation, the effect of the actuator mass was included as discussed in the Ph.D. dissertation of the first author [13]. The total mass of two controllers is 3.5 Kg, which includes two pair of actuators and actuator mechanisms. For the symmetric disturbance, the displacement responses within ten fundamental periods at one end are found for various feedback gains (g_s = 0, 1700, 9500, 19000 and 38000 Kg/sec), and the damping ratio versus g_s is shown in Figure 9. For the anti-symmetric disturbance, the applied loading is equivalent to two impulse-type anti-symmetric bending couples. The displacement responses within ten fundamental periods at one end are calculated for various feedback gains (g_a = 0, 1100, 5000, 10000 and 20000 Kg/sec) [13]. The damping ratio versus g_a is shown in Figure 10. Both cases demonstrate the existence of the optimal feedback gains. The optimal damping ratios for symmetric and anti-symmetric bending vibrations are around 13% and 17%, respectively. Because of the spill-over effect from the participation of the high-frequency modes, they are smaller than those predicted from numerical simulation. Nevertheless, in both analyses, it is shown that the anti-symmetric bending vibration can be damped out more efficiently than the symmetric one. The reason is that

the two controllers used only cover the regions which have the highest strain energy density for the second mode, but not for the first mode.

Due to the slenderness of the designed truss, it is very difficult to control the torsional vibration by using two-point self-equilibrated control forces. Even worse, the direction of the cross member in each bay is alternating from bay to bay on the experimental truss. The relative axial deflection between two adjacent bays caused by a torsional vibration will cancel out each other. Therefore, the sensors used in the experiment hardly detect the torsional motion, which also makes the control of the torsional vibration impossible. However, if the direction of the cross member in each bay were the same, the actuators used would have some ability to suppress the torsional vibration. In order to increase the effectiveness of the structural control, nonlocal self-equilibrated internal control couples are required. The search for an actuator mechanism to generate this type of control couple is under research.

Finally, extensive numerical experiments were conducted to look at the robustness of this vibration control system to control saturation and mechanical buckling nonlinearities. The results show that the control system should behave well in this nonlinear regime [13].

References

1. T. Kida, I. Yamaguchi, O. Okamoto, Y. Ohkami, Y. Shimamoto, A. Motoe, K. Hirako and S. Ueno, 1986. "A Preliminary Study on a Linear Inertia Actuator for LSS Control," 15th International Symposium on Space Technology and Science, Tokyo, Japan.

2. D.C. Zimmerman, G.C. Horner and D.J. Inman, 1988. "Microprocessor Controlled Force Actuator," Journal of Guidance, Control and Dynamics, 11: 230-236.

3. J. Shenhar and L. Meirovitch, 1986. "Minimum-fuel Control of High-order System," Journal of Optimization Theory and Applications, 48:469-491.

4. A.H. Von Flotow and B.E. Schäfer, "Wave-Absorbing Controllers for a Flexible Beam," Journal of Guidance, Control and Dynamics, 9:673-680.

5. J.L. Fanson and J.A. Garba, 1988. "Experimental Studies of Active Members in Control of Large Space Structures," AIAA/ASME/ASCE/AHS 29th Structures, Structural Dynamics and Materials Conference, Williamsburg, VA .

6. K. Takahara, F. Kuwao, M. Shigehara, T. Katoh, S. Motohashi and M. Natori, 1989. "Piezo Linear Actuators for Adaptive Truss Structures," ASME Winter Annual Meeting, San Francisco, CA.

7. C.A. Rogers, C. Liang and D.K. Barker, 1989. "Dynamic Control Concepts Using Shape Memory Alloy Reinforced Plates," Smart Materials, Structures and Mathematical Issues, Technomatic.

8. P. Gergely, L. Larson, A.R. Ingraffea, J.F. Abel, B. Aubert, L. Liao and M. Minter, 1988. "Experimental Trusses: Open-loop Active Control," URI Annual Report to AFOSR, Cornell University, Ithaca, NY.

9. M. Natori, S. Motohashi, K. Takahara and F. Kuwao, 1988. "Vibration Control of Truss Beam Structures Using Axial Force Actuators," AIAA/ASME/ASCE/AHS 29th Structures, Structural Dynamics and Materials Conference, Williamsburg, VA.

10. Y. Murotsu, H. Okubo and F. Terui, 1989. "Low-authority Control of Large Space Structures by Using a Tendon Control System," _Journal of Guidance, Control and Dynamics,_ 12:264-272.

11. E.O. Doebelin, _Measurement Systems: Application and Design,_ 3rd ed. New York, N.Y.: McGraw-Hill.

12. L.B. Larson, August 1990. "Experimental Program for Active Control of Flexible Space Structures," Cornell University, Ph.D. Dissertation.

13. P.-Y. Chen, May 1990. "Vibration Suppression of Flexible Structures Using Co-located Velocity Feedback and Nonlocal Actuator Control," Ph.D. Dissertation.

Acknowledgement

Figures

Figure 1. Sketch of experimental space truss and locations of suspension rubber strips.

Figure 2. Configurations of actuator and sensor in parallel and serial arrangements.

Figure 3. Schematic diagrams of actuator mechanisms for one and two controllers in the vibration control experiments.

Figure 4. Free vibration time histories of vertical acceleration at one end of truss with two actuators for different feedback gains from experimental test.

Figure 5. Filtered responses of the experimental results in Figure 4 by a band-pass digital filter with frequency bandwidth 20-30 Hz.

Figure 6. Contour plot of the damping ratio of first-mode vibration versus g_1 and g_2 for feedback control with two actuators from experimental test.

Figure 7. Optimal damping ratios versus input level for vibration control with two coupled actuators.

Figure 8. Damping ratios versus vibration amplitude at one end of truss with and without feedback control.

Figure 9. Damping ratios versus g_s from numerical simulation and experimental test with two actuators.

Figure 10. Damping ratios versus g_a from numerical simulation and experimental test with two actuators.

TABLE I - COMPARISON OF NATURAL FREQUENCIES BETWEEN ANALYTICAL TRUSS AND FRAME MODELS, AND MODAL TESTING

Natural frequencies of experimental space truss (Hz)			
	Experiment	Truss Model	Frame Model
SB1	10.37	10.50	10.49
SB1	10.37	10.50	10.49
AB1	27.75	28.44	28.39
AB1	27.87	28.44	28.40
AT1	28.00	28.67	28.54
SB2	52.75	54.32	54.05
SB2	53.37	54.32	54.06
ST1	55.62	57.16	56.89
AT2	82.50	85.41	84.97
AB2	84.12	86.94	86.01
AB2	84.75	86.94	86.01
ST2	109.50	113.10	112.42
SB3	119.75	124.75	121.98
SB3	119.75	124.76	121.98
SL1	127.50	132.88	130.66
ST3	136.00	140.45	139.36

SBn: Symmetric Bending Mode n

ABn: Anti-symmetric Bending Mode n

STn: Symmetric Torsional Mode n

ATn: Anti-symmetric Torsional Mode n

SLn: Symmetric Longitudinal Mode n

TABLE II - SPECIFICATIONS ON ACTUATORS AND SENSORS

Experiment with two controllers		
Velocity sensor	Induced voltage per unit velocity	1.95 V sec / m
Actuator	Resistance	14.7 Ω
	Inductance	20 mH
	Output force per unit current	1.88 Kgf / A
	Induced voltage per unit velocity	N.A.

Figure 1. Sketch of experimental space truss and locations of suspension rubber strips.

Actuator and sensor in serial configuration

Labels in figure: Fixed arm, Permanent magnet, Fixture, Moving magnet, Connecting rod, Sensor solenoid, Actuator coil

Figure 2.   Configurations of actuator and sensor in parallel and serial arrangements.

Actuator mechanism for two controllers

Figure 3.   Schematic diagrams of actuator mechanisms for one and two controllers in the vibration control experiments.

Figure 4.   Free vibration time histories of vertical acceleration at one end of truss with two actuators for different feedback gains from experimental test.

Figure 5.   Filtered responses of the experimental results in Figure 4 by a band-pass digital filter with frequency bandwidth 20-30 Hz.

Figure 6. Contour plot of the damping ratio of first-mode vibration versus g_1 and g_2 for feedback control with two actuators from experimental test.

Figure 7. Optimal damping ratios versus input level for vibration control with two coupled actuators.

Figure 8.   Damping ratios versus vibration amplitude at one end of truss with and without feedback control.

Figure 9. Damping ratios versus g_s from numerical simulation and experimental test with two actuators.

Figure 10. Damping ratios versus g_a from numerical simulation and experimental test with two actuators.

PROJECT SUMMARY

Project Title:
Experimental Truss: Closed-loop Active Control

Faculty Leader:
Professor Peter Gergely
Structural Engineering

Graduate Research Assistant:
Lauran B. Larson

Other Participants:
Professor John F. Abel
Brian Aubert, GRA
Li-Zhi Liao, GRA

Executive Summary:

The first phase of the experimental program, the testing of a 10 meter truss, has been completed. Non-collocated closed-loop active control was achieved using eccentric tendons. A detailed system characterization was first established as input for the control parameter optimization. Active control increased effective damping to about 5% in the first mode from about 0.5% in the uncontrolled case.

Project Description:

The geometric configuration of the 10 meter test specimen is shown in Figure 1. The test setup consists of the specimen itself, the eccentric tendons, linear motor actuator, accelerometers providing the required feedback state variables, signal conditioning, digital motor controller, and the 286 PC with integral A/D conversion board.

Closed loop active control has been implemented by execution of the following sequence during each 15 millisecond timestep of the test:

- Acquisition of 13 state variables (accelerations) hardware integrated and amplified to yield velocities.
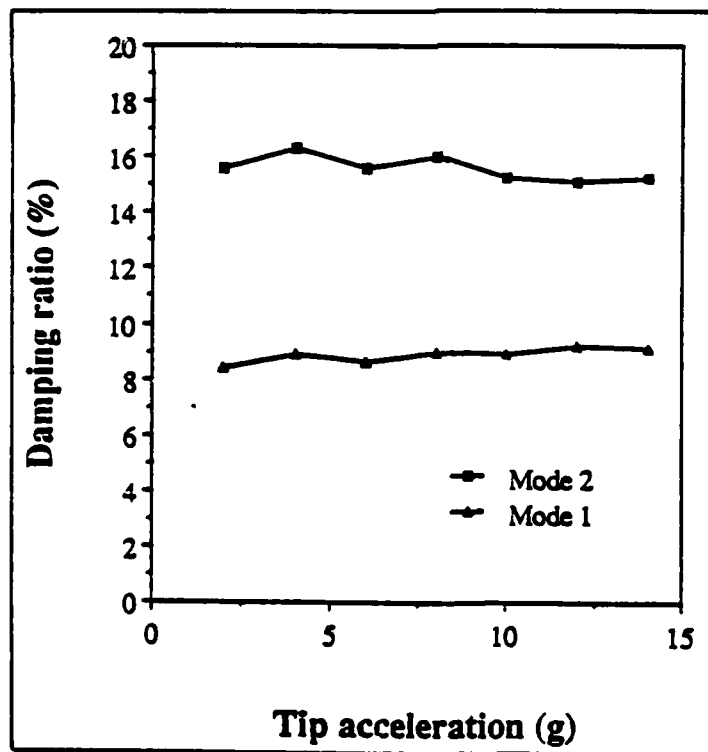- Analog to digital conversion of the velocities.
- Execution of the control algorithm yielding a single acceleration control variable from the 13 velocity feedback variables.
- Writing both the feedback state variables and the resulting acceleration control variable to file for later analysis.
- Transmission of the acceleration control variable to the motor controller and implementation of the commanded acceleration.

Figure 2 shows a block diagram representation of the above live control sequence.

The 10 meter specimen geometry has a high aspect ratio in the direction of primary motion to model the flexibility of satellite structures. The effecting of control by delivery of rotations to joints was investigated in several static simulations wherein the deformed geometry resulting from pure rotations was compared to the expected mode shapes. Diagonals are absent in the primary direction of motion so that the implementation of control through the eccentric tendon can deliver small rotations to the joints as well as translations.

The eccentric tendon control scheme was selected for its efficient delivery of accelerations in the primary direction of motion at each node throughout the length of the specimen. This contrasts previously investigated single or dual actuator location schemes which attempt to counteract vibrations throughout the length of the specimen with forces directed to only a few nodes.

Preliminary tests completed on a small scale specimen resulted in the selection of electromagnetic linear actuators rather than servohydraulic actuators in an effort to eliminate the dynamic non-linearities inherent in servohydraulic systems. The DC linear motors are controlled by a digital controller board in the 286 PC.

The presence of gravity field-induced accelerations in the feedback signals has been investigated by laboratory tests and simulations. We have concluded that, due to the geometry and expected mode shapes of the specimen, the state variables of interest will be read from joints which undergo rotations sufficiently small to make the presence of the gravity field negligible in the feedback signals. These accelerations are then hardware integrated to provide velocities to the control algorithm in the 286 PC.

Since the placement and length of the eccentric tendon offsets were based on an optimization algorithm which targeted the first and second modes, the excitation source for the first series of tests has been an initial displacement and release of the free end of the cantilevered specimen.

A detailed program of static and dynamic characterization of the truss specimen was performed to provide a reference of uncontrolled specimen behavior for comparison with active control results and to provide data used in adjustment of the finite element used in optimizing the control parameters. This characterization process consisted of static stiffness tests of individual specimen components and dynamic tests for identification of system natural frequencies, mode shapes, and damping values. Dynamic characterization tests included experimental model testing for verification of mode shapes, frequency domain testing for accurate identification of model frequencies, and free vibration testing for determination of

uncontrolled damping values.

Feedback data consisted of accelerations recorded at each of the 11 vertical bays of the truss which were digitally integrated to provide velocity feedback. The active control tests consisted of introducing a relatively small lateral disturbance to the free end of the truss specimen immediately after activation of the control system hardware and software. The test data recorded and available for post-processing and analysis included the velocity data at the sensor locations, tendon force data measured at the connection to the tensioning device, and the control force output signal resulting from the control algorithm. Analysis of this data combined with visual observations made during the control tests provided a basis for determining the effectiveness of the active control system and the conditions and causes of control instability.

Results:

The eccentric tendon active control scheme considered in this work provided stable and effective active damping in the range of 5% of critical for random lateral disturbance below a threshold excitation velocity level of approximately 16 cm/sec applied symmetrically at the free end of the truss. The effect of active control is illustrated in Figures 3 and 4. The magnitude of this excitation velocity threshold level appeared to be related to the relationship between the dynamic capability of the control system mechanics and the frequency content of the disturbance.

For disturbances below the threshold, the system mechanics (the linear motor and amplifier) were able to deliver the small tendon force demanded by the control algorithm to the truss specimen sufficiently fast enough to avoid significant phase lags in the achieved control force waveform. When the disturbance was in excess of the threshold level, the system mechanics could not accurately deliver the control force profile demanded by the control algorithm. The result of this phenomena was a significant phase and/or time lag in the achieved control which would at some frequency represent 180 degrees of phase shift which would then drive, rather than damp, the system.

The magnitude of control force effort demanded during stable test runs near the excitation threshold of stability was approximately 40 Newtons. However, repeated tests indicated that this quantity did not, itself, appear to be a criteria for stability since its magnitude varied within both stable and unstable test runs. What appeared to be more important to control success was the frequency content of the excitation source.

Another source of control system instability was observed during the control tests performed prior to installation of the acceleration signal anti-aliasing filters. The aliasing of signals above the sampling frequency into the acceleration data record would, when digitally integrated, result in

corruption of the feedback velocity data used in the control algorithm. Although it was found that the introduction of these filters caused a small reduction in the amount of active damping achieved, control tests conducted subsequent to their installation no longer showed evidence of aliasing-related control instability.

In an effort to identify the individual components of phase and/or tim lag in the control loop, swept-sine input vs. response tests were run for the controller-feedback circuit alone and for the controller with linear motor activated and connected to the truss specimen. In the case of complete control loop, recording accurate phase-lag test data was very difficult as the drive signal passed through a region of resonance with a truss natural frequency. Since the specimen had very little damping, the truss motion would quickly become violent at system resonances.

For the controller-feedback circuit alone, an achieved control signal phase lag of approximately 60 degrees was observed near 6 Hz. The primary reason for this phase las was the need to insert a single stage R/C filter in the load cell conditioning circuit to attenuate a problematic high frequency signal resident in this circuitry. For the complete control system, the control signal phase lag at 6 Hz was closer to 180 degrees, depending on the demanded amplitude of force drive signal.

At the time they were installed on the truss, the control tendons were pretensioned to 50 Newtons. This relatively small degree of tension appeared to be sufficient to prevent slackening and the associated impulse behavior during active control tests.

The data sampling rate of 73 Hz in the outer loop, although not fast by signal processing standards, appeared to be sufficient for acquiring acceleration data used in generating feedback velocities. Although a faster sampling rate would likely improve the resolution of velocity feedback states, the low frequency nature of this test made improvement of the sampling rate a low priority with respect to active control success.

<u>Publications and Reports</u>

"Experimental Program for Active Control of Flexible Space Structures", L.B. Larson, M.S. Thesis, Cornell University, August 1990.

LINEAR MOTOR

TENSION CABLE (shown only on single side of truss for clarity)

MOMENT RESISTING JOINTS IN THIS PLANE OF MOTION

10 m

0.5 m

DIRECTION OF MOTION

ELEVATION

TEST BAY COLUMN INTEGRAL WITH WALL
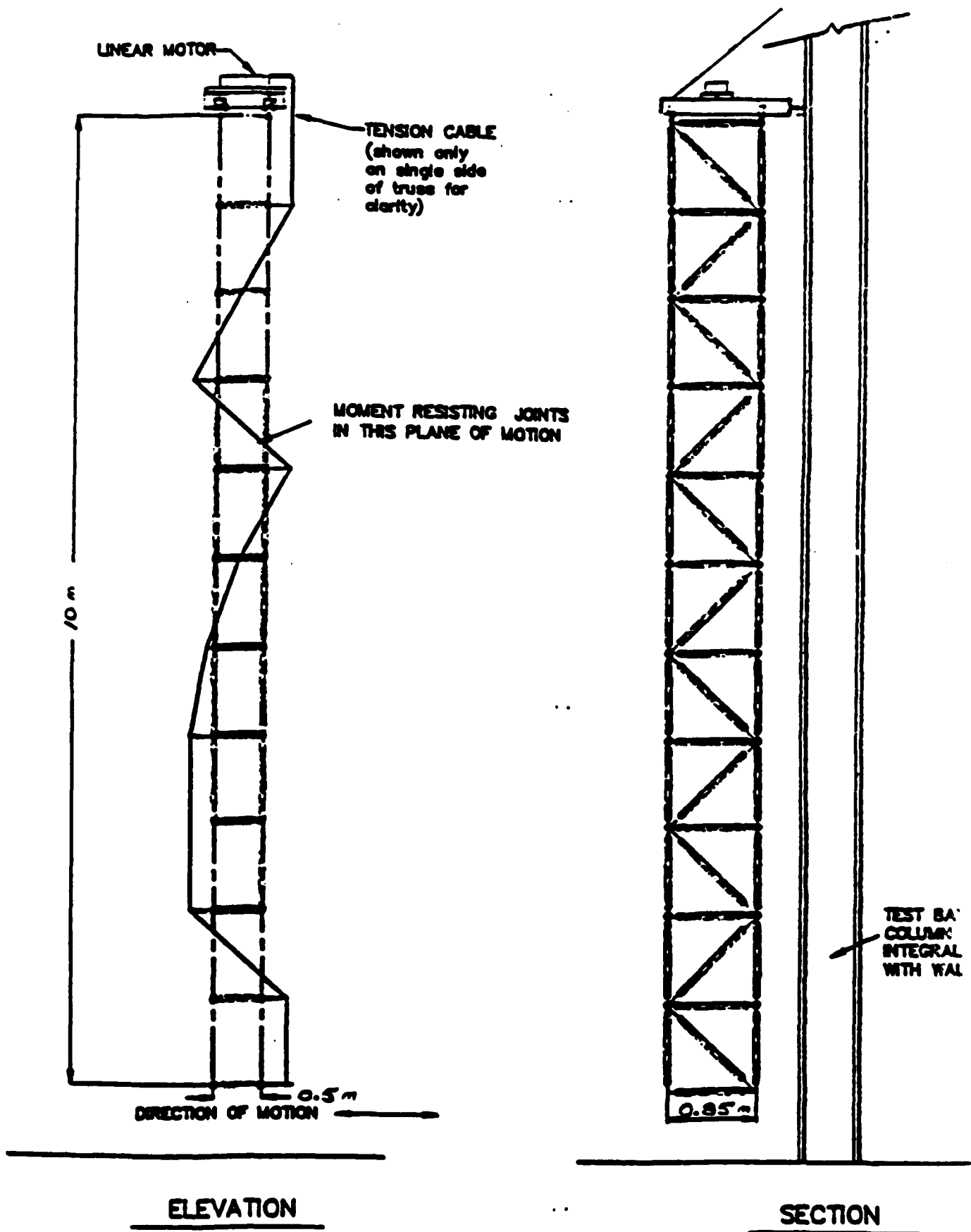
0.85 m
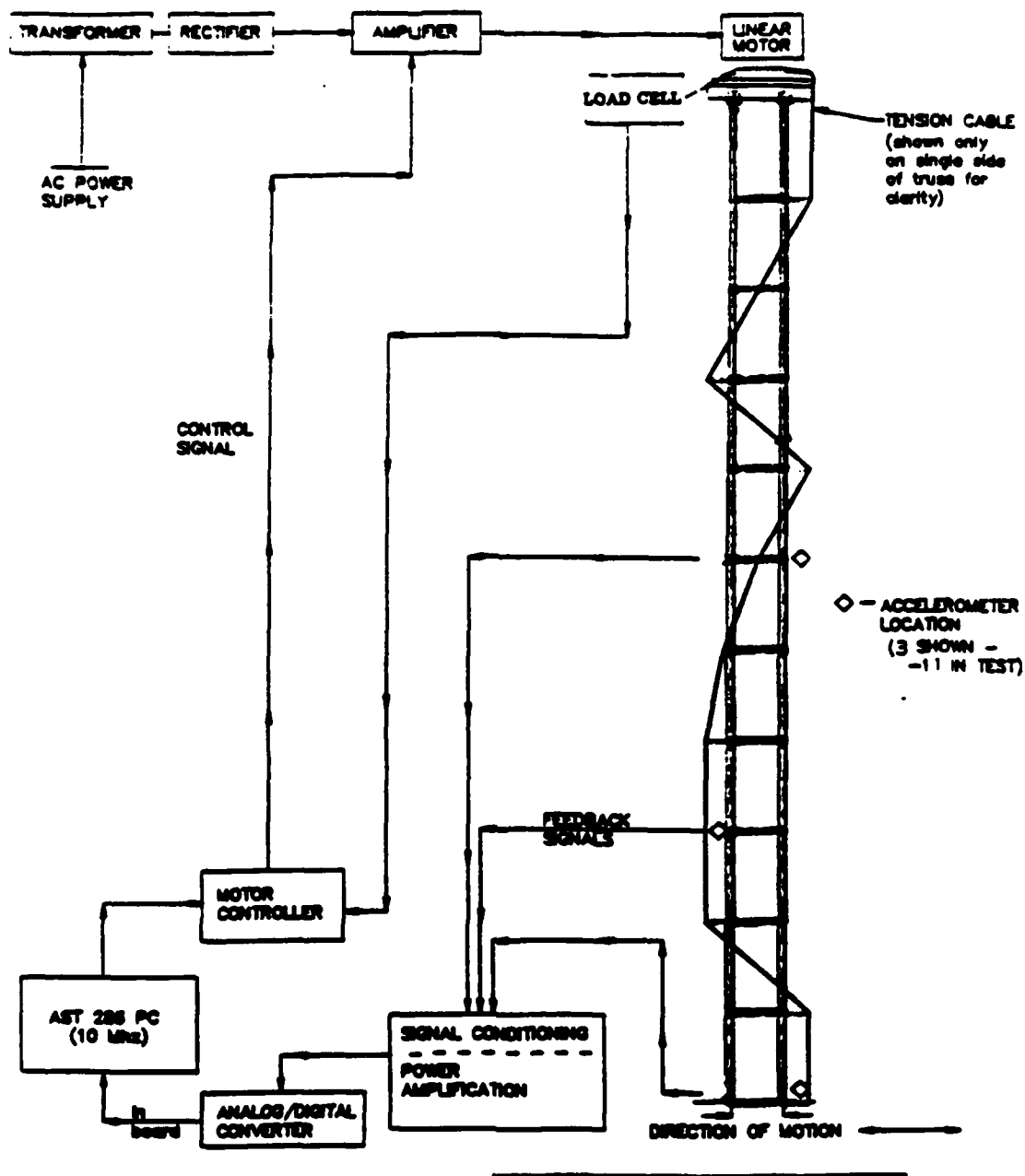
SECTION

Figure 1 Geometry of truss
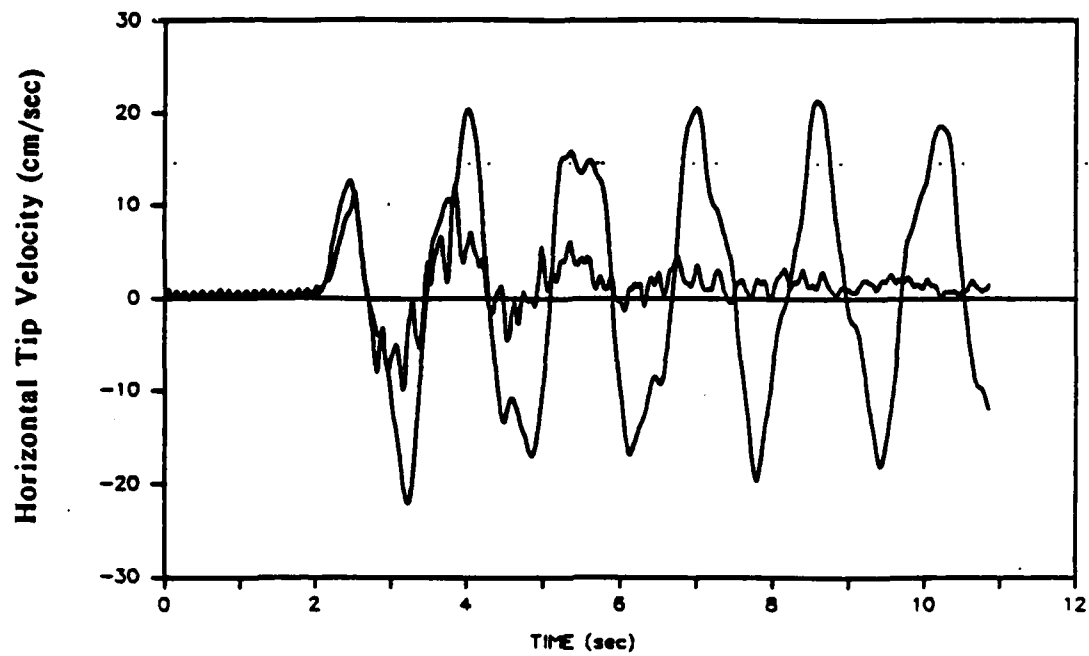
105

Figure 2 Active Control Block Diagram

Figure 3 Ch. 1 controlled and uncontrolled response. No anti-aliasing, V_o= 12 cm/sec
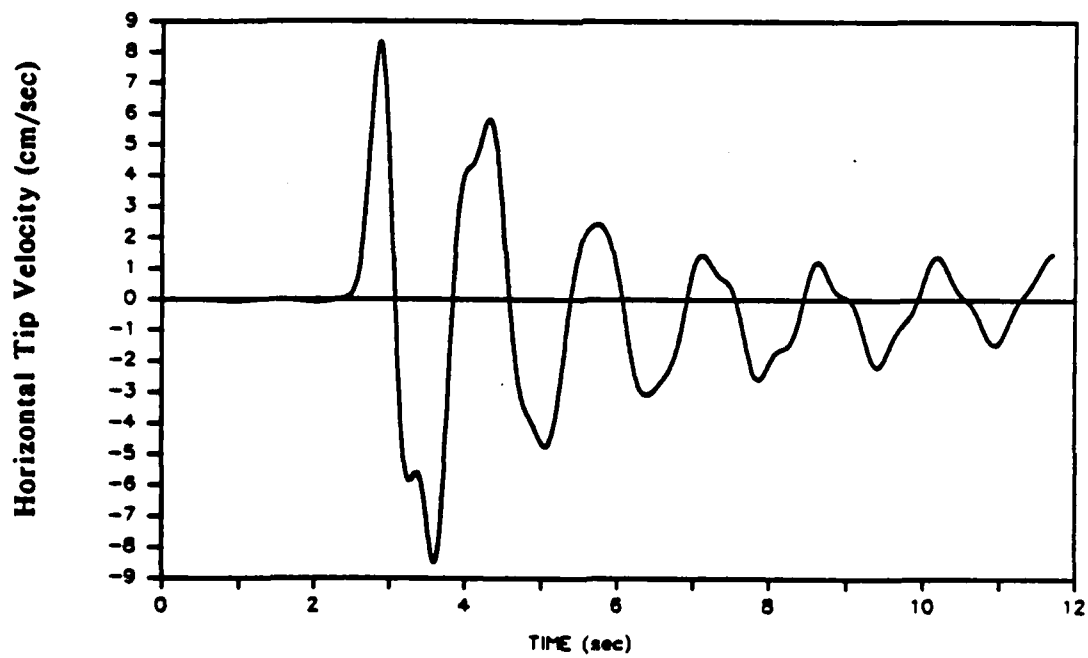
Figure 4 Ch. 1 active control with anti-aliasing. V_o = 16 cm/sec. Modes 1-2.

PROJECT SUMMARY

Project Title:
Control of Large Flexible Structures

Faculty Leader:
James S. Thorp, Electrical Engineering

Graduate Research Assistant:
Jin Lu, Electrical Engineering

Other Participants:
Professor John F. Abel, Civil and Environmental Engineering and Program of Computer Graphics
Brian H. Aubert, Graduate Research Assistant, Civil Engineering and Environmental Engineering and Program of Computer Graphics

Executive Summary:

Problems related to the decentralized active control of large flexible structures to suppress structural vibration are investigated. Attention is focused on the following two problems: (1) optimal locations of actuators and sensors for active control of large flexible structures, in particular, the optimal actuator placement for a 3-D 11-bay truss; (2) characterization of the decentralized controllers which achieve the desired pole placement of large flexible structures, in particular, characterization of velocity feedback control using collocated actuators and sensors. Theories and algorithms are developed for these problems.

Project Description:

The design process of a control system for a large 3-D flexible structure built at Cornell University involves two steps: (1) selection of actuator and sensor locations; (2) design of control law so that the structural damping is enhanced. Theories and algorithms are developed for the two design steps. The theories and algorithms developed are applicable to general large flexible structures.

Selection of actuator locations:
A fundamental problem towards the control of a large flexible structures (LFS) is the determination of optimal actuator locations. Since the choices of actuator locations for an LFS are numerous, the problem of determining optimal actuator locations is by no means a trivial one.

A common approach towards the problem of optimal actuator locations is to optimize actuator locations in the context of LQ regulator (or LQG regulator), i.e.,

to minimize a quadratic performance index over a parameter vector p representing actuator locations and control command u[1]. To solve this problem, one needs to compute matrix Riccati equations for every value of the parameter vector p over its domain (p is a vector of discrete numbers in many cases). This is numerically complicated.

Another approach towards this problem is to assess the sensitivities of critical modes with respect to actuator locations through system eigenstructure analysis, e.g., modal participation factors method. If only one critical mode is considered, the optimal actuator locations can be chosen as the ones with respect to which the mode is most sensitive. However, if more than one critical modes are considered and the sensitivities of modes with respect to actuator locations are inconsistent with each other, this approach does not give a systematic way to make trade-off among actuator locations.

Recently, the problem of optimal actuator locations is studied from the standpoint of controllability [4]. Criteria measuring system controllability are maximized as functions of actuator locations to determine the actuator locations from which the system is strongly controllable. This optimization is generally a combinatorial optimization and there is no efficient way to solve it.

We approached the problem of determining a given number of optimal actuator locations for damping enhancement of critical modes from the standpoint of controllability. First, a new criterion measuring the controllability of critical modes from actuator locations is introduced. Optimization of this criterion leads to a given number of actuator locations from which the critical modes are strongly controllable. These actuator locations are defined as optimal actuator locations. Second, an efficient method is presented for determining the optimal actuator locations. With this method, the optimal actuator locations are easily found by solving a constrained optimization (nonlinear programming) problem.

Optimal tendon placement of a tendon control system for a 2-D 11-bay truss structure

Control systems using different types of actuators for active vibration suppression of large flexible structures (LFS) have been studied intensively in recent years, for example, proof-mass actuator control systems, piezoelectric actuator control systems and tendon control systems. For such flexible structures as beamlike structures and trusslike structures, tendon control systems have been shown to be easy to implement and effective in suppressing vibration[5]. This fact makes tendon control systems an attractive candidate for control systems to be used in a real LFS in the future. Despite its importance, however, there are many unsolved problems related to the design of tendon control systems.

We considered the optimal tendon placement of a tendon control system for the 2-D version of the 11-bay truss built in the Geoge Winter Structural Laboratory, Cornell University (Fig.1). The 2-D 11-bay truss is modeled as a lumped-parameter

linear time-invariant system via finite element method. The control objective is to enhance the damping of critical modes using output feedback control.

Although we may use the method described in the previous section to determine the optimal tendon placement, we found that with the criterion of optimality for the tendon placement being the effectiveness and robustness of the tendon control system, the optimal tendon placement problem can be formulated as a constrained optimization problem which can be solved using dynamic programming; therefore the globely optimal solution to the tendon placement problem can be obtained efficiently.

Eigenstructure(eigenvalues/eigenvectors) assignment using decentralized control

The problem of eigenstructure assignment (simultaneous assignment of eigenvalues and eigenvectors) is of great importance in control theory and applications due to the fact that the stability and dynamic behavior of a linear multivariable system is governed by the eigenstructure of the system. In general, the speed of the dynamic response of the system depends on the eigenvalues whereas the "relative shape" of the dynamic response depends on the associated eigenvectors and generalized eigenvectors. Eigenstructure assignment by state feedback control and output feedback control has received considerable attention over the last decade. Eigenstructure assignment has been used successfully in incorporating highly desirable control requirements, such as robustness of eigenvalue assignment and least gain controller, into eigenvalue assignment by state feedback control and output feedback control[9-12].

Due to the large size of a large flexible structure and the high dimension of its system model, full state feedback control and output feedback control are impractical. This is the reason that decentralized feedback control (an actuator uses only local measurements) is widely used for large space structures. We investigated the problem of eigenstructure assignment of large flexible structure using decentralized control.

Over the past decade, many methods have been proposed for eigenvalue (pole) assignment by decentralized control[13-14]. The philosophy of these methods is to obtain a set of nonlinear equations of the decentralized feedback gain by equating the closed-loop characteristic polynomial of the system with a desired polynomial; then solve this nonlinear equations for the decentralized feedback gain. Since no connection between the closed-loop eigenvectors and the feedback gain is given, these methods do not accommodate eigenvector assignment. We introduce a parametric expression for decentralized feedback gain which achieves the desired eigenvalue assignment. The expression is parameterized by parameters satisfying a set of nonlinear equations. The closed-loop eigenvectors are also expressed as functions of these parameters. With the parametric expression, the parameters can be chosen to assign the eigenvalues and eigenvectors simultaneously. This method is a significant extension of those for eigenstructure assignment by state feedback control and output feedback control.

Modal control of large flexible space structures using collocated actua-

tors and sensors

Direct velocity feedback control(DVFC) using collocated actuators and sensors has been commonly employed in active vibration suppression on large flexible space structures(LFS) due to its inherent property of being energy dissipative and thus robustly stable with respect to the uncertainties in the modeling of LFS [6]. However, it is known that DVFC using collocated actuators and sensors does not achieve as good closed-loop performance as do some control schemes using non-collocated actuators and sensors. For example, a DVFC using collocated actuators and sensors cannot assign the eigenvalues associated with critical modes (low frequency modes) of a LFS arbitrarily. Furthermore, there exists no systematic method for designing the DVFC that achieves the desired eigenvalue assignment when it is possible; it is more often than not that the control is designed on a trial and error basis.

We considered the problem of assigning the eigenvalues associated with critical modes of a LFS into a specified region in the left half plane (LHP) via DVFC using collocated actuators and sensors. The specified region in LHP is chosen so that the critical modes have desired damping. Conditions for the existence of a DVFC using collocated actuators and sensors that can achieve the eigenvalue assignment are derived. When there exist nonunique feasible DVFCs, the one with least Frobenius norm feedback gain is determined. An experimental four-bay truss is used to illustrate the results.

Conclusion

We considered a number of problems related to the active control of large flexible structures. New theories and algorithms are developed to find the optimal actuator locations and design decentralized controllers. These theories and algorithms are applicable to general control systems.

Reference

[1] C. S. Kubrusly and H. Malebranche, "Sensors and Controller Location in Distributed System–A survey," *Automatica*, Vol 21, No.2, pp. 117-128, 1985.

[2] A. M. A. Hamdan and A. H. Hayfeh, "Measure of Modal Controllability and Observability for First- and Second-order Linear Systems," *Journal of Guidance, Control and Dynamics*, Vol. 13, No. 3, May-June, 1990 , pp. 421-428.

[3] M. L. DeLorenzo, "Sensor and Actuator Selection for Large Space Structure Control," *Journal of Guidance, Control and Dynamics*, Vol. 13, No. 2, March-April, 1990 , pp. 249-257.

[4] William N. McCasland, "Fault-Tolerant Sensor and Actuator Selection for Control of Flexible Structures," *Proc. of 1989 American Control Conference*, pp. 1111-1113, 1989.

[5] Y.Murotsu, H.Okubo and F.Terui, "Low-Authority Control of Large Space Structures by Using a Tendon Control System," *Journal of Guidance, Control and Dynamics*, Vol.12, March-April, 1989, pp. 264-272.

[6] Balas, M. J., "Direct Velocity Feedback Control of Large Space Structure," *Journal of Guidance and Control*, vol. 2, May-June 1979, pp. 252-253.

[7] Balas, M. J., "Trends in Space Structure Control Theory: Fondest Hopes, Wildest Dreams," *IEEE Trans. Automat. Contr.*, vol. AC-27, No. 3, pp. 522-535, June, 1982.

[8] T. W. C. Williams and P. J. Antsaklis, "Limitations of Vibration Suppression in Flexible Space Structures," *Proc. of the IEEE Conference on Decision and Control*, Dec. 1989, pp. 2218-2222.

[9] G. Roppenecker and J. O'Reilly, "Parametric Output Feedback Controller Design," *Automatic*, vol. 25, No. 2, pp. 259-265, 1989.

[10] M. Tarokh, "Approach to pole assignment by centralized and decentralized output feedback," *IEE Proceeding*, vol. 136, Pt. D, No.2 pp. 89-97, March 1989.

[11] B. C. Moore, "On the Flexibility Offered by State Feedback in Multivariable Systems Beyond Closed Loop Eigenvalue Assignment," *IEEE Transactions on Automatic Control*, vol. AC-21, pp. 689-692, Oct. 1976.

[12] A. N. Andry,Jr, E. Y. Shapiro, and J. C. Chung, "Eigenstructure Assignment for Linear Systems," *IEEE Transactions on Aerospace and Electronic Systems*, vol. AES-19, No. 5, pp. 711-729, Sept. 1983.

[13] J. H. Chow and M. A. Kale, "Decentralized Local Pole-Placement Control Designs Using Static Output Feedback," *Proc. 1989 American Control Conference*, pp. 236-241, June. 1989.

[14] S. Lefebvre, S. Richter and R. DeCarlo, "A continuation algorithm for eigenvalue assignment by decentralized constant output feedback," *Int. J. Control*, vol. 41, pp. 1273-1292, 1985.

Published Papers and Reports

Jin Lu, Hsiao-Dong Chiang and James S. Thorp, "Partial Eigenstructure Assignment and Its Application to Large Scale Systems" to appear in *IEEE Transactions on Automatic Control*, January, 1991.

Jin Lu and James S. Thorp, "Modal Control of Large Flexible Structures Using Collocated Actuators and Sensors," to appear in *IEEE Transactions on Automatic Control*, July, 1991 (also in *Proceeding of 1990 Conference on Information Sciences and Systems*, Princeton, NJ).

James S. Thorp, Jin Lu, and H. D. Chiang, "Actuator Placement for Modal Control of Large Flexible Structures," revised and under re-review for publication in *Journal of Dynamic Systems, Measurement, and Control*.

Jin Lu, Hsiao-Dong Chiang and James S. Thorp, "Eigenstructure Assignment by Decentralized Feedback Control," submitted to *IEEE Transactions on Automatic Control*.

Jin Lu, James S. Thorp and Brian H. Aubert, "Optimal Tendon Placement of Tendon Control Systems for Large Flexible Space Structures", accepted for presentation at the *1990 CDC*, Honolulu, Hawaii, Dec. 5-7, 1990.

Jin Lu, Hsiao-Dong Chiang and James S. Thorp, "Velocity Feedback Control and Its Application to the Design of Stabilizers in Multimachine Power Systems," *Proceeding of 1989 American Control Conference*, pp. 1252-1257, Pittsburgh, PA, June, 1989.

Jin Lu, James S. Thorp and H. D. Chiang, "Design of Linear Multifunctional Observers with Unfixed Feedback Gain," *Proceeding of 1989 Conference on Information Sciences and Systems*, pp. 562-566, Baltimore, MD, March, 1989.

H. D. Chiang, James S. Thorp, Jincheng Wang and Jin Lu, " Optimal Controller Placements and Designs in Large Scale Linear Systems," *Proceeding of 1989 American Control Conference*, pp. 1615-1620, Pittsburgh, PA, June, 1989.

Aubert B, Abel J., Lu J., and Thorp J., "Effects of Structural Imperfections on Constant-Feedback-Gain Control of a Spatial Structure," to appear in *Computing Systems in Engineering*.
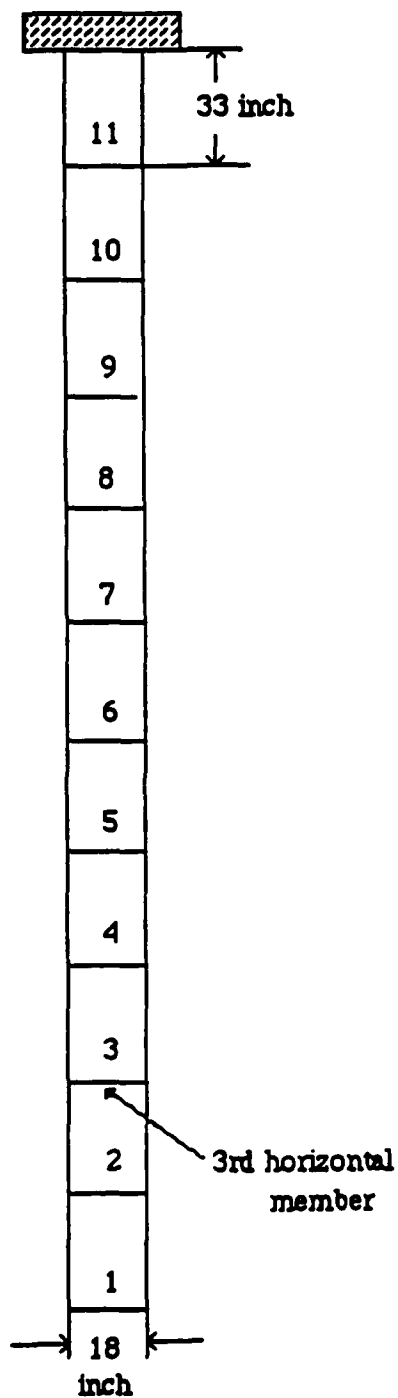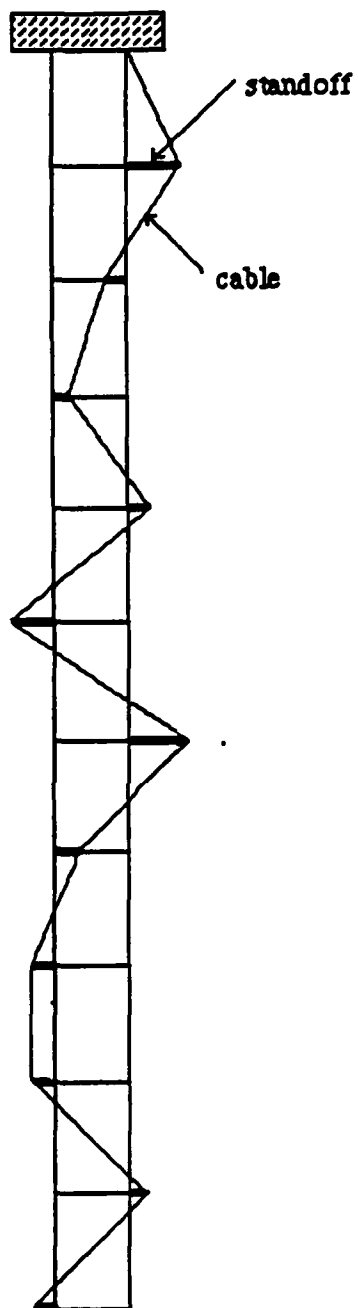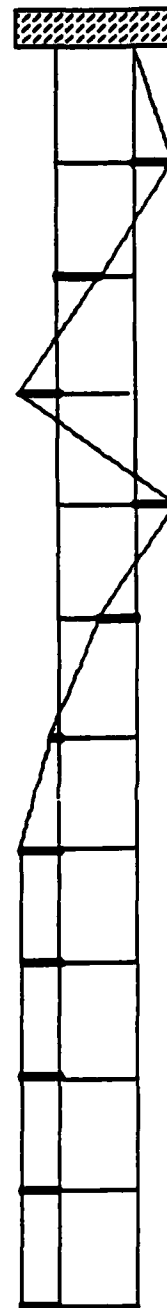
Fig. 1: 11-bay truss

Fig.2: Feasible actuator

Fig.3 : The optimal feasible actuator

PROJECT SUMMARY

Project Title:
Optimal Nonlinear Control with Geometrically Nonlinear Finite Element Analysis for Flexible Structures: Some Preliminary Results[1]

Faculty Leader:
Dr. Christine A. Shoemaker
Civil and Environmental Engineering

Graduate Research Assistants:
Li-Zhi Liao and Brian Aubert

Other Participant:
Dr. John F. Abel
Civil and Environmental Engineering

Executive Summary:

There is an extensive literature on the application of optimal control techniques to flexible structures but the majority of this research deals with LQ (Linear system dynamics, Quadratic Performance Function) techniques that assume the system dynamics are linear. There is little literature on nonlinear control of structures and, to the authors' knowledge no previous research on the coupling of nonlinear optimization and nonlinear finite element structural models. The major advantage of LQ is that feedback control can be rapidly computed. It has been hoped that LQ control policies computed on the basis of a linear approximation of nonlinear dyanmics will work reasonably well on nonlinear systems.

The optimization algorithm used in this analysis is Differential Dynamic Programming (DDP) which was originally introduced by Jacobson and Mayne (1971). Computational advances and a DDP algorithm for constrained optimization have been reported recently (Yakowitz, 1986).

This paper reports preliminary development of computational algorithms to compute the optimal control of systems described by geometrically nonlinear finite element equations and the application of these methods to the

---

[1]Published in <u>Computational Mechanics</u>, A.N. Atluri and G. Yagawa (eds.), Springer-Verlag, 1988.

active control of flexible structures. The initial results indicate that nonlinear DDP optimal control policies based on the nonlinear dynamics of a structure perform significantly better for nonlinear structures than do the conventional linear control policies.

The dynamics of the structure are described by:

$$M \ddot{d}_t + C \dot{d}_t + K(d_t) \, d_t = p_t + B(d_t) \, u_t \tag{1}$$

where:

d_t — the vector of nodal displacements at time t

$K(d) = K_0 + K_1(d) + K_2(d^2)$ — the stiffness matrix

M — diagonal mass matrix

C — mass proportional viscous damping matrix

$B(d_t)$ — control influence matrix

p_t — external load history vector

u_t — control forces vector

The criterion used to select the optimal policy is the objective function suggested by Miller et al. (1985):

$$\sum_{t=1}^{T} \theta_{mt} \, \dot{d}_t^T M \, \dot{d}_t + \theta_{kt} \, d_t^T K_0 \, d_t + \theta_{bt} \, u_t^T B_0^T K_0^{-1} B_0 \, u_t \tag{2}$$

where the θ's are weighting functions and:

$\dot{d}_t^T M \, \dot{d}_t$ — a measure of kinetic energy

$d_t^T K_0 \, d_t$ — a measure of strain energy

$u_t^T B_0^T K_0^{-1} B_0 \, u_t$ — a measure of potential energy

The terms K and B introduce geometric nonlinearities into the system because they are functions of d. The control force is assumed to act on a diagonal between two nodes; hence the nonlinear terms in B depend upon trigonometric functions of the nodal displacements. The system in eq. (1) is integrated with an explicit time-marching scheme because such an approach permits closed-form expressions for the partial derivatives of the transition-function matrices needed in the DDP equations.

The difference between linear and nonlinear controllers is demonstrated by the dynamics of controlled and uncontrolled systems described in Figures 1 and 2. Figure 1 depicts the two-bay truss analyzed, and compares the uncontrolled behavior of a linear system and a nonlinear system due to a transverse impact load on a tip node. Figure 1 demonstrates that the two uncontrolled responses are quite similar, enough so that one could be led to predict that a linear control policy would work quite well on the nonlinear as well as the linear structure.

116

Figure 2 compares linear control policies on the nonlinear structure to the DDP policy derived for the nonlinear structure. In one case the linear policy is applied open loop, i.e., the control law is not based on an obserrvation of the state vector (d_t, $\dot{d}_t$). The results indicate that much better control is achieved by using the DDP nonlinear control than by using the open loop linear control. The third curve in Figure 2 is the result of the application of the the linear control law with feedback. In this case the control law is based on the displacements and velocities one time step (.025 sec) before the implementation of the control law. Both simulations and actual practice would require some delay between the measurement of the state and the implementation of the control. Although the concept of a feedback control is attractive, it is also difficult and probably infeasible in practice to be able to measure accurately all displacements and velocities. Figure 2 indicates that even if perfect measurements could be made at each time step, the linear control with feedback does not perform as well as the nonlinear DDP control that is obtained from the true nonlinear dynamics of the system.

The computational requirements of DDP are of the order of

N^3 · T · Number of Iterations

if N > M where

N — dimension of the state vector (which includes nodal displacements and nodal velocities)

M — dimension of the control forces vector

T — the number of time steps

For the problem described in Figures 1 and 2, N — 16, M — 1, and T — 200. DDP applied to explicit structural dynamic simulation requires a large number of time steps. DDP, which depends only linearly on the numer of time steps, is more efficient for these problems since other noninear optimal control methods have computational requirements that grow in a polynomial or exponential fashion with the number of time steps. However, any nonlinear method, DDP included, is much more demanding comuationally than are the linear procedures. We are exploring ways to increase the efficiency of DDP and to reduce the number of time steps required for the analysis.

REFERENCES

1. Jacobson, D. H. and Mayne, D. Q., <u>Differential Dynamic Programming</u>, American Elsevier Publishing Company, Inc., New York, 1970.

2. Miller, D. F., Venkeyya, V. B., and Tischler, V. A., "Integration of Structures and Controls — Some Computational Issues," Proceedings of 24th Conf. on Decision and Control, pp. 934-941, 1985.

3. Yakowitz, S. J., "The Stagewise Kuhn-Tucker Condition and Differential Dynamic Programming," <u>IEEE Trans. Auto. Control</u>, vol. AC-31, pp. 25-30, 1986.
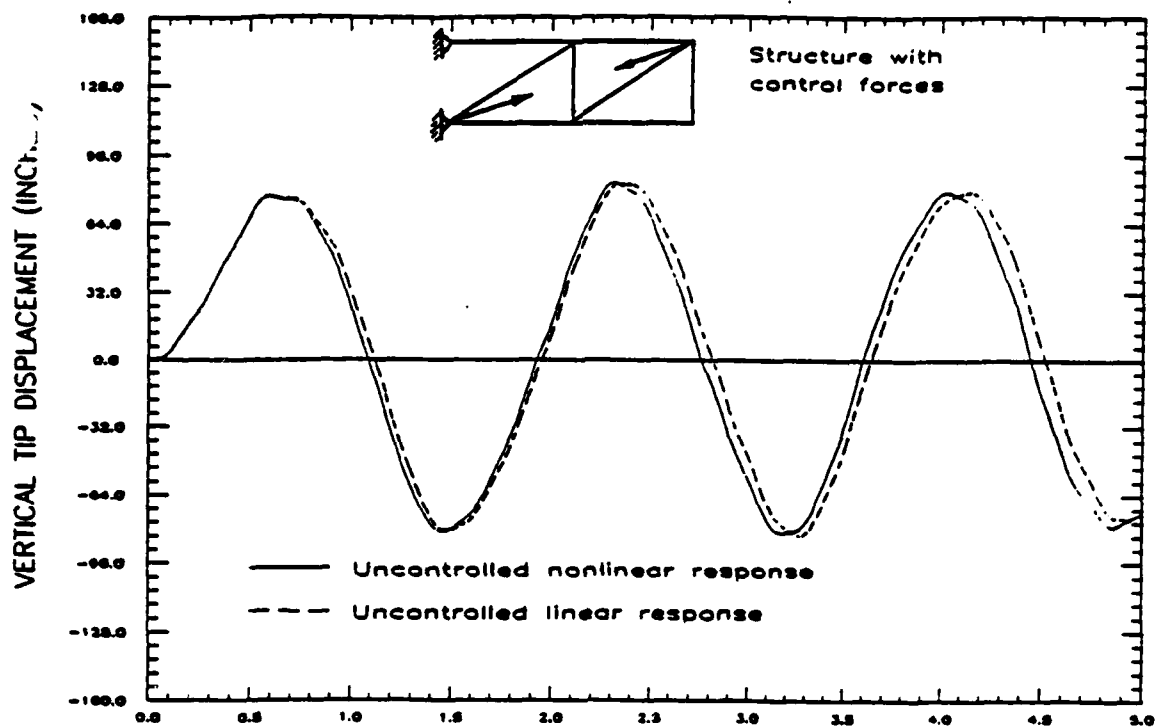
Figure 1. Truss analyzed, with nonlinear and linear uncontrolled
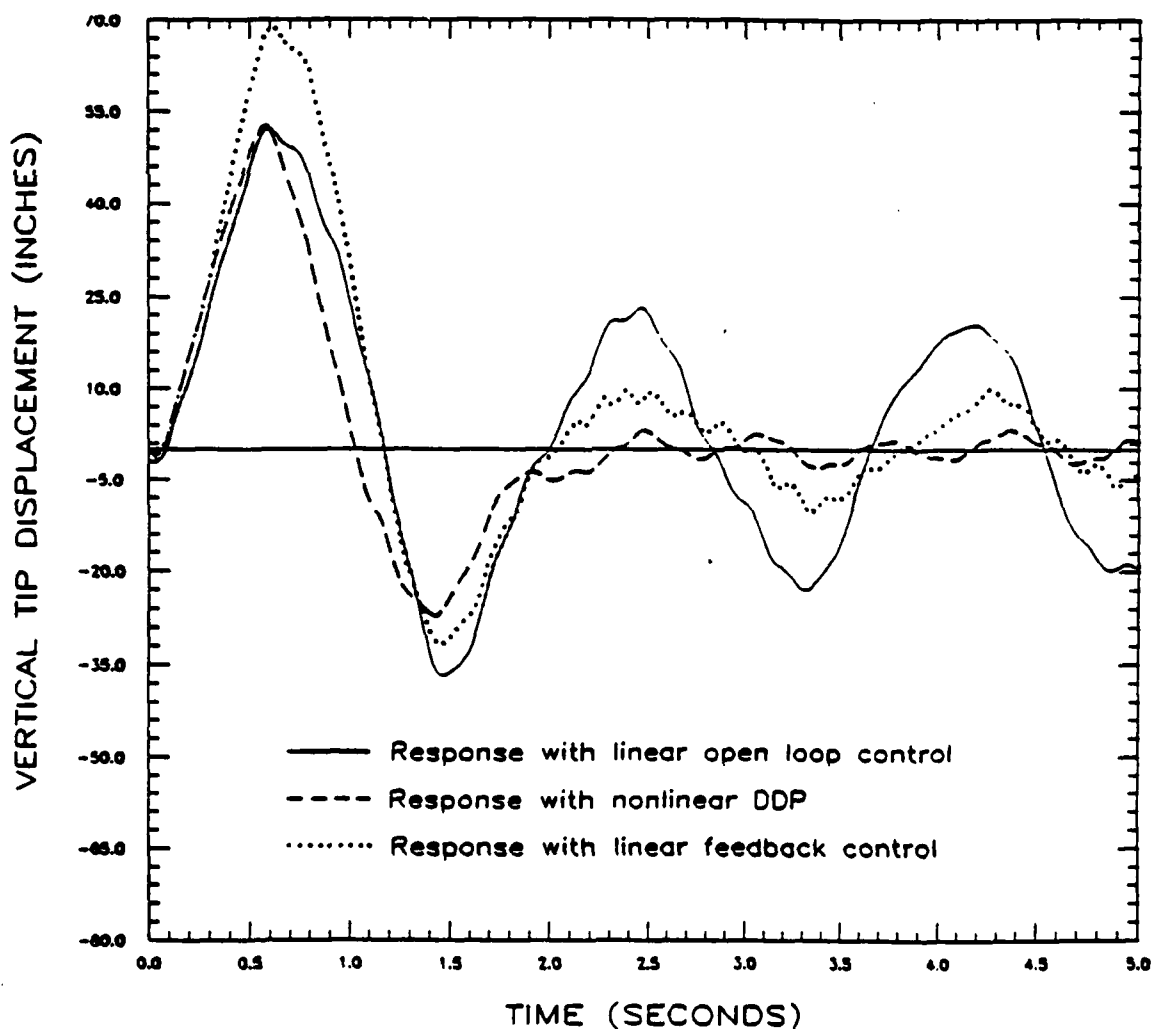responses -- vertical deflection of top, free-end node.

Figure 2. Comparison of controlled responses of nonlinear structure.

PROJECT SUMMARY

Project Title:
Finite-Precision Effects in Feedback Control Systems for Flexible Space Structures

Faculty Leader:
Assistant Professor David F. Delchamps
Electrical Engineering

Graduate Research Assistants:
None

Other Participants:
None

Executive Summary:

Analytical models for lightly damped systems are close to being unstable over a range of operating conditions. If finite-precision measurements are employed by a feedback controller designed to stabilize or place the closed loop poles of the linearization of such a system, then complicated dynamical behavior often results. We have discovered that the design of stabilizing controllers for such systems must pay close attention to finite-precision constraints on measurements and on arithmetic in potential digital implementations. Moreover, we have discovered ways in which long records of finite-precision measurements can be employed in designing feedback controllers for lightly damped systems that are more effective than standard schemes based on instantaneous feedback laws. We have also recently begun investigating the question of whether some of the techniques we have employed in analyzing spatial quantization in control systems will eventually contribute to our understanding of the behavior of finite-element-based control strategies for lightly-damped distributed systems.

Project Description:

We have subjected to a careful analysis the dynamical behavior that arises in control systems that employ feedback based on quantized measurements of real-valued time functions. The models we have considered are all discrete-time, but have important continuous-time analogues. Of particular interest to us have been two general questions. First, how does the finite-precision constraint on measurements affect one's ability to stabilize unstable systems or place the poles of lightly damped systems by means of feedback? Second, how can one make intelligent use of long records of finite-precision measurements in more general control problems involving trajectory following or trajectory optimization? Many established techniques from the ergodic theory of dynamical systems and from information theory have proven extremely useful to us in our research.

With regard to the stabilization problem, we have established under some mild assumptions the existence of a bounded invariant region in the state space of a closed loop system

whose controller is based on the instantaneous feedback of a finite-precision measurement of the system's state that would stabilize the system if perfect measurements were available. In this invariant region, almost all trajectories are chaotic, and under additional assumptions there exists on the region an invariant measure that is absolutely continuous with respect to Lebesgue measure and with respect to which the closed-loop dynamics are ergodic. The ergodicity would seem to make such systems amenable to computer simulation. The invariant measure differs significantly from the measure that one would obtain by modeling the quantization errors as uniform white noise. For details, see [1-2] and [5-6].

Furthermore, we have discovered ways of using feedback to make a long record of finite-precision measurements of a system's state reveal asymptotically perfect knowledge of the current state if the system is stable or just barely unstable. If the system is too unstable for such strategies to work, there exist other schemes that give a current state estimate which is asymptotically quite a bit better than that which may be calculated from instantaneous finite-precision measurements. We have obtained an upper bound on the amount of information about the state that can be rendered available by such strategies; this bound might be construed as an upper bound on the useful arithmetic precision in a digital controller for the system. See [3] for a complete discussion.

Papers Published or to Appear

[1] "Expanding Maps and the Statistical Stabilization of Linear Control Systems With Quantized Measurements, *Proceedings of the 1989 Conference on Information Sciences and Systems*, Baltimore, MD, March, 1989, pp. 112-118.

[2] "Some Chaotic Consequences of Quantization in Digital Filters and Digital Control Systems," in *Proceedings of the IEEE International Symposium on Circuits and Systems*, Portland, OR, May, 1989, pp. 602-605.

[3] "Extracting State Information From a Quantized Output Record," to appear in *Systems and Control Letters*, 1990.

[4] "Controlling the Flow of Information in Feedback Systems With Measurement Quantization," to appear in *Proceedings of the 28th IEEE Conference on Decision and Control*, Tampa, FL, December, 1989.

[5] "Asymptotic Statistical Properties of Linear Systems Operating Under Quantized Feedback," to appear in *Proceedings of the Twenty-Seventh Annual Allerton Conference on Communications, Control, and Computing*, Urbana, IL, September, 1989.

Papers Submitted or in Preparation

[6] "Stabilizing a Linear System With Quantized State Feedback," submitted to *IEEE Transactions on Automatic Control*.

Conference Presentations

[7] "Information and Uncertainty in Feedback Systems With Measurement Quantization," presented at the SIAM Conference on Control in the 90's, San Francisco, CA, May, 1989.

[8] "Stabilization and Pole Assignment for Linear Systems Using Quantized Measurements," presented at the 1989 Conference on the Mathematical Theory of Networks and Systems (MTNS-89), Amsterdam, The Netherlands, June, 1989.

[9] "The Pseudorandom Asymptotic Behavior of Digitally Controlled Analog Systems," to be presented at the 28th IEEE Conference on Decision and Control, Tampa, FL, December, 1989.

PROJECT SUMMARY

Project Title:
Optimal Controller Placements in Large Scale Linear Systems

Faculty Leader:
Dr. Hsiao-Dong Chiang - Assistant Professor
Electrical Engineering

Graduate Research Assistant:
Jin-Cheng Wang and Jin Lu

Other Participant: Professor James S. Thorp
Electrical Engineering

Executive Summary:

The problem of controller placements in large scale linear systems is investigated. Specifically, given a large scale linear system, it is desired to find the optimal number of linear controllers, the optimal locations in the system to place these controllers and the optimal feedback gain of each controller so that an objective function is optimized, and also so that other desirable properties of the controlled system, such as eigenstructure assignment, occur. A new formulation of the controller placement problem is presented. A general solution algorithm based on simulated annealing is developed for the controller placement problem. The solution algorithm can arrive at the global optimal solution. The solution algorithm has been implemented into a computer package an applied to an eleven bays structure of 132-dimension linear system with very promising results.

Description of Project and Results

A. Introduction

Consider a large-scale, linear time-invariant system

$$\dot{x} = Ax \tag{1}$$

where $x \in R^n$ is a state vector and A is a matrix of large dimension. Suppose one attempts to improve the dynamical behavior of (1) by applying linear state-feedback controllers to modify its eigenstructure. One of the first questions facing the designer for such a large-scale system is

(1) how many controllers to specify,

(2) where to place these controllers, and

(3) what is the associated feedback gain

such that an objective function is optimized and certain constraints are satisfied. This problem is termed the *controller placement problem*, which is especially important from the point of view of economy and effectiveness. For instance, poorly chosen locations for controllers may cause large feedback gain (this induces high control efforts). Since the choices of controller locations for a large-scale system are enormous, this problem is by no means a trivial one.

Despite its importance, very little has been done on the controller placement problem. A great majority of control schemes developed thus far are based on the assumption that locations to place controllers are given. Indeed, the controller placement problem is difficult to solve analytically.

B. Problem Formulation

Let u(t) be a m dimensional vector of control input. Since the type of controllers we consider is linear state-feedback, the control input vector u(t) is expressed as

$$u(t) = -Fx \tag{2}$$

where the feedback gain matrix $F = [f_{ij}]$ is a $m \times n$ matrix. Applying the linear state-feedback controllers (2) into (1) we have the following closed-loop system

$$\dot{x} = (A - BF)x \tag{3}$$

(A, B) is assumed to be completely controllable. Let the open-loop eigenvalues of (1) be $\lambda(A) = \{ \lambda_i, i = 1,2,...,n \}$, where $\{ \lambda_i, i = 1,2,...,k \}$ (k < n) is a symmetric set. The controller placement problem is to seek a control matrix $\hat{B}$ (which determines the optimal number of controllers and the optimal locations to place these controllers) and a feedback gain matrix $\hat{F}$ (which determines the optimal feedback gain of each controller) so that a desired objective function is optimized and the following conditions are satisfied :

(i) (partial eigenvalue assignment)

the closed-loop eigenvalues are

$$\Lambda(A - BF) = \{\lambda_i, i = 1,2,...,k\} \cup \{u_i, i = k+1,...,n\}$$

where $\{\lambda_i, i = 1,2,...,k\}$ are also the open-loop eigenvalues, $\{u_i \in \Omega, i = k+1,...,n\}$ is a symmetric set of distinct complex numbers, where Ω represents a desired region in the complex plane. And $\lambda_i \neq u_i$.

(ii) (partial eigenvector assignment)

the closed-loop eigenvectors associated with $\{\lambda_i, i = 1,2,...,k\}$ are h_i, i = 1,2,...,k, h_i need not be the corresponding eigenvector of (1-1).

(iii) (constraints on feedback gain matrix)

The feedback gain of each controller satisfies certain required constraints

$$g(F) \leq 0$$

Let the number of all the interested locations to place controllers be m and B be the corresponding control matrix of dimension $n \times m$; i.e. $B = [b_1, b_2, ..., b_m]$. Each column of B represents a control location. Let the number of controllers to be exerted on the system be n_c, $n_c \leq m$. The controller placement problem is formulated as follows:

$$\underset{F^i, B_i}{minimize\ C(F^i)} \tag{4}$$

subject to

$$\Lambda(A - B_i F^i) = \{\lambda_i, i = 1,2,...,k\} \cup \{u_i, i = k+1,...,n\}$$

where $\{\lambda_i, i = 1,2,...,k\}$ are also the open-loop eigenvalues, $\{u_i \in \Omega, i = k+1,...,n\}$ is a symmetric set of distinct complex numbers, where Ω represents a desired region in the complex plane.

$$(A - B_i F^i)h_i = \lambda_i h_i, \quad i=1,2,...,k.$$

$$B_i = \{ b_{i1}, b_{i2}, ..., b_{ij} \} \qquad j \leq n_c$$

$$b_{ik} \in \{b_1, b_2, ...b_m\} \qquad 1 \leq k \leq j$$

$$F^i = [f_1^i, f_2^i, ..., f_j^i]^T \qquad j \leq n_c$$

$$f_k^i = [f_{k,1}^i, f_{k,2}^i, ..., f_{k,n}^i]$$

$$f_{r,s}^i \in R \qquad 1 \leq r \leq m \text{ and } 1 \leq s \leq n$$

$$g(F^i) \leq 0$$

where the adjustable "variables" B_i, F^i are the control matrix and the feedback gain matrix. (A, B_i) is assumed to be completely controllable. Note that the feedback gain matrix F depends on the controller matrix B and the eigenstructure of the closed-loop system (4). C(F^i), a desired objective function which depends only on feedback gain matrix F^i, could be a non-differentiable function. $g(F^i) \le 0$ represents further constraints on the feedback gain matrix, where $g : R^p \rightarrow R^q$, p, q are appropriate integers. The above formulation is a combinatorial optimization problem. The matrix B_i determines the number of controllers to be placed and the locations to place controllers while the matrix F^i gives the corresponding feedback gain of each controller.

C. Simulated Annealing

There are two possible approaches to solve combinatorial optimization problems: one is via exact optimization algorithms and the other is through approximation algorithms. The former yields a globally optimal solution in a possibly prohibitive amount of computation time while the latter yields an approximate solution in an acceptable amount of computation time. Among the approximation algorithms, the most common one is the greedy search technique which accepts only changes that produce immediate improvement, with the disadvantage that it often gets stuck at local optima rather than at global optima. This problem becomes particularly severe as the problem size becomes large, because the number of local optima usually increases with the problem size. One technique to circumvent this problem is the technique based on simulated annealing.

Simulated annealing is a powerful general-purpose technique for solving combinatorial optimization problems. This technique is based on the analogy between the simulation and the annealing process used for crystallization in physical systems. Annealing is the physical process of heating up a solid to a melting point, followed by cooling it down until it crystalizes into a state with a perfect lattice. In this technique, a parameter called *temperature* is defined, which is of the same dimension as the cost. Just as in a physical system, the temperature is closely related to the freedom with which the entities of the system can move around. The system to be optimized starts at a high temperature, and all the entities of the system move about freely. The temperature is then gradually lowered until the system "freezes", at which point all the entities of the system are virtually fixed. This frozen configuration will be close to the lowest energy (or cost) configuration. It has been shown that this technique converges asymptotically to the global optimum solution with probability one, provided that certain conditions are satisfied.

The design of an algorithm based on simulated annealing consists of four important elements: (1) a set of allowed system configurations (configuration space), (2) a set of feasible moves (move set), (3) a cost function and (4) a cooling schedule. The system to be optimized starts at a high "temperature" and is slowly cooled down, until the system "freezes" and reaches the global optimum in a manner similar to annealing of a crystal during growth to reach a perfect structure. At each "temperature", the simulated annealing algorithm is represented in the following pseudo-code

```
repeat (
        1. perturb
            2. check feasibility/discard
            3. evaluate cost function
            4. accept/update
    ) until stop criterion = true
```

Step 1. **perturb** the current system configuration to a new configuration by choosing either at random an element (in the configuration space) from the neighborhood of current configuration or according to a certain rule. Step 2. **check** the equality and inequality constraints. If these constraints are satisfied, then proceed to step 3. Otherwise, the move is discarded and the configuration before this move is used and go to step 1.　　　Step 3. **evaluate** the change of the cost function dc $:= \hat{c}$ - c, where c and $\hat{c}$ are the value of the cost function before and after the move has been executed. Step 4. **accept/update**: if the move decreases the value of the cost function, i.e. dc < 0, the move is accepted and the new configuration is retained. On the other hand, when dc > 0 (i.e. the move is up-hill) acceptance is treated

probabilistically in the following way: the Boltzman factor $e^{-\frac{dc}{kT}}$ is first calculated, where the parameter T is the "temperature" and k is a constant whose dimension depends on c and T. Then, a random number r uniformly distributed in the interval [0,1) is chosen. If $r \leq e^{-\frac{dc}{kT}}$, the new configuration is retained; otherwise, if $r < e^{-\frac{dc}{kT}}$, the move is discarded and the configuration before this move is used for next step. The algorithm stops when no significant improvement in the cost function has been found for a number of consecutive iterations. It is due to the probabilistic selection rule, the process can always get out of a local minimum in which it could get trapped and proceed to the desired global optimum. This feature distincts approaches based on the simulated annealing technique from the greedy search approach.

Although the simulated annealing framework is conceptually straightforward, design of a successful algorithm based on simulated annealing requires considerable engineering judgement in the design of the four elements described above. Details regarding the design of an algorithm based on the simulated annealing for solving the controller placement problem is contained in [1,2].

D. Application to Modal Control of Large Flexible Scale Systems

We have developed a solution algorithm based on the simulated annealing technique and applied the solution algorithm to an experimental 11-bay truss system. The three dimensional structure used in the experimental portion of the research is shown in Fig. 1. The structure consists of eleven 33 inch by 33 inch by 18 inch bays, suspended vertically. The upper four nodes are fixed against translation and rotation, while the other nodes are free to translate and rotate in all three directions. Because of the desire to reduce the size of the state vector, a two dimensional model of the structure, shown in Fig. 2, was selected for use in the numerical simulations. The structure consists of eleven 33 inch by 18 inch bays, suspended vertically. The top two nodes are fixed against translation and rotation, while the other nodes are free to translate in the x and y directions and rotate about the z axis. The loading of the structure precludes both out-of-plane and torsional excitation of the structure, thus allowing the reduction in dimensionality without affecting the accuracy.

The elements used are standard 2-D beam-column elements with two translational and one rotational degree of freedom at each end. The members are modelled as aluminum tubular sections with an inside diameter of 0.54 inches and a wall thickness of 0.088 inches. The members have a cross-sectional area of 0.125 in^2 and a moment of inertia of 0.0033 in^4. The Young's modulus of the tubes is 10,000,000 psi. The angles between members framing in at a node are assumed to remain constant.

The structural stiffness matrix, K, is assembled using linear assumptions of small displacements, rotations and strains. The mass matrix, M, is lumped at the nodes. The translational mass contributions come from both the nodal masses and the tributary mass of the members. The translational mass at each node is 0.01035 pound-second^2/inch. The rotational mass is based on the rotational inertia of the members framing in at a node. The rotational mass at the tip nodes in 0.0173 pound-second^2/radian. The damping matrix, if required, is proportional to the mass and stiffness matrices. The mass proportional damping is primarily effective in the low modes while the stiffness proportional damping is primarily effective in the high modes.

The undamped system is described by the following oscillatory system

$$M\ddot{y} + Ky = 0 \qquad\qquad (5)$$

where y is a 66-vector of displacement at 22 nodes shown in Fig. 1. M and K are 66×66 mass and stiffness matrices, respectively. In state space, system (5) can be written as

$$\dot{x} = Ax \qquad\qquad (6)$$

where x=$[y \ \dot{y}]^T$ is a 132 vector, A=$\begin{bmatrix} 0 & I \\ -M^{-1}K & 0 \end{bmatrix}$ is a 132×132 matrix. The eigenvalues of the open-loop system (6) are listed in Table 1. System (6) is a uncontrolled system. Applying linear controllers to (5) we have the following system

126

$$M\ddot{y} + Ky = Du \tag{7}$$

where u is an m (>1) vector of control input, and D is an 66×m control matrix. The matrix D = $[d_1, d_2, ..., d_{275}]$, is formed in the following way: ith column of D corresponds to ith controller. For instance, d_1 is a 66-dimension column vector with

$$d_1 = [\ \cos\alpha,\ \sin\alpha,\ 0,\ 0,...,0\ ]^T$$

where all the components but the first two are zero, α is the angle between the controller and the horizontal axis (see Fig. 3). d_{122} is a 66-dimension column vector with

$$d_{122} = [\ \cos\beta,\ \sin\beta,\ 0,...,0,\ -\cos\beta,\ -\sin\beta,\ 0,...,0\ ]^T$$

where all the components but the 1th, 2nd, 22th and 23th are zero, β is the angle between the controller and the horizontal axis (see Fig. 4).

In state space, system (7) can be written as

$$\dot{x} = Ax + Bu \tag{8}$$

where $B = \begin{bmatrix} 0 \\ -M^{-1}D \end{bmatrix}$ is a 132×m matrix. There are 275 prospective controller locations. It is easy to show that the system (8) is completely controllable provided any one controller is placed in the system.

Now, we seek two optimal locations to place these two controllers and the optimal feedback gain of each controller such that the objective function $C(F^i) = \sum_{r=1}^{n_c}\sum_{s=1}^{n} w_{ij}f_{r,s}^i{}^2$ is minimized with the following constraints: the two lowest frequency self-conjugate pairs of open-loop system (6) are to be moved to another distinct and self-conjugate pairs lying in the region of $\Omega = \{\ -10.0 < \text{Re}\{u_{129}, u_{130}\} < -3.75, 5.0 < \text{Im}\{u_{129}, -u_{130}\} < 7.0, -10.0 < \text{Re}\{u_{131}, u_{132}\} < -3.75, 2.5 < \text{Im}\{u_{131}, -u_{132}\} < 3.5\}$ while keeping the other open-loop eigenvalues and their associated eigenvectors unchanged (Fig. 5). For the purpose of illustration, we let the open-loop eigenvectors associated with unchanged open-loop eigenvalues be the corresponding closed-loop eigenvectors. Other choices of preassigned eigenvectors associated with unchanged eigenvalues are allowed. Since it is desired to use only the velocity $\dot{y}$ as feedback signal, we let $w_j = 10^6$, $j = 1, ...,66$, $w_j = 1$, $j = 67,...,132$, so that the feedback gain from displacement can be forced to become so small during the optimization process as to be neglected.

The optimal locations to place two controllers are the locations connecting nodes 19, 24 and 7, 24 (see Fig. 6). The optimal feedback gains of these two controllers are tabulated in Table 2 (we only display the feedback gain matrix F_c, from which the feedback gain matrix F can be obtained). The corresponding eigenvalues are $u_{129} = -4.051094 + j\ 5.1855471$, $u_{130} = -4.051094 - j\ 5.1855471$, $u_{131} = -3.999249 + j\ 2.7875621$, $u_{132} = -3.999249 - j\ 2.7875621$. The other closed-loop eigenvalues remain unchanged.

Papers:

[1]   H.D. Chiang, J.S. Thorp, J.C. Wang and J. Lu, "Optimal Linear Controller Placements for Large Scale Systems" 1989 American Control Conference, June 1989, pp. 1615-1620.
[2]   H.D. Chiang, J.S. Thorp, J.C. Wang and J. Lu, "Optimal Controller Placements for Large Scale Linear Systems" submitted to *IEEE Trans. on Automatic Control* for publication.
[3]   J. Lu, H.D. Chiang and J.S. Thorp, "Partial Eigenstructure Assignment and its Application to Model Control of Large Space Structures", submitted to *IEEE Trans. on Automatic Control* for publication.
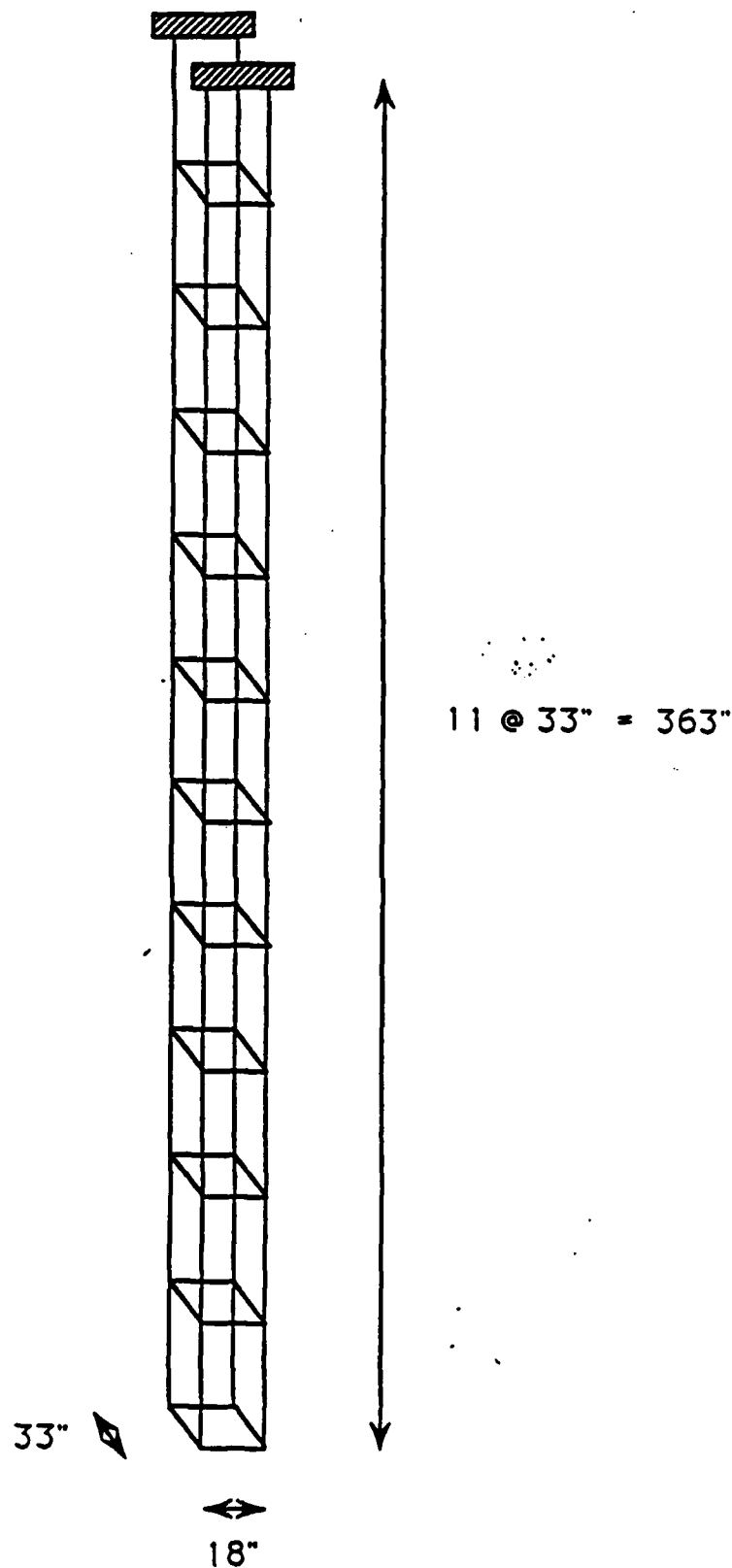
11 @ 33" = 363"

33"

18"

Fig. 1.   The three dimensional structure of an experimental 11-bay truss system. The structure consists of eleven 33 inch by 33 inch by 18 inch bays, suspended vertically.

11 @ 33" = 363"
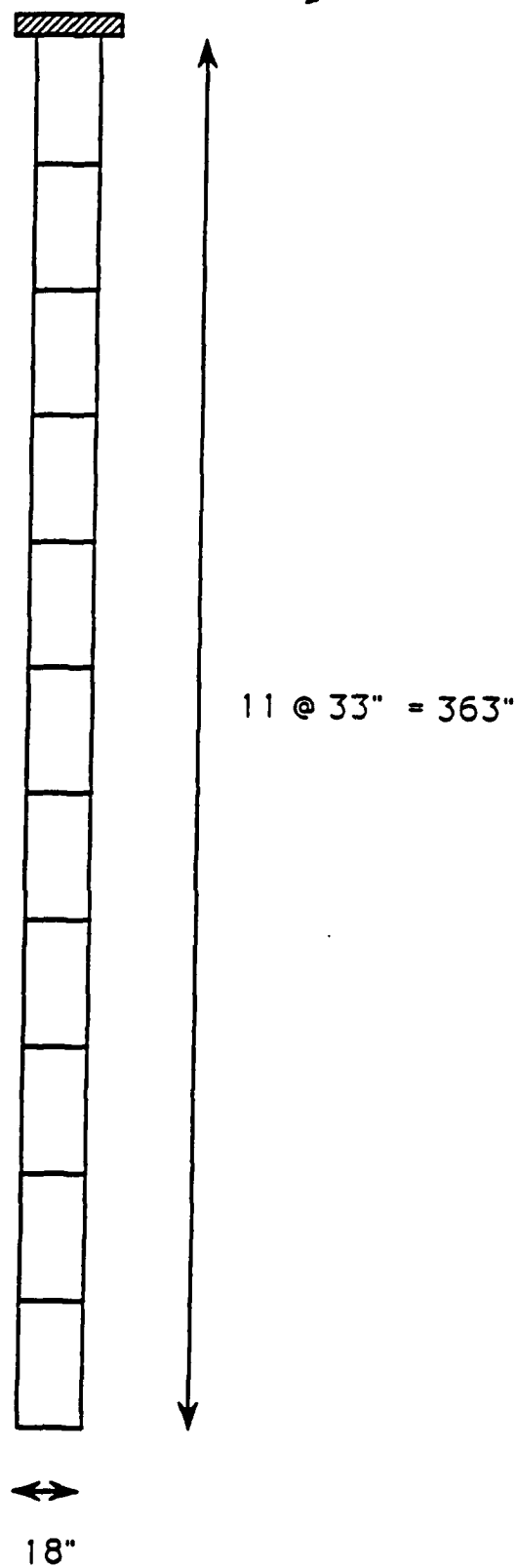
18"

Fig. 2.   A two dimensional model of the structure in Fig. 1 was selected for use in
          the numerical simulations.
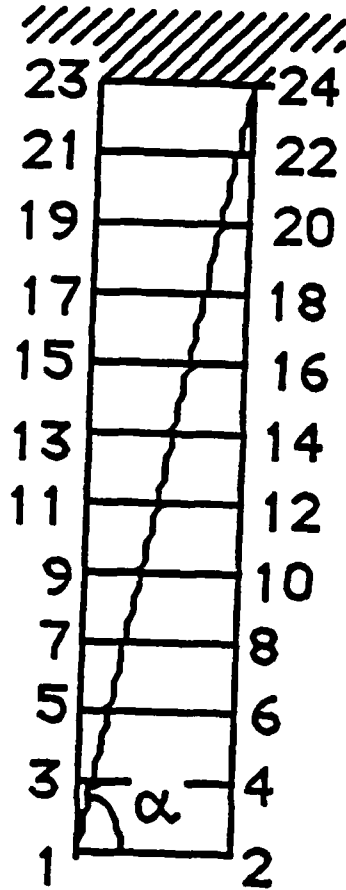
Fig. 3.   A controller is placed between nodes 1 and 24 with α being the angle between the controller and the horizontal axis.
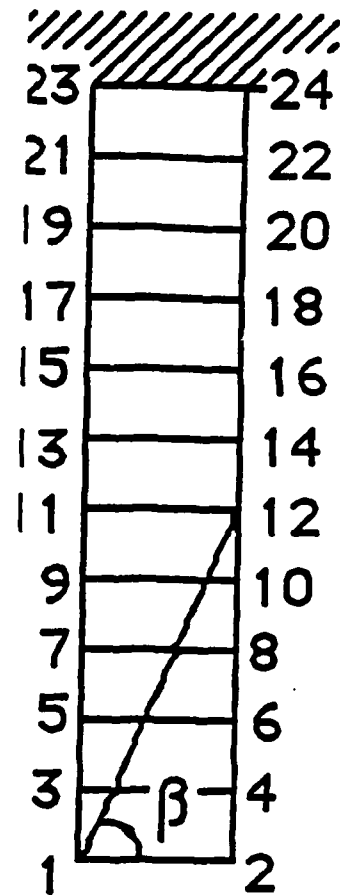
Fig. 4.   A controller is placed between nodes 1 and 12 with β being the angle between the controller and the horizontal axis.

130
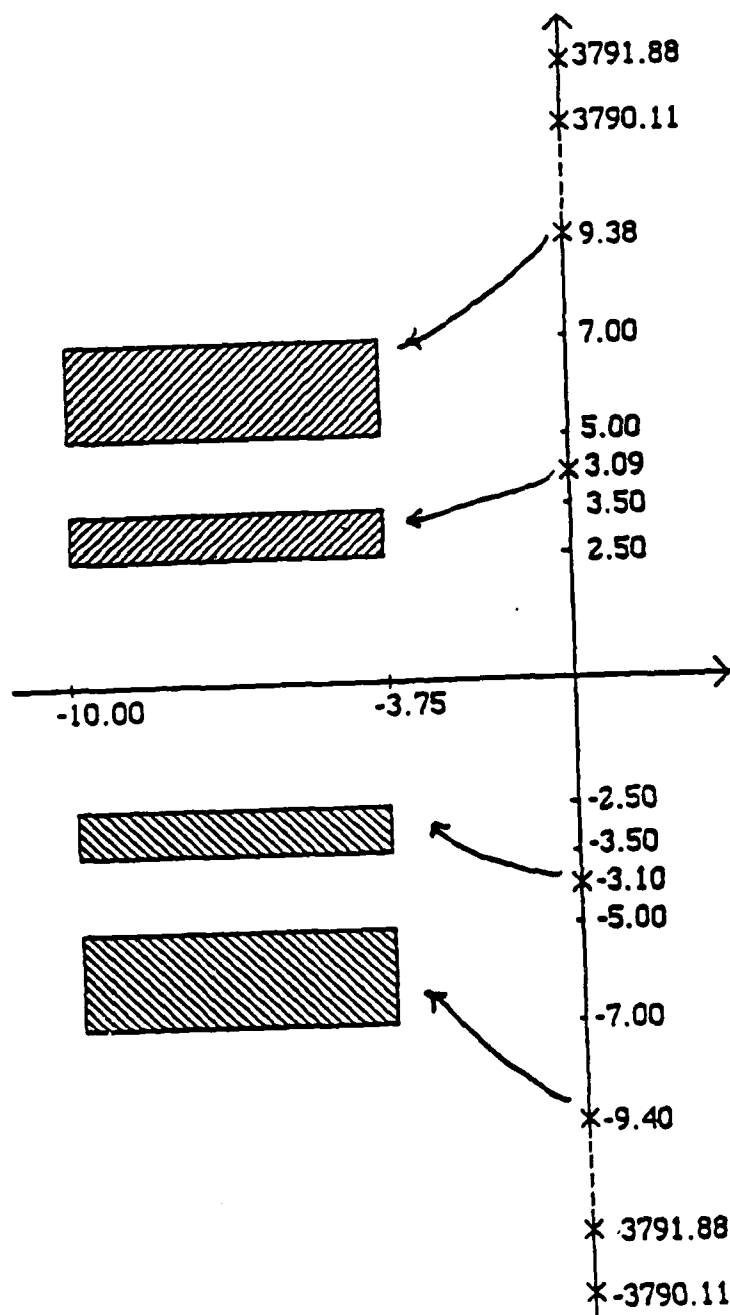
Fig. 5. The two lowest frequency self-conjugate pairs of open-loop system (7-2) are to be moved to another distinct and self-conjugate pairs lying in the region of $\Omega = \{ -10.0 < \text{Re}\{u_{129}, u_{130}\} < -3.75, 5.0 < \text{Im}\{u_{129}, -u_{130}\} < 7.0, -10.0 < \text{Re}\{u_{131}, u_{132}\} < -3.75, 2.5 < \text{Im}\{u_{131}, -u_{132}\} < 3.5 \}$. The others remain unchanged.

Fig. 6. The optimal locations to place two controllers are the locations connecting nodes 19, 24 and 7, 24.

Table 1: The open loop eigenvalues:

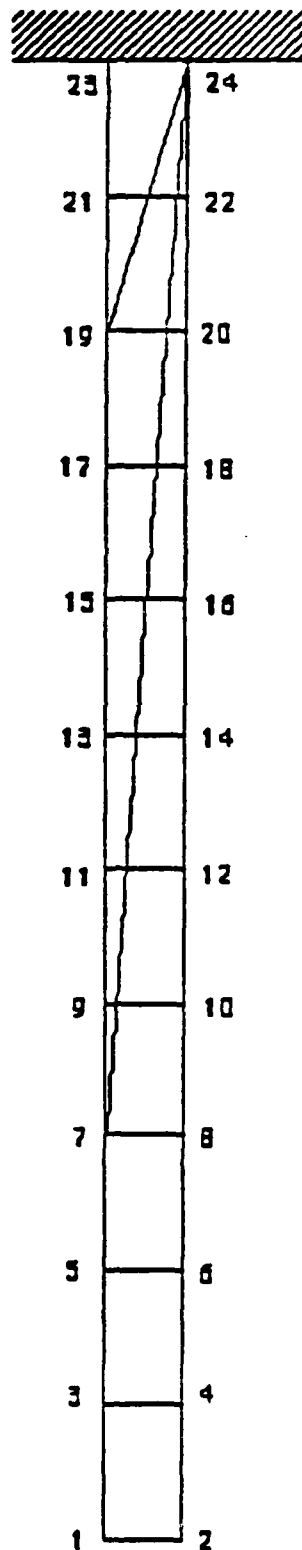| nonzero # mult. by 10^3.	nozero # mult. by 10^2.	nozero # mult. by 10^1.
0.000000 ± 3.791884 i	0.000000 ± 9.477749 i	0.000000 ± 6.421722 i
0.000000 ± 3.790111 i	0.000000 ± 8.555062 i	0.000000 ± 6.122129 i
0.000000 ± 3.685702 i	0.000000 ± 8.346887 i	0.000000 ± 5.656770 i
0.000000 ± 3.683875 i	0.000000 ± 8.168735 i	0.000000 ± 5.067614 i
0.000000 ± 3.663998 i	0.000000 ± 7.982516 i	0.000000 ± 4.400687 i
0.000000 ± 3.663443 i	0.000000 ± 7.766917 i	0.000000 ± 3.695159 i
0.000000 ± 3.663412 i	0.000000 ± 7.641387 i	0.000000 ± 2.983468 i
0.000000 ± 3.663364 i	0.000000 ± 7.531739 i	0.000000 ± 2.281989 i
0.000000 ± 3.663300 i	0.000000 ± 7.310173 i	0.000000 ± 1.604270 i
0.000000 ± 3.663226 i	0.000000 ± 7.122772 i	0.000000 ± 0.937866 i
0.000000 ± 3.663147 i	0.000000 ± 7.111580 i	0.000000 ± 0.309464 i
0.000000 ± 3.663069 i	0.000000 ± 6.954832 i	
0.000000 ± 3.662998 i	0.000000 ± 6.924232 i	
0.000000 ± 3.662939 i	0.000000 ± 6.854425 i	
0.000000 ± 3.662897 i	0.000000 ± 6.793822 i	
0.000000 ± 3.662875 i	0.000000 ± 6.598525 i	
0.000000 ± 3.510940 i	0.000000 ± 6.352853 i	
0.000000 ± 3.509016 i	0.000000 ± 6.072997 i	
0.000000 ± 2.967673 i	0.000000 ± 5.238789 i	
0.000000 ± 2.969979 i	0.000000 ± 5.041897 i	
0.000000 ± 2.613933 i	0.000000 ± 4.918793 i	
0.000000 ± 2.611274 i	0.000000 ± 5.492153 i	
0.000000 ± 2.206231 i	0.000000 ± 5.778485 i	
0.000000 ± 1.764405 i	0.000000 ± 7.783706 i	
0.000000 ± 1.760091 i	0.000000 ± 2.718264 i	
0.000000 ± 1.288449 i	0.000000 ± 2.610780 i	
0.000000 ± 2.969974 i		
0.000000 ± 2.613933 i		
0.000000 ± 2.209467 i		

Table 2		
	$F_e(1,k)$	$F_e(2,k)$
k=1	0.0010965	-0.0008940
k=2	0.0009768	0.0001474
k=3	-0.0001997	-0.0003619
k=4	-0.0014071	-0.0023362

C

PROJECT SUMMARY

Project Title:
Nonlinear Random Vibration of Pin-Jointed Trusses with Imperfections

Faculty Leader:
Professor Mircea Grigoriu
Structural Engineering

Executive Summary:

The equivalent linearization and harmonic balance methods are applied to develop approximations of the response of pin-jointed trusses with imperfections that are subject to narrow-band stationary Gaussian excitations. The imperfections consist of gaps in joints and can cause dynamic responses that differ significantly from responses of ideal pin-jointed trusses, referred to as auxiliary trusses. Joint imperfections are modeled by trilinear restoring forces as shown in Fig. 1.

Results for single-degree-of-freedom systems indicate that the assumption of ideal joints is only satisfactory when joint gaps are small and/or excitation magnitude is large. It is found that joint imperfections may generally cause significant changes in response intensity and frequency relative to the response of corresponding auxiliary systems. On the other hand, Monte Carlo simulation studies show that the equivalent linearization method has a much broader range of validity. The method gives satisfactory estimates of response variances provided nonlinearities are not excessive, e.g., large joint gaps and small excitations. Figure 2 illustrates the dependence of normalized response standard deviation σ_x obtained by the equivalent linearization method on ratio of joint gap δ to a parameter σ_0 related to excitation intensity for several damping coefficients β. Estimates of σ_x compare satisfactorily with simulation results for values of $\delta/\sigma_0 \leq 2.0$. The equivalent linearization method is unsatisfactory when $\delta/\sigma_0 > 2.0$, i.e., the case of large nonlinearities that may result in chaotic vibrations.

Studies of a three bay pin-jointed truss with imperfection by the equivalent linearization method lead to similar conclusions. As for simple oscillators, the equivalent linearization method can be applied for combinations of joint gaps and excitation intensities that do not result in excessive nonlinearities.

Cornell Reports:

Islam, S., and Grigoriu, M., "Nonlinear Random Vibration of Pin-Jointed Trusses with Imperfections."

Reports/Papers to be Published:

Grigoriu, M., "A New Closure Technique for Solution of Nonlinear Random Vibration Problems."

Conference Presentations:

Grigoriu, M., "Probabilistic Analysis of Response of Duffing Oscillators to Narrow Band Stationary Gaussian Excitations," *Proceedings, I Pan American Congress of Applied Mechanics* (PACAM), Rio de Janeiro, Brazil, January, 1989, pp. 652-655.

Grigoriu, M., "Reliability of Degrading Dynamic Systems," *Proceedings, Euromech 250: Nonlinear Systems Under Random Conditions*, Como, Italy, June, 1989.
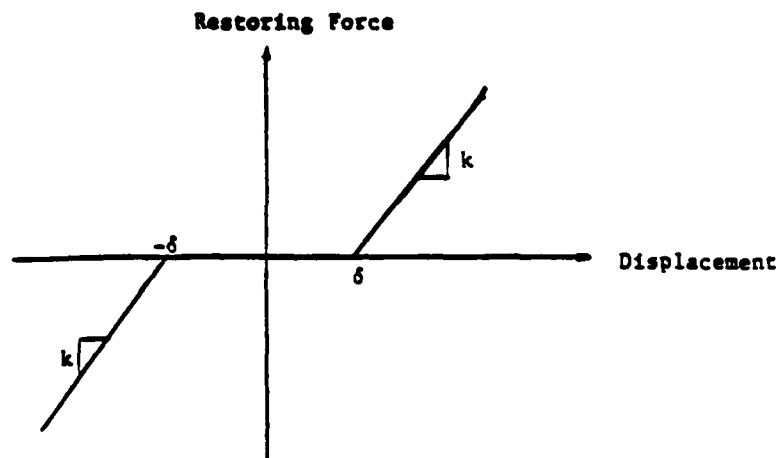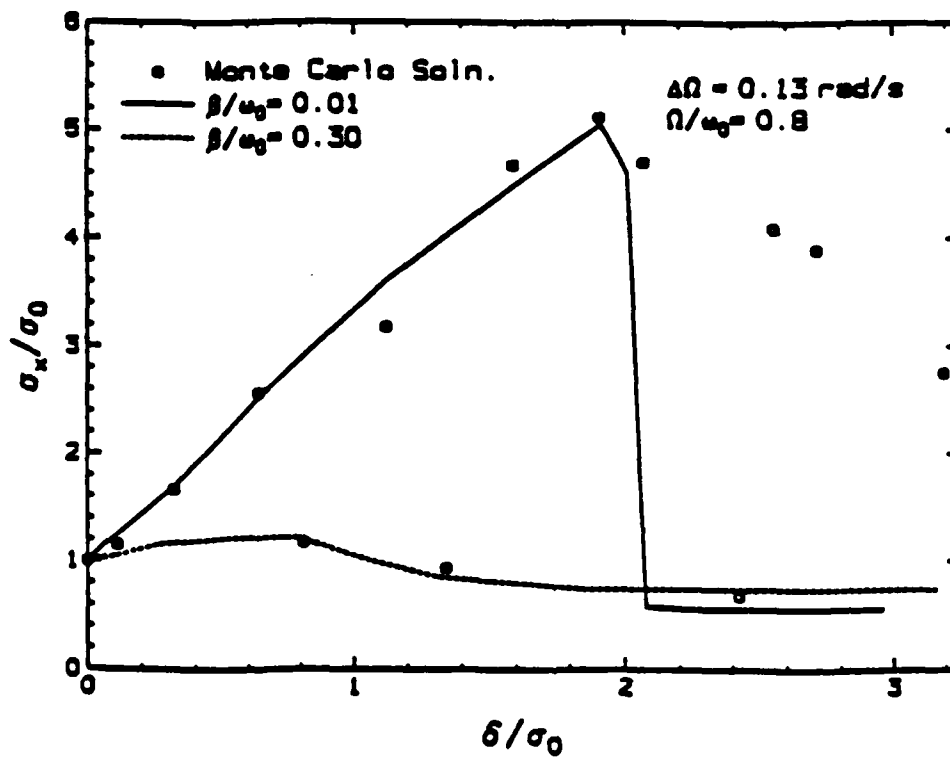
Figure 1. Model of Joint Gap.

Figure 2. Standard Deviation of Approximate Response
by Equivalent Linearization Method.

Project Title:
Vibration of a Shallow Arch Under Axial Loading

Faculty Leader:
Professor S. Mukherjee
Theoretical and Applied Mechanics

Graduate Research Assistant:
Rudra Pratap
Theoretical and Applied Mechanics

EXECUTIVE SUMMARY

The present work is an analytical study of the vibration of a shallow arch under periodically varying axial load, using theory of linear elasticity. The dynamic analysis under dead load is carried out first. In the second section, the analysis incorporates the dynamic load. Using Galerkin's projection the assumed solution of the equation of motion is then reduced to a non-homogeneous Mathieu equation for the time dependent amplitudes. A particular solution, based on the variation of parameters, is used to derive a system of equations for the amplitudes. The resonance conditions for the amplitudes are derived and the corresponding subspace of the parameters is separated. The subspace is presentsd in the form of parametric plots. Any point in the interior of the stable region of the Strutt chart can thus be conveniently tested whether it can cause resonance or not by simply checking its location in the separated subspace.

1. DYNAMIC ANALYSIS UNDER DEAD LOAD

Governing equation of motion is:

$$EI\, w_{,xxxx} + P_0 \left(\frac{1}{R} + w_{,xx} \right) = -\rho\, w_{,tt}$$

where

w = transverse displacement

EI = modulus of rigidity

R = radius of curvature

P_0 = dead load

ρ = mass/unit length.

Assumed solution is

$$w = e^{\lambda t}\, \phi(x) + \psi(x)$$

where $\psi(x)$ satisfies the corresponding static equation

$$\psi_{,xxxx} + \frac{P_0}{EI} = -\frac{1}{R}\frac{P_0}{EI}$$

Assuming $\phi(x) = \sin\frac{n\pi}{L}x$ gives

$$\lambda = \frac{n\pi}{L\beta}\sqrt{\alpha^2 - \left(\frac{n\pi}{L}\right)^2}$$

where $\alpha = \frac{P_0}{EI}$ and $\beta = \frac{\rho}{EI}$

i) If $P_0 > \dfrac{n^2\pi^2}{L^2} EI$, then it gives rise to unbounded solution and hence is unstable.

ii) if $P_0 < \dfrac{n^2\pi^2}{L^2} EI$, λ has complex roots and

$$w = \sin\frac{n\pi x}{L}\, (a_n\cos \omega_n t + b_n\sin \omega_n t) + \frac{1}{2R}\left(\frac{L^2}{\sin \alpha L} \sin \alpha x - x^2 \right)$$

where

$$\omega_n = \frac{n^2\pi^2}{\rho L^2}\left(EI\, \frac{n^2\pi^2}{L^2} - P_0 \right)$$

Thus, in this case, the arch exhibits harmonic oscillation with amplitude determined by initial conditions. Initial curvature of the arch does not play any significant role in vibration.

2. DYNAMIC ANALYSIS UNDER PULSATING LOAD

Governing equation of motion is:

$$EI\ w_{,xxxx} + [P_0 + P(t)]\ w_{,xx} + \rho w_{,tt} = -\frac{1}{R}[P_0 + P_t]$$

where $\qquad P_0$ = dead load

$\qquad\qquad\quad P(t)$ = dynamically varying load

Assume solution as:

$$w(x,t) = \sum_{j=1}^{N} a_j(t)\ \sin\frac{j\pi x}{L}$$

then using Galerkin's projection the equation of motion becomes

$$\sum_{j=1}^{N}\left(\frac{j\pi}{L}\right)^4 a_j\int_0^L \sin\frac{j\pi x}{L}\sin\frac{k\pi x}{L}\ dx - \sum_{j=1}^{N}\alpha\ [P_0 + P_t]\left(\frac{j\pi}{L}\right)^2 a_j\int_0^L \sin\frac{j\pi x}{L}\sin\frac{k\pi x}{L}\ dx$$

$$+ \sum_{j=1}^{N}\beta\ddot{a}_j\int_0^L \sin\frac{j\pi x}{L}\sin\frac{k\pi x}{L}\ dx + \frac{\alpha}{R}\ [P_0 + P_t]\ \int_0^L \sin\frac{k\pi x}{L}\ dx = 0.$$

This gives the following equation for $a_k(t)$:

$$\ddot{a}_k(t) + \frac{\alpha^2}{\beta}\ P_k^c\ [P_k^c - \{P_0 + P_t\}]\ a_k(t) = 0, \quad \forall\ \text{even } k \text{ and}$$

$$= -\frac{2k\pi}{RL}\ \frac{\{P_0 + P_t\}}{P_k^c}\ \forall\ \text{odd } k$$

where $\qquad P_k^c = \dfrac{n^2\pi^2}{L^2}\ EI.$

Introducing parameters,

$$\Omega_k = \frac{k^2\pi^2}{\beta L^2}\sqrt{1 - \frac{P_0}{P_k^c}}$$

and $\qquad \mu = \dfrac{P_t}{2(P_k^c - P_0)}$

with loading $\qquad P(t) = P_t \cos \omega t,$

139

the final equation is obtained as,

$$\ddot{a}_k(t) + \Omega^2[\, 1 - 2\mu\cos\omega t\,]\, a_k(t) = -\frac{2k\pi}{LR}\frac{P_0}{P_k^c}\left[\, 1+\frac{P_t}{P_k^c}\cos\omega t\,\right],\ \forall\ \text{odd } k$$

$$= 0 \qquad \forall\ \text{even } k.$$

We will only consider the amplitudes corresponding to odd k. With this understanding we can drop the subscript k and cosider the following equation:

$$\ddot{a}(t) + \Omega^2[\, 1 - 2\mu\cos\omega t\,]\, a(t) = C_1 + C_2\cos\omega t \qquad (1)$$

where
$$C_1 = -\frac{2\pi}{LR}\frac{P_0}{P_c},$$

and
$$C_2 = -\frac{2\pi}{LR}\frac{P_t}{P_c}.$$

Equation (1) is the famous non-homogeneous Mathieu equation.

The homogeneous part of the solution of equation (1) is well known and the resulting stability diagram is given by the Strutt chart, figure 2. The homogeneous solution corresponds to the forced vibration of a straight beam under dynamic axial load. As is clear from the equation, the initial curvature of the beam results into the non-homogeneity of the equation. Hence, it is the particular solution which is of interest here. A suitable method to find the particular solution is outlined in [1]. Based on this method Kotowski [2] has derived the form of the particular solution which is valid everywhere except on the limiting curves of the Strutt chart. Using that form of the solution, the resonance conditions for the arch vibration have been obtained in the following section.

3. RESONANCE CONDITIONS

This is of interest to us only for those points in the parameter space which lie in the stable region. On the limiting curves the solution is known to be unstable anyway. In the stable region, the form of the particular solution is:

$$a_{part}(t) = \sum_0^{\infty} A_n\cos n\omega t$$

A substitution of this in eqation (1) gives the infinite system of algebraic equations for the resulting amplitudes A_n.

$$
\begin{bmatrix}
\Omega^2 & -\mu\Omega^2 & 0 & 0 & \cdots \\
-2\mu\Omega^2 & \Omega^2 - \omega^2 & -\mu\Omega^2 & 0 & \cdots \\
0 & -\mu\Omega^2 & \Omega^2 - (2\omega)^2 & -\mu\Omega^2 & \cdots \\
0 & 0 & -\mu\Omega^2 & \Omega^2 - (3\omega)^2 & -\mu\Omega^2 \\
\vdots & \vdots & \vdots & \vdots & \ddots
\end{bmatrix}
\begin{Bmatrix} A_1 \\ A_2 \\ A_3 \\ A_4 \\ \vdots \end{Bmatrix}
=
\begin{Bmatrix} C_1 \\ C_2 \\ 0 \\ 0 \\ \vdots \end{Bmatrix}
\tag{2}
$$

Now we define the width of resonance as that frequency range for which the amplitudes in $a_{part}(t)$ ensuing from the unit amplitudes of the pururbing function are greater than |1|.

The infinite system (2) is a very fast converging system and for all practical purposes it is sufficient to consider the first 5 by 5 submatrix. It has also been observed that only the first three amplitudes are significant enough to be considered. As is clear from the system of equations (2), one needs to look into only that subspace spanned by the first two columns of the inverse of the co-efficient matrix, because the non-homogenous vector is normal to the complementary subspace. Normalizing the system by using ω/Ω as the frequency ratio r, we get explicit expressions for A1, A2 and A3 in terms of parametrs r and μ. Figures 3, 4 and 5 show the parametric plot for these amplitudes. All those points in the stable region of the parametric space which fall into the contour plots for A1, A2 and A3 > 1 give us resonance conditions. There are infinite number of such points because for each pair of (μ, r) there are many pairs of (ω, Ω) which give us the same value of r.

4. REFERENCES

[1] McLachlan, N.W., Theory and Applications of Mathieu Functions. Dover Publication Inc., New York (1964), pp 132-134.

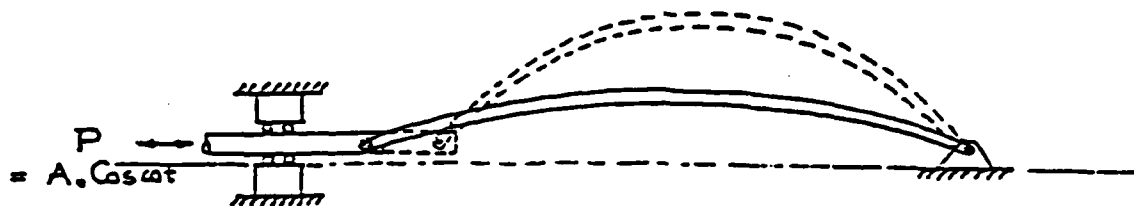[2] Kotowski, G., Lösungen der inhomogenen Mathieuschen Differentialgleichung mit periodischer Störfunktion beliebiger Frequenz. Z. Angew. Math Mech. Bd.23, Nr.4, (1943).
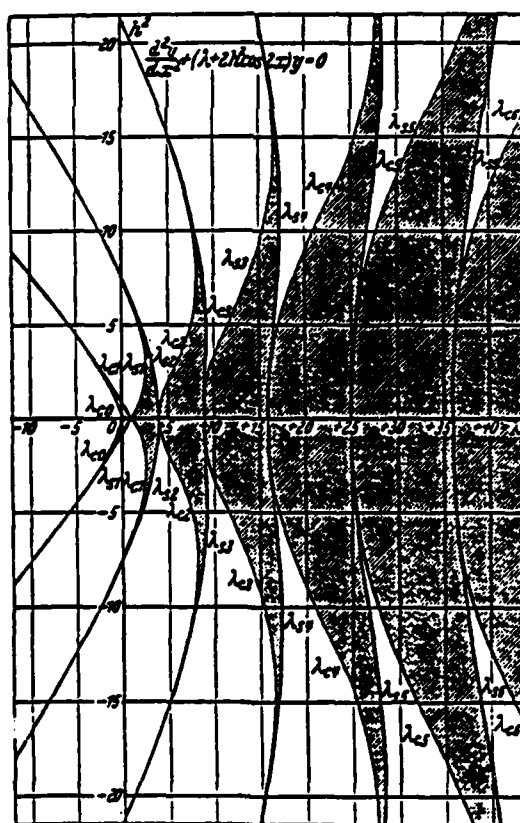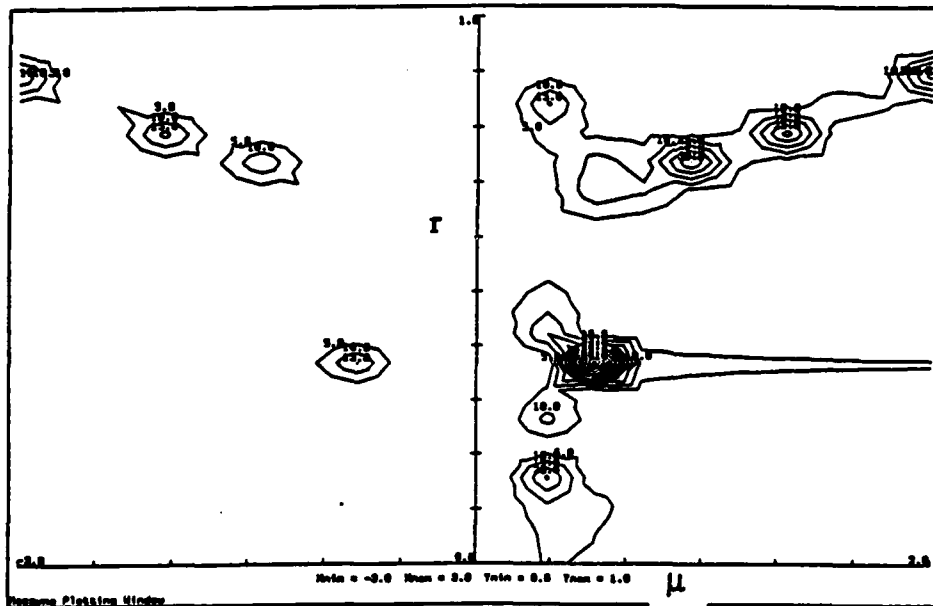
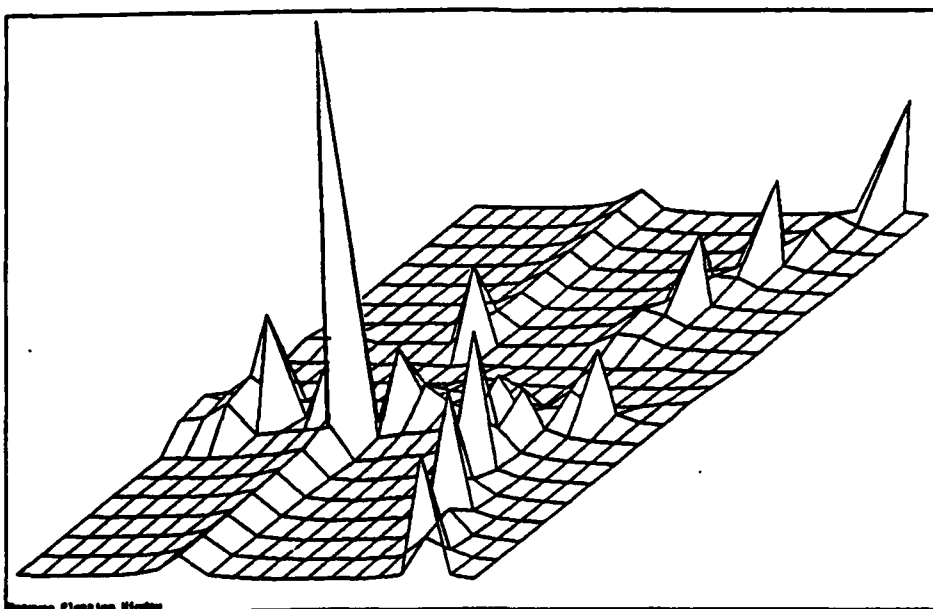Figure 1

Figure 2

Contour plot of A_1

Figure 3
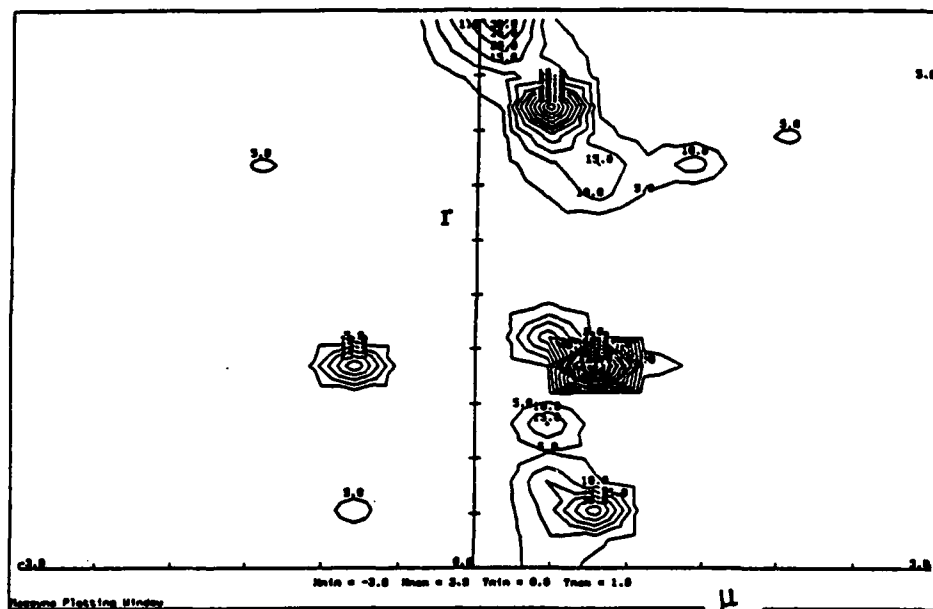
Contour plot of A_2
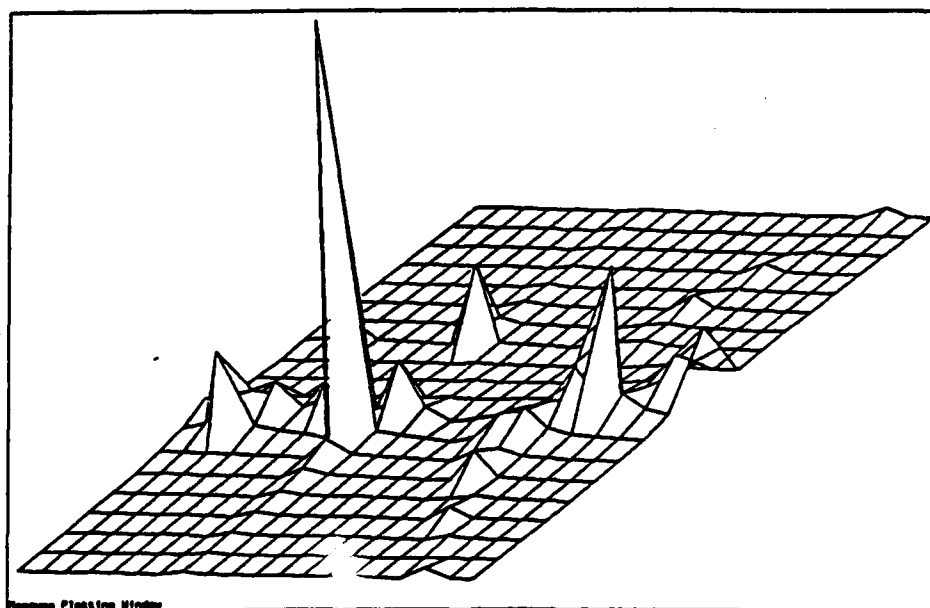
Figure 4
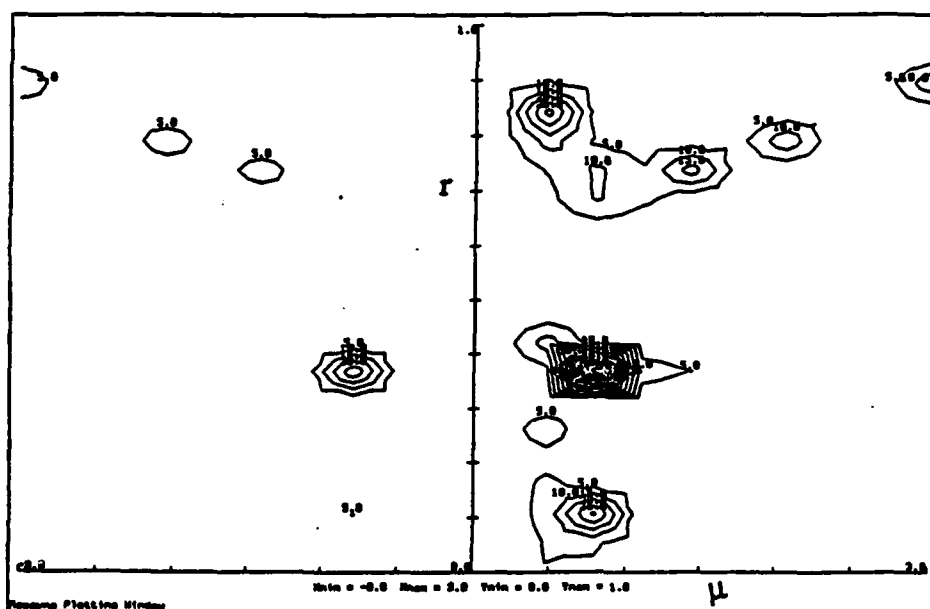
Contour plot of A3
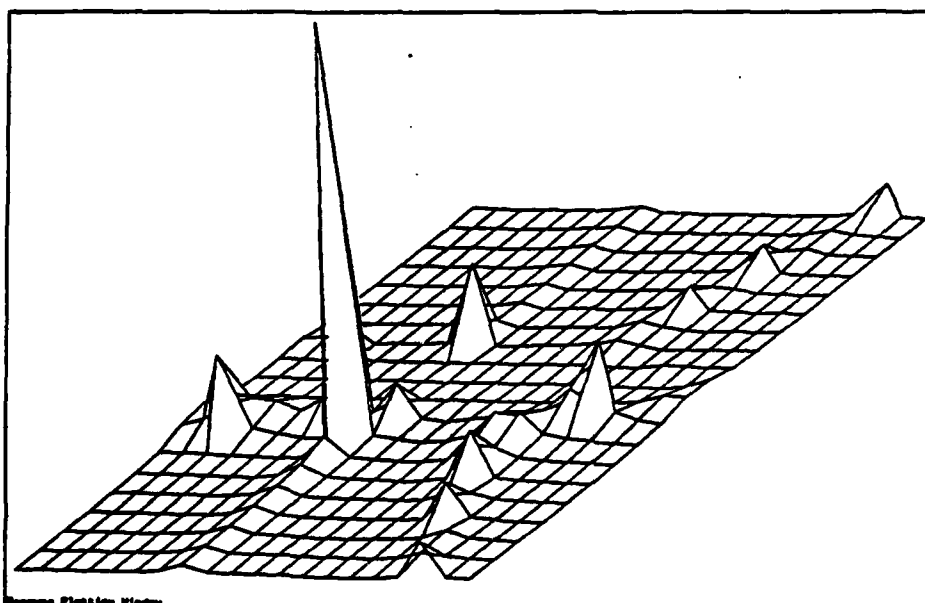
Figure 5

145

Numerical Simulation of the Transient Nonlinear Dynamics of Actively

Controlled Space Structures

Brian H. Aubert, Ph.D.

Cornell University 1991

Advisor: Professor John Abel
Civil and Environmental Engineering

Abstract

The dynamic behavior of large, flexible space structures is typically characterized by a significant number of low frequency modes of vibration which exhibit limited amounts of passive damping. The low frequency modes and the lack of inherent damping can result in long duration transient responses for even limited duration dynamic excitations. To avoid extended periods of motion which may conflict with mission requirements, it is necessary to provide an additional source of energy dissipation. The use of an active control system which has the capability to provide a set of forces to counteract the effects of the structural vibrations is one possible solution.

A research software package which has the capability of modelling the behavior of the actively-controlled response of nonlinear structures subject to dynamic excitation has been developed. The numerical simulation of the dynamic behavior of

an actively-controlled space structure requires an accurate idealization of the physical system. Finite elements have been used to represent the structural members. The analysis software allows for the inclusion of both geometric and material nonlinear behaviors. Implicit and explicit direct integration methods are available for analysis of the dynamic response in the time domain. Modal analysis capabilities are available for evaluation of the characteristic properties of the structural modes of vibration.

Two basic classes of active control algorithms exist, open-loop methods and closed-loop methods. Open-loop methods assume knowledge of the structure and the external forcing functions throughout a specified interval of time. Based on the assumed knowledge of the response of the structure, open-loop methods seek a set of control forces which rapidly damp out the undesired motion. Closed-loop methods assume knowledge of the system but not of the future forcing functions. The control forces necessary to provide rapid energy dissipation in a closed-loop method are calculated based on periodic sets of measurements of the actual dynamic response of the structural system.

Three basic methods of active control have been included in the software. An optimal, nonlinear open-loop method known as differential dynamic programming (DDP) has been implemented. Two closed-loop methods, collocated-velocity feedback and constant-feedback-gains, are also available for use. Active control methods introduce a new class of possible nonlinear responses into the structural dynamics problem. Modelling features such as control saturation, observation and actuation lags have been implemented in the software as a first step towards more accurate representation of the response of physical control systems.

The results of transient, dynamic analyses for large three-dimensional structures generate a large amount of response data which must be effectively interpreted. Interactive computer graphics have provided a convenient means of performing modelling operations and response visualization. In order to reduce the amount of clock time required to perform a given analysis, a parallel multiple-instruction, multiple-data (MIMD) version of the explicit central difference integration method has been implemented. The parallel version of the analysis software is designed using distributed memory in a message passing environment on groups of high performance workstations. The parallel communication is provided by ISIS, a parallel application management package developed at Cornell.

VIBRATION SUPPRESSION OF FLEXIBLE STRUCTURES

USING COLOCATED VELOCITY FEEDBACK AND NONLOCAL ACTUATOR CONTROL

Chen, Pei-Yen, Ph. D.

Cornell University, 1990

Advisor: Professor Francis C. Moon
Theoretical and Applied Mechanics

In this dissertation, a generalized colocated velocity feedback control system is proposed as an active damper which never pumps energy into the structure, and is applied to suppress the vibration in large flexible structures. Some fundamental characteristics of this system are exploited, as well as locations of poles and zeros for the open loop, and root loci for the closed loop. Due to the colocation between actuators and sensors, these properties are unique, and reveal the necessity of introducing optimization to design the controller. By minimizing a quadratic objective function defined by structural states and control forces, a suitable optimization procedure is presented to determine the optimal feedback gains in the form of general, symmetric, diagonal and proportional matrices, where the robustness property is preserved.

A six-and-half-meter long experimental space truss with rigid joints was manufactured to implement the concept of generalized colocated velocity feedback control. The self-equilibrated internal control forces are generated through new magnetic actuators with a high force-to-mass ratio. The corresponding velocity signals are picked up by magnetic sensors which were designed as an integral part of the actuators. In order to transmit these nonlocal torque-free control forces, an actuator

mechanism was also invented. All of the results from theoretical analysis, numerical simulation and experimental testing demonstrate that the transient vibration of the lowest modes in the experimental truss can be suppressed efficiently by using this control strategy with an optimal feedback gain.

Although a conventional optimal feedback control may achieve a better performance in an ideal situation, the main attractive feature of the generalized colocated velocity feedback control is its reliable robustness property. A comparison of the performance between colocated and noncolocated controls is examined. In addition, the effects on the robustness of this system due to non-ideal conditions are investigated, such as dynamic characteristics of control elements, unmodelled masses, nonlinear buckling behavior of structural members, and saturation limits on control forces.

Therefore, by using a few special actuators and sensors, the generalized colocated velocity feedback control is a feasible and robust control scheme for increasing the damping capability of large flexible structures in practical applications.

LOW-DIMENSIONAL BEHAVIOR IN CHAOTIC

NONPLANAR MOTIONS OF A FORCED LINEARLY

ELASTIC ROD: EXPERIMENT AND THEORY

Joseph Paul Cusumano, Ph. D.

Cornell University, 1989

Advisor: Professor Francis C. Moon
Theoretical and Applied Mechanics

New analytical and experimental techniques from dynamical systems theory are combined with a geometrically exact rod theory to yield insight into the source of complex dynamical phenomena observed in a thin prismatic steel rod. Because of the system's geometry, one would expect motions to remain planar. However, experiments show that planar motions become unstable in wedged-shaped regions of the forcing frequency, forcing amplitude parameter plane, with each wedge centered on a resonant frequency of the system. The motions inside of these wedges are observed to be nonplanar and chaotic. A family of asymmetric bending-torsion nonlinear modes are found experimentally, and the frequency/amplitude characteristic of the family is obtained.

Other phenomena discovered include dynamic two-well behavior and energy cascading from high to low frequencies. The fractal dimension of the attracting sets in different resonant wedges are estimated from experimental scalar time series using a numerical code. The dimension estimates, with one exception, are below 5, implying from dimension theory that it may be possible to model the dynamics of the rod with as few as two degrees of freedom.

Starting with a geometrically exact, linearly elastic rod theory, a

model system of two nonlinearly coupled partial differential equations is derived. The dynamics of a two-mode model incorporating a single bending and a single torsional mode are explored, and a simple mechanical analogue is described. Nonlinear modes analagous to those found experimentally in the rod are discovered numerically in the two-mode model. A wedge of planar instability is found for the model inside of which the motions are chaotic and nonplanar. The nonplanar motions also exhibit the dynamic two-well behavior observed in the rod experiments.

Numerically obtained Poincare sections for a related Hamiltonian system reveal that the nonlinear modes are born by a pitchfork bifurcation in the energy. It is conjectured that the homoclinic structure which results from the pitchfork bifurcation is responsible for the dynamic two-well behavior observed in the damped-driven system. A similar pitchfork bifurcation is observed experimentally in the rod.

CHAOS AND FRICTION

Brian Feeny, Ph.D.

Cornell University 1990

Advisor: Professor Francis C. Moon
Theoretical and Applied Mechanics

We study the dynamics of a forced oscillator with dry friction. The magnitude of the friction in the oscillator varies with displacement. The primary concern is in the chaotic response to a harmonic excitation. Experimental data is compared with numerical simulations. In both the experiments and the simulations, the dynamics are reducible to one-dimensional maps. The motion is characterized using symbol dynamics. Bifurcations in a simulation with a Coulomb friction law are compared with universal bifurcation properties of standard one-dimensional maps. Theoretical analysis is performed qualitatively for the Coulomb model. The Coulomb model exhibits unlikely dynamical properties, stemming from noninvertibility in the flow which results from the multivalued discontinuity in Coulomb friction.

The friction is measured experimentally during oscillations. There is evidence of the presence of unseen state variables in the friction mechanism. A friction law is constructed based on observations in the measurements, and applied to simulations of the chaotic oscillator.

High frequency excitation is used experimentally to reduce friction and regulate chaos.

153

PARALLEL PROCESSING FOR TRANSIENT NONLINEAR

STRUCTURAL DYNAMICS OF THREE-DIMENSIONAL FRAMED STRUCTURES

Jerome Frederick Hajjar, Ph.D.

Cornell University 1988

Advisor: Professor John Abel
Civil and Environmental Engineering

A variety of strategies are developed for the practical solution of the fully nonlinear transient structural dynamics problem in a coarse-grained parallel processing environment. Emphasis is placed on the analysis of three-dimensional framed structures subjected to arbitrary dynamic loading and, in particular, steel building frames subject to earthquake loading. The parallel algorithms developed and investigated are intended to be appropriate for finite element models which use structural elements (e.g., beam-columns). Concerns include long-duration dynamic loading, geometric and material nonlinearity, and the wide distribution of vibrational frequencies found in frame models.

Explicit algorithms require no simultaneous solution of equations, employ simple communication, and are thus efficient for parallel processing. Parallel analysis using the central difference algorithm is examined and implemented. The strict stability limit on time step makes this method best suited for short-duration loadings.

Implicit techniques require the solution of simultaneous equations, and several strategies are discussed to implement these algorithms in parallel. The domain decomposition method is described in detail,

154

implemented, and tested. This method employs substructuring techniques and then a preconditioned conjugate gradient algorithm for the iterative solution of the reduced set of unknowns along the substructure interfaces. Substructuring is shown to provide a natural preconditioner for effective parallel iterative solution.

In addition, several partitioned time integration algorithms are investigated which attempt to include the advantageous aspects of both explicit and implicit analysis. Two algorithms, the alternating group explicit method and the group implicit method, are developed and described in detail. The group implicit algorithm is implemented and tested in parallel for frame dynamic analysis. For practical time step sizes, current forms of both algorithms are shown to be inaccurate.

The parallel algorithms studied are amenable to several common parallel hardware architectures but are implemented on a bus architecture, with the number of processors in this work varying from one to four. Database considerations and message passing constructs are investigated. Also, a flexible interactive computer graphics environment is described for the preparation of the input data to, and for the playback of, the parallel analysis simulation.

Transient Stress Waves in Trusses and Frames

Samuel Moss Howard, Ph.D.

Cornell University 1990

Advisor: Y.-H. Pao
Theoretical and Applied Mechanics

The dynamics of lattice-type structures in the form of planar trusses and frames are investigated in terms of axial (longitudinal) and flexural (transverse) waves which propagate along members and scatter at structural joints. Theoretical and experimental results are presented for pin-jointed trusses and frames with rigid joints.

The first part of the analysis considers only the axial waves, whose reflection and transmission at joints are related by analytical scattering coefficients. The complex reverberations of waves within a structure are calculated in the frequency domain with a new technique called the reverberation method, which is implemented on a digital computer. Transient waves are then computed by Fourier synthesis. This technique has been successfully applied to calculate hundreds of reverberations, revealing the growth of early wave transients into modal vibration of the entire structure.

Results of extensive laboratory experiments are also presented. New techniques were developed for the generation and measurement of broadband stress waves in truss structures, using foil strain gages and an elaborate digital data processing

system. The results of these experiments are compared to theoretical simulations based on the axial wave theory. Good agreement was found only for the very early response to about eight reverberations between two joints. Also, bending waves, which are neglected by the axial wave theory, appear to dominate the later portions of the experimental data.

In order to correct this later discrepancy, a general theory including both axial and flexural waves is developed, where the latter are predicted with either the Euler-Bernoulli or Timoshenko theories of bending, which introduce two modes of flexural waves in each member. First, general scattering coefficients for all three modes of waves at a joint are derived, and are shown to agree closely with experiments done on a single joint. The reverberation method is then generalized to include these general scattering coefficients, with the simplification that the mode conversion from flexural waves to axial waves at each joint is negligible. Simulated axial waves based on this assumption are found to be in much better agreement with the aforementioned experimental data over a longer duration (over 15 reverberations) of observation.

EXPERIMENTAL PROGRAM FOR ACTIVE CONTROL OF FLEXIBLE SPACE STRUCTURES

Lauran B. Larson, M.S., 1990

Advisor: Professor Peter Gergely
Civil and Environmental Engineering

ABSTRACT

The purpose of this work was the development and experimental testing of a constant velocity feedback gain, eccentric tendon active vibration control scheme for applications to flexible space structures. A large-scale 10-meter truss specimen, designed to behave dynamically similar to space structures, was built in the laboratory. A control tendon, draped eccentrically to the truss neutral axis, delivered control forces lateral to truss motions throughout the specimen length. The single control force was based on a vector multiplication of 11 feedback gains with 11 velocity feedback states recorded at locations throughout the length of the truss at each interval of data sampling. Both the feedback gain vector entries and the tendon eccentricity dimensions were derived by application of optimization theory to the control solution.

A detailed program of static and dynamic system characterization was applied to the truss specimen to establish a reference of uncontrolled behavior and to provide modal data used in adjustment of the finite element model upon which the control parameter optimizations were based.

The results of active control tests indicated that the control scheme was effective in providing approximately 5% of critical damping in the first mode as compared to 0.5% in the uncontrolled case. Two sources of system instability were observed. The first was found to be related to aliasing of the feedback data and was resolved by installing anti-aliasing analog filters in the feedback signal conditioning circuit. The second and more difficult instability was

caused by phase/time lag in the response of the electromagnetic linear motor used to tension the control tendon. When the time lag in linear motor response represented a 180 degree phase difference between demanded and achieved control, the control system would begin to drive, rather than damp the truss motions.

NUMERICALLY EFFICIENT ALGORITHMS FOR UNCONSTRAINED AND CONSTRAINED DIFFERENTIAL DYNAMIC PROGRAMMING IN DISCRETE-TIME, NONLINEAR SYSTEMS

Li-zhi Liao, Ph.D.

Cornell University, 1990

Advisor: Professor Christine Shoemaker
Civil and Environmental Engineering

The research reported in this dissertation focuses on the development of more efficient differential dynamic programming algorithms for solving general nonlinear discrete-time optimal control problems. The thesis reports both theoretical results on algorithm behavior and numerical applications of these algorithms to difficult large scale nonconvex problems.

The first part of this dissertation studies the detailed structure of unconstrained discrete-time optimal control problems and differential dynamic programming. This analysis makes it possible 1) to provide a new proof for quadratic convergence of differential dynamic programming; 2) to obtain sufficient conditions on the characteristics of the objective and transition functions required for quadratic convergence of differential dynamic programming; and 3) to introduce an adaptive shift procedure to guarantee good convergence of differential dynamic programming in nonconvex situations. Results are provided to demonstrate the numerical performance of this adaptive shift procedure.

The second part of the dissertation focuses on the development of an efficient algorithm called Constrained Differential Dynamic Programming to solve general nonlinear constrained discrete-time optimal control problems. In the process of developing this algorithm, matrix partition and QR factorization techniques are introduced in the traditional penalty function method to avoid the loss of information and an ill-conditioned Hessian matrix. After the completion of the improved penalty function method, the constrained differential dynamic programming method is developed by combining this improved penalty function method

with the unconstrained differential dynamic programming algorithm and the adaptive shift procedure. The convergence and numerical stability of this method are also examined. A very difficult, nonconvex, large dimensional test problem is created to test the numerical performance of this algorithm. Following the discussion of unconstrained and constrained differential dynamic programming algorithms, we compute the computational complexities and storage requirements of these two algorithms.

At the end of this dissertation, both unconstrained and constrained differential dynamic programming algorithms are applied to solve a four-bay nonlinear structural control problem. The dynamics of the structure are described by a nonlinear finite element model with 10,000 time steps. The results for this four-bay truss and other large scale numerical applications have shown that constrained differential dynamic programming is a very efficient algorithm for solving general nonlinear constrained discrete-time optimal control problems.

A PSEUDO EXPONENT FOR THE CHARACTERIZATION OF PERIODIC AND CHAOTIC DATA SETS FROM FORCED SYSTEMS

by

Oliver M. O'Reilly
M.S. Thesis, Cornell University, 1988

Advisor: Francis C. Moon
Theoretical and Applied Mechanics

ABSTRACT

A pseudo maximal Lyapunov Exponent is developed which classifies a time series of data from a system as chaotic or periodic. This exponent is based on the maximal Lyapunov Characteristic Exponent (L.C.E.). As is not the case with the maximal L.C.E., knowledge of the equation of motion of the system in terms of a set of ordinary different equations is not necessary.

The development of this exponent is due to Wolf (1985), however the number of independent variables involved in determining the exponent is reduced, resulting in a more efficient method to differentiate periodic and chaotic motions. The primary interest lies in characterizing the parameter space of experimental systems, in particular the forced buckled beam in a two well potential (Moon, 1980)). In order to verify the exponent's ability to differentiate periodic and chaotic motions efficiently, the exponent's behavior is verified initially using single degree of freedom systems with external forcing. The results of these calculations demonstrate the ability of the exponent to differentiate between periodic and chaotic motions.

The parameter space of the magneto-elastic system consisting of a forced buckled beam in a two well potential is then characterized, and the results correlated to those of spectrum analysis and Poincaré sections. Finally, noise is added to the numerical integrated equations of motion for a Duffing equation (Holmes, 1979)). The addition of noise, especially for periodic motions highlight the difficulties involved in using the exponent; the exponent correctly characterizes chaotic motions, but has considerable difficulty with "noisy" periodic motions.

The pseudo exponent is a new method in investigating experimental data and infinite dimensional systems, and compliments the currently used techniques of spectrum analysis and Poincaré sections.

THE CHAOTIC VIBRATION OF A STRING

Oliver Mary O'Reilly, Ph.D.

Cornell University, 1990

Advisor: Professor Philip Holmes
Theoretical and Applied Mechanics

A pretensioned string that is fixed at one end and forced harmonically in a plane transverse to its longitudinal axis at the other end, is found to exhibit chaotic motions. These chaotic motions involve vibrations in both transverse directions and occur when the forcing frequency is close to the fundamental transverse harmonic of the string. A three mode model, which assumes a linearly elastic string, is developed for the experimental system. Two of these modes correspond to the fundamental transverse modes and the third corresponds to the fundamental longitudinal mode.

The equations of motion for the aforementioned model are averaged, whereupon the longitudinal mode terms are eliminated. This reduces the system to four coupled, autonomous ordinary differential equations. A local bifurcation analysis of these equations is performed and chaotic motions are found numerically, both in the presence and absence of linear viscous damping. The mechanisms of chaos for these equations are discussed and shown to involve homoclinic orbits to fixed points of saddle-focus and saddle-center type. Finally a comparison of the analytical and experimental results is performed. Good qualitative agreement is obtained, however poor quantitative agreement is found and some reasons for this are discussed.

Symmetry and Bifurcation in Frame Structures with Bending Degrees Of Freedom

James A. Treacy

Advisor: Professor Timothy Healey
Theoretical and Applied Mechanics

There has been a great deal of effort in the last fifteen years to create finite element formulations of rods which will deal with large displacements. Most of these formulations are limited to small curvatures and only approximately deal with the change in geometry. It is also common to treat incremental rotations as if they are additive. This leads to increased error as the total rotation becomes large.

While there has been a proliferation of theoretical work done in bifurcation theory there is still a large amount of work to be done in the area of computational bifurcation theory. In industry, most 'bifurcation' analysis is little more than the analysis of the structure with the introduction of an imperfection into the structure to avoid numerical difficulties.

The main goal of my thesis is to use a geometrically exact rod model to study the bifurcation of structures with symmetry. A one-director Cosserat rod model is used. This essentially models a rod with shear but no deformation of the cross sections. To deal with the large rotations essential for such a model, the configuration space of a rod is taken to be a nonlinear manifold. The linearization of the equilibrium equations at each configuration is the tangent space to the manifold. The linearized equations are then solved and projected onto the manifold so that we always remain in configuration space. This is crucial for dealing with large motions.

The most common way of dealing with symmetry is the use of 'symmetry and anti-symmetry'. This is simply not practical in dealing with more complex symmetries because one can not use intuition in breaking up the problem. A group-theoretic approach is used which relies on a single a priori analysis of the structure. This analysis gives a set of symmetry basis vectors which are used to separate the problem into a number of invariant subspaces. When iterating along a solution branch all computations can be done in the subspace corresponding to the symmetry of that branch. The use of these subspaces avoids many numerical difficulties in the accurate detection of bifurcation points and branch switching. I have already used this technique in the study of truss structures. The study of rods is a natural next step in the generalization of this technique since bending degrees of freedom must be accounted for.